Chemical Engineering Journal 98 (2004) 1–38

Chemical Engineering Journal

www.elsevier.com/locate/cej

Review

Micro-structured reactors for gas phase reactions

Gunther Kolb*, Volker Hessel

Institut für Mikrotechnik Mainz GmbH, Carl-Zeiss-Str. 18-20, 55129 Mainz, Germany

Received 3 April 2003; accepted 16 October 2003

Abstract

This paper deals with reviewing on the application of micro-structured reactors for heterogeneously catalysed gas phase reactions. After a brief introduction covering some estimation criteria for the performance of micro-structured reactors, an overview of the work performed to date in the field is given. The reactors are classified by the type of catalyst applied (porous or non-porous) and according to their basic design criteria. At the end, a small chapter is dedicated to applications employing reactors combined with other micro-structured devices like heat exchangers. Finally, some alternative ways of achieving micro-structures, besides relying on micro-fabrication, are discussed.

Diverse gas-phase reactions have been investigated in micro-reactors, among them (partial) oxidations, hydrogenations, dehydrogenations, dehydrations, and reforming processes. Particular attention has been drawn to achieve excellent temperature control and to prevent hot-spots. So, for many reactions increases in selectivity were found. Especially, many examples of partial oxidations were described, including processes of utmost industrial importance such as ethylene oxide synthesis. Within consecutive processes, as e.g. given for multiple hydrogenations, high selectivity was achieved for species that are thermodynamically not the most stable molecule of all species serially generated such as monoenes yielded by hydrogenation of polyenes. Also, increases in conversion were achieved, e.g. by processing at high pressure and high temperature, often in the explosive regime. As a consequence, high space–time yields were reported as well. In many cases, reactor performance better compared to fixed-bed technology was achieved. Process safety was found to be high when using micro-reaction devices; intrinsic safety in former explosive regimes was ascribed. With respect to process optimisation, fast serial screening of process parameter variation was conducted, at low sample consumption.

Keywords: Mico-structured; Micro-fabrication; Gas phase reactions

1. Introduction

In this paper, reactors are regarded as being micro-structured, when carrying channel(s) or similar fluid paths with a size below 1 mm.

The well-known, specific advantages of micro-structured reactors were summarised in an early report of Fichtner et al. [1]. Firstly, enhanced heat transfer is observed, which may be exploited for highly exothermic reactions due to the removal of the heat generated and the suppression of hot spot formation. Another aspect is the optimisation of slow reactions getting close to the thermodynamic equilibrium. An example for this was demonstrated by TeGrotenhuis et al. [2] for the water-gas-shift reaction, which is investigated as a gas purification reaction in the scope of a future application of micro-technology for reforming applications. In conventional technical reactors, the conversion of reactions close to their thermodynamic equilibrium is improved by intermediate direct (cold gas/water injection) or indirect (coolers switched between several stages of the reactor) cooling. In micro-reactors, heat-exchanging channels may be introduced which allow for temperature profiling of the reactor according to the specific needs of the reaction. This was quantified by simulation work [2] as shown in Fig. 1. Thus, the typical two-stage design of water-gas-shift reactors might become obsolete in micro-structured reactors. Another way of exploiting the improved heat transfer is the combination of exothermic and endothermic reactions in a single reactor designed like a heat exchanger.

As therefore the overcome of heat and mass-transfer limitations is a crucial driver for applying micro-reactors instead of conventional apparatus, suitable criteria have to be identified which allow proper judging of such limitations. The Anderson criterion [3] may be applied for checking the effect of intra-particle (or intra-coating) temperature gradients:

$$\frac{-\Delta H_r r_{eff} d_h E_a}{\alpha R T_r^2} < 1 \quad (1)$$

* Corresponding author. Tel.: +49-613-1990-341; fax: +49-613-1990-305.
E-mail addresses: hessel@imm-mainz.de, kolb@imm-mainz.de (G. Kolb).

1385-8947/$ – see front matter © 2003 Elsevier B.V. All rights reserved.
doi:10.1016/j.cej.2003.10.005

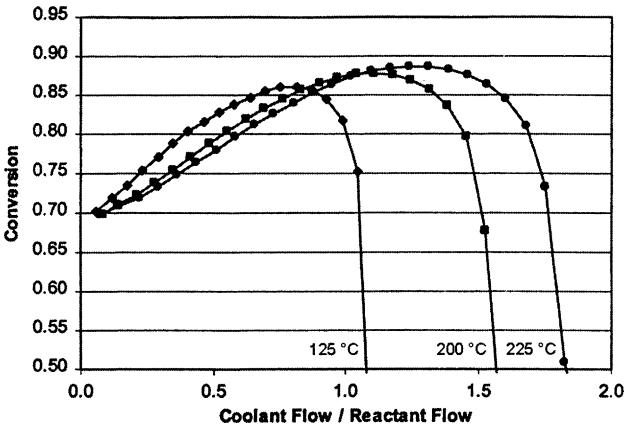

Fig. 1. CO conversion of the water-gas shift reaction vs. ratio of coolant/reactant flow at constant steam reformate feed at 350 °C, a feed composition of 9% CO, 9% CO_2, 36% H_2O, and 45% H_2. Coolant temperature 125 °C (◆), 200 °C (■), and 225 °C (●); from TeGrotenhuis et al. [2].

ΔH_r indicating the reaction enthalpy, r_{eff} the measured rate of reaction, d_h the hydraulic diameter, E_a the activation energy, α the heat transfer coefficient, R the gas constant, and T_r the temperature in the gaseous phase. If the criterion is fulfilled, heat transfer limitation in the gas phase of the micro-channel is negligible. This was the case for the Pt-catalysed oxidation of hydrogen as found by Görke et al. [86].

A modification of the Anderson criterion was applied by Ajmera et al. [49] to check for intra-particle temperature gradients for the oxidation of CO. Again, no indication for such a limitation was found.

Secondly, an enhancement of mass transfer is observed, which is closely coupled to the dimensions of the micro-channels. A simple estimation of the mass transport coefficient k_g gets possible due to the fact, that in the fully developed laminar flow of a micro-channel the Sherwood number *Sh* in most applications approaches a constant value:

$$Sh = \frac{k_g d_h}{D} = 3.66 \quad (2)$$

d_h being the hydraulic diameter and D the diffusion coefficient. This demonstrates that the mass transfer gets more and more dominant the smaller the channels are.

The equation discussed above gives a hint to an experimental method of checking mass-transfer limitations by modifying the hydraulic diameter of the channels. This was applied by Fichtner et al. [125] for the partial oxidation of methane to syngas. No indication for mass-transfer limitations was determined by the experiments.

Another way of checking for mass transport limitations experimentally was demonstrated by Pfeifer et al. [65]. They carried out experiments on methanol steam reforming at one, two and four micro-structured platelets of decreasing length L, $L/2$ and $L/4$. By decreasing the flow velocity u at the same time from u to $u/2$ and $u/4$, the modified residence time $\tau = m_{cat}/Q$, m_{cat} being the catalyst mass and Q being the total flow rate, remained unchanged allowing thus for direct comparison of the experiments. Fig. 2 shows, that no mass transport limitations were found for the reaction system.

Among others, Görke et al. [86] applied the Mears criterion:

$$\frac{r_{eff} d_h}{2 k_g c} < 0.15 \quad (3)$$

to check for mass-transfer limitations. d_h stands here for the hydraulic diameter of the micro-channel, r_{eff} for the determined (effective) rate of reaction, k_g for the mass transfer coefficient and c for the concentration of the species under investigation. No mass-transfer limitation for the hydrogen oxidation reaction at Pt catalyst was found.

Commenge et al. [4] developed by numerical simulations a criterion for the heterogeneous Damköhler number *Da*:

$$Da = \frac{k_s r}{D} < 0.1 \quad (4)$$

where k_s is the rate constant of a first-order wall reaction, r the channel radius and D the diffusion coefficient. If the criterion is fulfilled, the effect of mass transport limitations is limited to 3%.

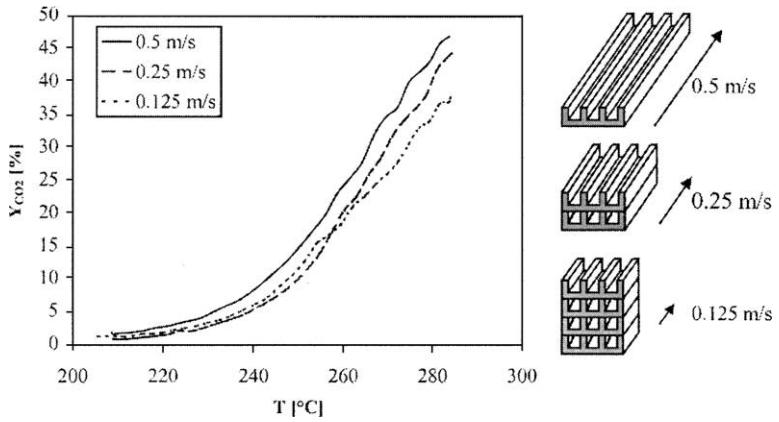

Fig. 2. CO_2 yield from methanol steam reforming vs. temperature at a constant residence time of 125 ms and different channel geometries from Pfeifer et al. [65].

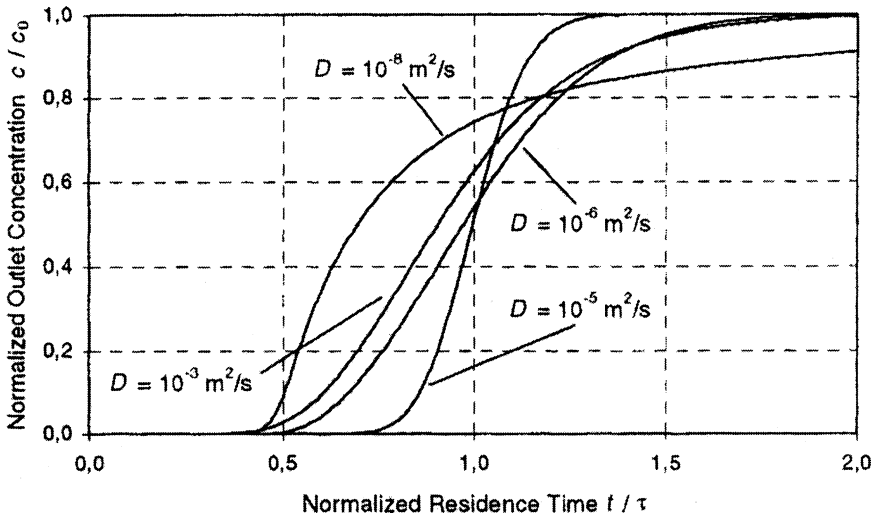

Fig. 3. RTD curve for a channel of 300 μm × 300 μm × 20 mm size, a flow velocity of 1 m/s and a time of 10 ms from Walter et al. [6].

The Weisz-modulus [5] Ψ allows for the estimation of intra-particle (or intra-coating) diffusion limitations:

$$\Psi = L_c \frac{m+1}{2} \frac{r_{eff}}{D c_s} < 0.1 \quad (5)$$

where L_c is the characteristic length of the particle or coating defined by the ratio of volume to surface, m the reaction order, r_{eff} the effectively measured rate of the reaction. For a first-order reaction, values of $\Psi < 0.1$ indicate the absence of intra-catalyst diffusion limitation. This criterion was applied by Ajmera et al. [49] to the oxidation of carbon monoxide for catalyst particles incorporated into a micro-channel reactor. Mass transport in the coating was not limiting the reactor performance in this case.

Assuming a rate law of first order for the selective catalytic reduction of NO with ammonia, Rebrov et al. [69] determined the Thiele modulus:

$$\varphi = L_c \sqrt{\frac{k_s}{D}} \quad (6)$$

L_c is the characteristic length of the catalyst, k_s the rate constant and D the diffusion coefficient. Applying φ, the effectiveness factor of the catalyst may be calculated:

$$\eta = \frac{3}{\varphi}\left(\frac{1}{\tanh\varphi} - \frac{1}{\varphi}\right) \quad (7)$$

Values of η around 0.85 were found for the zeolitic coating under investigation.

The residence time distribution in a micro-channel with its laminar flow regime strongly depends on the diffusion coefficients of the species involved and on the channel dimensions (see Figs. 3 and 4). Walter et al. [6] demon-

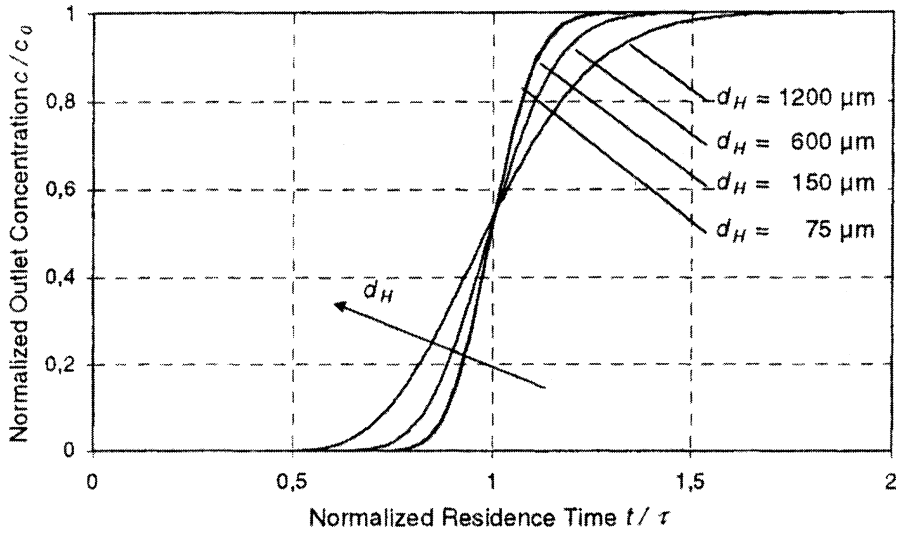

Fig. 4. RTD curve for various channel dimensions, 20 mm channel length, a flow velocity of 1 m/s and a diffusion coefficient of 3×10^{-5} m^2/s from Walter et al. [6].

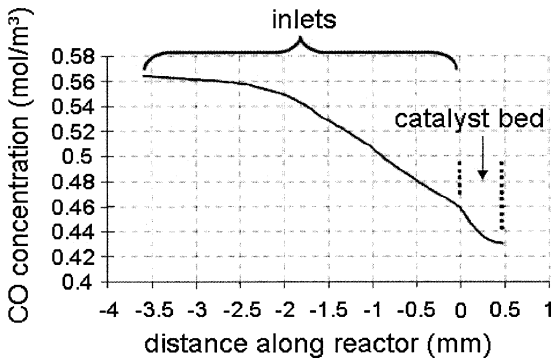

Fig. 5. CO concentration in a cross-flow micro-reactor for CO oxidation at a temperature of 540 K, a pressure of 2.5 bar and a CO concentration of 0.564 mol/m^3 along the reactor including 2.75 mm upstream determined by Ajmera et al. [49].

strated the existence of an optimum diffusion coefficient for a micro-channel to achieve a performance similar to ideal plug flow. It was determined to a value of 10^{-5} m^2/g for a $300 \times 300\,\mu m^2$ channel. The origin of this phenomenon may be explained by the effective axial diffusion coefficient as defined by Aris [7]:

$$D_{ax,eff} = D + \chi \frac{(d/2)^2 u^2}{D} \quad (8)$$

where D stands for the diffusion coefficient, χ for a shape factor, d for the channel diameter, and u for the flow velocity. High values of D make the first term dominant, small values the second. Decreasing the channel diameter makes only the second term smaller.

The effects of axial diffusion were demonstrated by Ajmera et al. [49] for the inlet channels of a micro-structured reactor. As shown in Fig. 5, the concentration of the reaction educts already decreases significantly before the feed enters the reaction zone. Claus et al. [114] had to take the same effect into consideration when sampling at the open outlet of their micro-structured screening reactor.

Another important aspect is the flow uniformity in micro-channel reactors. Commenge et al. [8] developed a dimensionless approach for a channel system. The velocity profile in the channels was found to depend strongly on the geometry of the inlet and outlet chambers. For 20 channels, the ratio of chamber width to duct thickness lead to a concave velocity profile for a value of 0.5, to an even profile for 1.6, and to a convex profile for a value of 10. This was valid for a wide range of *Re* numbers. The channel length was inversely proportional to the maximum deviation from the normalised maximum velocity difference. Increasing the channel width increased rapidly the normalised maximum velocity difference for narrow channels, but only weakly for channels which are wider than deep. An almost linear relationship between the width of inlet and outlet zones was found, which gives a normalised maximum velocity difference of less than 3% as a function of the number of channels.

The specific surface area is generally high for micro-structured reactors. This increased surface-to-volume ratio allows for the suppression of homogeneous reactions [34], however, may also promote undesired follow-up reactions, such as total oxidations, at active, but unselective construction materials, such as stainless steel at high temperature.

Micro-reactors allow safe processing in otherwise explosive regimes. Many partial oxidations can thus be carried out using pure oxygen and at elevated pressures. By this, space–time yields can be increased, as e.g. demonstrated for the ethylene oxide synthesis [36,39]. A very instructive example for safe processing is given by the hydrogen–oxygen reaction which, according to all experience gained so far with micro-reactors, can be handled very safely when operating within the explosive regime [34,86]. In this content, intrinsic safety is an often quoted and recently theoretically confirmed term for such micro-reactor processing [34].

Finally, micro-reactors allow for easier scale-up, as the geometry of the "unit cell" (the micro-channel) does not need to be changed. However, when numbering-up of micro-structured reactors is done, it needs to be taken into consideration that the housing material has to be minimised to reduce heat-losses, start-up energy demand and time demand. Therefore, the practical needs might result in more macro-sized reactors carrying micro-channels as far as scale-up is concerned.

There may be more, so far unidentified reasons to choose micro-reactors for heterogeneous gas-phase processing. For instance, investigations with regard to hydrodynamics in micro-channels and their role on processing are not at all completed. Prior literature, partly giving such information, needs more time for 'penetrating the micro-reactor community' as a result of the deeply interdisciplinary nature of the field. Hence, one can say that with increasing work in the field within the next years the above given list of possible advantages of micro-reactors will be supplemented, revised and differently weighted.

2. Non-porous catalyst systems

2.1. Chip-like micro-structured reactors with a thin-film catalytic coating

Jensen et al. [9,10] pointed out the advantages of designing and manufacturing reactors similar to micro-electro-mechanical systems (MEMS): heaters and sensors may be integrated [11] and short response times for heat exchanging tasks are found due to the thin walls applied. He propagates the application of aerosol and technologies similar to the inkjet method besides wet preparations and thin film technologies. Even though some publications [24,26] assembled here work with porous catalyst coatings, most of the work is done applying sputtered catalyst coatings.

Srinivasan et al. [12] performed in an early work published in 1997 ammonia oxidation in a chip-like micro-reactor. The main intention was to demonstrate the feasibility of decentralised and safe production of hazardous chemicals by ap-

plying micro-technology. A single T-shaped channel was etched by KOH into a silicon wafer. The wafer was covered by a SiN membrane carrying a thin-film Pt layer for heating on the outer side and a Pt catalyst layer on the inner side. Temperature and flow sensors were integrated into the device as well. The reactor was mounted on an Al-block and sealed by O-rings. A temperature as high as 800 °C could be achieved in the reaction zone because all other parts did not heat up. Fifteen molar percent ammonia in oxygen was fed to the reactor. The reaction ignited at 200 °C. At flow rates below 15 scm^3/min the ignition front travelled upstream. When the heating power was lowered, extinction occurred at 300 °C. Approaching stochiometric feed-composition, the temperature rise increased due to the higher heat generation of the reaction. The experiments were limited to 650 °C, because high temperatures caused deformations and rupture of the membrane. As products nitrogen, nitrogen monoxide and also to nitrous oxide were found the latter at concentrations smaller than 15 vol.% below 350 °C. At temperatures exceeding 400 °C N_2O decomposed completely. Increasing the heating power leads to a higher NO/N_2 ratio, which is in line with literature [13]. As a slow increase of conversion with increasing temperature after ignition of the reaction was found, mass-transfer limitations were expected at least at residence times lower than 9 ms. Complete conversion was found for higher residence times. Increasing the residence time decreased the NO/N_2 ratio as the NO had time to readsorb and decompose. In ammonia rich feed, conversion vanished due to an inhibition of NO desorption by ammonia. Problems occurred by an etching process of Pt in the ammonia/oxygen atmosphere which led to losses of the catalyst to the gas phase. The small reactor had a production capacity of 10 g NO per day.

A general finite element approach was developed by Hsing et al. [14] to simulate the reactor described by Srinivasan et al. [12]. The observed downstream ignition of the reaction and the reaction front travelling upstream were confirmed by the calculations. The effects were attributed to both heat conduction in the membrane and the presence of fresh reactants in the upstream area. The calculations revealed also, that temperature variations along the membrane should decrease with increasing flow rate due to the more even distribution of ammonia along the catalyst surface.

Jensen et al. [10] developed a silicon membrane reactor which was composed of an aluminium bottom plate, a microstructured silicon layer carrying the channel system and a 3 μm thick SiN membrane as a cover of the reactor. The reactor was manufactured by photolithography and plasma etching. The channels were introduced either by wet-etching or deep reactive ion etching.

The latter resulted in a more precise shape of the channels and therefore higher possible operating pressures as the unsupported membrane area was minimised. Again, Pt heaters and temperature sensors were integrated into the device. Pt as an active component was put on the membrane either by wet chemistry or by physical vapour deposition (PVD) on a Ti adhesion layer. The reactor was applied for ammonia oxidation. Heating the membrane, again an ignition/extinction behaviour of the reaction could be observed. At temperatures higher than 300 °C, deformations of the SiN membrane got visible, leading to rupture at temperatures exceeding 650 °C, as the heat removal by conduction was smaller than the heat generated by the reaction. It was proposed therefore to make use of the non-uniform temperature profile of the reactor for calorimetric measurements. A 1 μm thick SiN membrane did not show an ignition/extinction behaviour any-more but only an ignition followed by autothermal behaviour. By increasing the thickness of the membrane from 1 to 1.5 and 2.6 μm, and switching to pure silicon, the ability of the reactor membrane to dissipate heat was increased by an order of magnitude [16]. Only in the latter case, both membranes showed ignition/extinction behaviour. The 2.6 μm thick membrane ignited at a higher temperature and reached lower steady state temperatures. For the 1 μm thick membrane running in the autothermal mode, only one reaction temperature of 550 °C could be set. At this high temperature, a high selectivity to NO was found. The thicker membranes allowed for lower operation temperatures and thus lower NO selectivity [16]. Introducing silicon membranes into the reactor increased the heat conductivity by 25 times which improved the temperature uniformity. By using SiO_2 and Si_3N_4 as membrane material, stress compensated membranes of 0.25 and 0.3 μm thickness could be manufactured [16].

Franz et al. [15] applied a silicon membrane for highly exothermic reactions to improve the heat removal in this type of reactor by the higher heat conductivity of silicon as mentioned above. Pt was deposited by PVD and the membrane was tested applying ammonia oxidation. At temperatures higher than 200 °C formation of N_2, NO and N_2O (the latter, in line with Srinivasan et al. [12], up to 15 vol.%) started but no ignition/extinction behaviour was observed, which was attributed to the improved heat removal. The reactor showed a fast response on temperature changes in the order of 20 ms which makes a dynamic operation possible. Additionally, Franz et al. [16] developed an aerosol technique for the deposition of Pt, Ag and Rh salt solutions in micro-channels.

Later on, Franz et al. [17] fabricated a Pd membrane reactor for (de)hydrogenation reactions and hydrogen purification by buffered oxide etching (BOE) and other etching techniques. Thin membranes could be realised compared to the relatively thick membranes (10–25 μm) which are manufactured on porous ceramics in conventional reactors. Thin perforated layers of silicon nitride (0.3 μm) and silicon oxide (0.2 μm) were used as a support for the 0.2 μm thick Pd membrane which was deposited by an e-beam. Pt films for resistor heating and temperature sensing were integrated using the same technique. The membrane had dimensions of $12 \times 0.7\ mm^2$ and withstood a pressure difference of 5 bar at ambient temperature. A membrane separation factor of 1800 and a hydrogen flow rate of 600 $scm^3/(min\ cm^2)$ were calculated for the separation of hydrogen out of a mixture of ni-

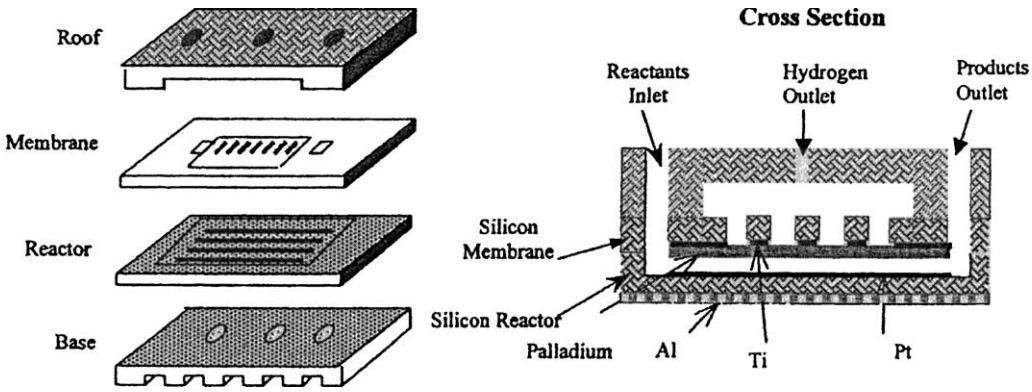

Fig. 6. Membrane micro-reactor designed by Cui et al. [19].

trogen and hydrogen. Other micro-reactors for gas-phase reactions were designed and manufactured according to techniques developed for micro-electronic devices based on silicon technology. In this way, two or several plates were connected and sensors were integrated into the devices. Zheng et al. [18] and Cui et al. [19] designed several membrane micro-reactors for the dehydrogenation of cyclohexane to benzene one of them shown in Fig. 6. The reactors were made of silicon and photo etching techniques were applied for manufacturing. Pt was used as a catalyst which was sputtered onto the reaction chamber. The micro-channels of the reaction chamber were 500 μm wide, 10 μm deep and 50 mm long, another type 400 μm deep, 50 μm wide and 8 mm long [19]. Additionally, a Pd-membrane was introduced into the reactor to continuously remove the hydrogen out of the reaction zone in order to enhance the conversion beyond the limitations of the thermodynamic equilibrium.

Another chip-like reactor was designed and manufactured by Besser et al. [20] for organic synthesis reactions. Modular reaction-chips were produced by electron beam lithography. Again, the Pt catalyst was introduced by sputtering into the 5–20 μm wide channels. Glass covers were sealed by anodic bonding, silicon covers by diffusion bonding.

Besser et al. [21,22], applied silicon reactors fabricated by both basic leaching and photolithography for cyclohexene dehydrogenation as an example for hydro-treating and reforming reactions for future fuel processing. The channel system was 19 mm in length and 100 μm × 100 μm wide. Anodic bonding was used to attach the Pyrex glass cover and vacuum sputtering of Pt to achieve a 20 nm thick catalyst coating. The reactor was heated externally. Experiments were performed at ambient pressure and feed rates between 0.2 and 2 scm^3/min. An increasing selectivity towards benzene up to 80% was found at reaction temperatures above 120 °C. Conversion increased up to 95% between 20 and 50 °C and maintained at this level up to 120 °C, then deactivation of the catalyst started which was explained by carbon deposition. Increasing the hydrogen partial pressure decreased the benzene yield and space–time yield at a temperature of 200 °C. However, residence time was changed accordingly to carry out that measurement. Increasing the residence time had a positive effect on the benzene yield, but did not affect the cyclohexane yields. A small amount of hydrogen was found to be necessary to condition the catalyst. Increasing the cyclohexene partial pressure increased the benzene yield. The maximum space–time yields found at 200 °C amounted to 8×10^{-4} kg/(m^2 cat min) for benzene and 4.3×10^4 kg/(m^2 cat min) for cyclohexane.

Surangalikar et al. [23] investigated cyclohexene (de) hydrogenation over Pt catalysts in another silicon reactor manufactured by photolithography and KOH etching. As for the other reactors developed by this group, it was covered with Pyrex glass by anodic bonding and heating was performed by an external block. Two reactors with different channel systems were used. Both channel types had a length of 1.8 mm and a depth of 100 μm. In the first reactor 39 channels of 100 μm width revealing a total surface area of 2 cm^2 were incorporated, the second one had 780 channels of 5 μm width manufactured by ion coupled plasma (ICP) etching with a total surface area of 28 cm^2. The Pt catalyst was introduced by sputtering. By estimation of the mass transfer coefficients external mass transport limitations could be excluded for the reaction system. A matrix of experiments was carried out by modification of the H_2 (0.1/0.3/1.0 scm^3/min) and cyclohexene (0.6/0.3/1.0 scm^3/min) flow rates. The pressure was kept at 1 bar and the temperature was set to 200 °C. The catalyst showed deactivation, but only a maximum 10% activity loss was accepted for the experiments. Increasing the residence time from 200 to 600 ms revealed an increase of the conversion from 20 to 80% in the 100 μm channels, whereas an almost constant conversion of approximately 90% was found independent of the residence time for the smaller channels. This was attributed to the higher surface area and thus catalyst mass of the smaller channel system, which results in a higher modified residence time (catalyst mass/flow rate). Conversion was also found to be dependent on the ratio of hydrogen to cyclohexene partial pressure showing maximum conversion at a value of 5. The increasing conversion measured for low values of the ratio was attributed to the conditioning, which is necessary for the catalyst to get ac-

Table 1
Surface area of coatings generated by various methods for the hydrogenation of cyclocyclohexene (according to Zhao et al. [24])

	Channel size (μm)			
	5	5	100	100
Coating method	Spin-coating	Dip-coating	Drop-coating	Dip-coating
SA (m^2) after coating	3.5	6.7	1.2	4.4

tive. Hydrogen was determined to be mandatory to achieve catalyst activity. The decreasing conversion derived for values of the ratio of hydrogen to cyclohexene partial pressure higher than 5 was explained by the low residence times of the corresponding experiments. An increasing hydrogen partial pressure was determined to be beneficial for the selectivity towards cyclohexane versus benzene. Cyclohexane selectivity was found to be close to 100% for the 100 μm channels in a temperature range between 50 and 130 °C and fluctuating around 90% in a temperature range between about 70 and 150 °C for the 5 μm channels. The decrease of conversion at elevated temperatures was attributed to the deactivation of the catalyst. Generally, lower space–time yields were found for the 5 μm channels, but due to their higher surface area the tendency to deactivation was smaller.

Zhao et al. [24] applied dip-coating, spin-coating and drop-coating to introduce silica as a porous layer into both channel systems of the reactor described by Surangalikar [23]. Pt was then introduced by both sputtering and wet impregnation. The resulting surface areas are summarised in Table 1 and revealed a surface area increase from 1000 to 15,000 times. At temperatures below 50 °C a conversion of 20% was found for cyclohexene hydrogenation which increased to 70% at 120 °C. Selectivity towards benzene was favoured at temperatures exceeding 150 °C. Similar to the findings of Surangalikar et al. [23] for unsupported catalyst, the conversion was found to be independent of the residence time. In contrast to the results of Surangalikar et al. [23], no effect of the ratio of hydrogen to cyclohexene partial pressure was given. The lifetime of the supported catalyst was 3.5 times higher compared to their unsupported counterparts.

Ouyang et al. [25] applied a silicon-chip-based microreactor for the Fischer–Tropsch synthesis at an iron catalyst. The chips had outer dimensions of 1 cm × 3 cm with channel dimensions of 5 or 100 μm width at 50–100 μm depth. The reaction was carried out at a H_2/CO ratio of 3, and flow rates of 0.4 scm^3/min between 200 and 250 °C. Conversions between 50 and 70% were found after 12 h activation of the catalyst under reaction conditions. Changing the H_2/CO ratio from 1 to 10, increased the conversion only from 50 to 56%.

Kusakabe et al. [26] developed a chip-like silicon-based process engineering device consisting of a preheater, a reactor and an integrated thermocouple mainly applying photolithographic techniques (see Fig. 7). The preheater was a single channel meander 95 mm long with channel dimensions of 200 μm width and 60 μm depth. The reactor was a 78 mm long meander of 500–600 μm width and 60 μm depth. The reactor was heated by an integrated Pt wire at the bottom. Top and bottom of the reactor were made of glass and attached to the silicon core by anodic bonding. Both sputtering of the silicon surface and wet impregnation of alumina precipitated by the sol–gel method were used to introduce Pt as active component. After activation in H_2 at 500 °C the catalyst was tested for benzene hydrogenation at temperatures between 100 and 150 °C, a flow rate of 1 cm^3/min and residence times from 100 to 600 ms. First-order kinetics were found for the reaction. The sputtered catalyst showed a 10 times lower reaction rate compared to its alumina-based counterpart.

Cao et al. [27] applied a micro-structured testing device consisting of a preheating unit, a mixer, a reactor and a quenching zone for the oxidative dehydrogenation of methanol to formaldehyde. This process is performed industrially in shallow beds with feed temperatures of 150 °C at residence times below 10 ms. The reaction is exothermic resulting in high temperatures of the product gas between 600 and 650 °C. Thus quenching is applied to prevent further oxidation of formaldehyde downstream the reactor. Oxidation and dehydrogenation of methanol takes place in approximately equal parts and CO, CO_2, formic acid and methyl formate are formed as by-products. Sixty to seventy percent conversion is achieved at selectivities up to 95%. The reactor was manufactured by photolithography and etching followed by the catalyst deposition and anodic bonding of the Pyrex glass cover. The channels

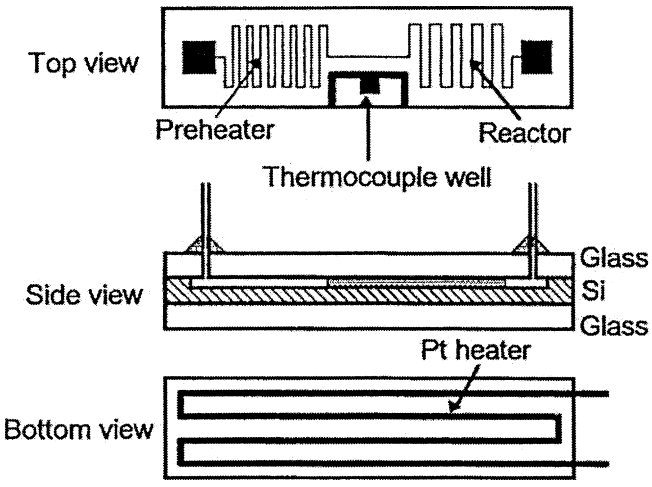

Fig. 7. Self-heating micro-reactor designed by Kusakabe et al. [26].

were 200 μm wide and 20 mm long. The channel depth was varied in two reactors between 70 and 130 μm. Ag was introduced as catalyst by sputtering. The reaction was carried out at residence times between 4 and 25 ms and temperatures between 430 and 530 °C at an inlet methanol concentration of 8.5 vol.%. Only CO_2 and formic acid were found as products, the carbon monoxide formation being successfully suppressed. Conversion (75–70%) and selectivities (10 and 90% to carbon dioxide and formic acid, respectively) were found to be independent of the oxygen inlet concentration. As methanol is known to react with the adsorbed oxygen, the zero-order dependency found for the oxygen concentration is in agreement with literature [28]. Conversion increased from 40 to 75% when increasing the temperature from 430 to 530 °C and below 420 °C rapid deactivation of the catalyst occurred. An activation energy of 14.3 kcal/mol was determined by an Arrhenius plot which is a smaller value compared to literature [28] and was attributed to product inhibition and thus different kinetics compared to other systems. Increasing the residence time from 4 to 24 ms increased the conversion from 57 to 73%, but hardly affected the selectivities. Generally, in the deeper channels higher conversion was achieved.

Pattekar et al. [29] made use of a silicon-chip for hydrogen production from methanol steam reforming. The reactor housing was made of stainless steel, electrically heated and sealed with graphite. The micro-channel was a long serpentine of 1000 μm width and 230 μm depth fabricated by photolithography and KOH etching. Cu catalyst was sputtered to a thickness of 33 nm onto the chip. Preliminary simulations revealed non-uniform temperature distribution in the reactor housing pointing at the importance of proper insulation especially in low power systems. At a feed composition of 76 mol% methanol in steam less than 7% conversion was achieved at 250 °C. Selectivity to carbon monoxide was higher than to carbon dioxide and 7 mol% hydrogen was found in the product.

Alepee et al. [30] investigated the dehydrogenation of methanol to formaldehyde at temperatures exceeding 600 °C applying a chip-like reactor. The main reason for applying micro-technology was the potential of achieving extremely fast heating and cooling and ultra-short residence times in the micro-channel system. An integrated heater/reactor/cooler was constructed therefore. The heater was composed of silicon micro-structured by KOH etching and capped with a SiN membrane. The channel was 7.4 mm long and had a trapezoidal cross-section 1.3 mm wide and 380 μm deep. Pt–Ta filaments were used to heat the bottom made of Pyrex. At a flow rate of 30 scm^3/min which corresponds to a residence time of 4 ms, a heating power as low as 1.7 W was able to increase the exit temperature of the test gas nitrogen up to 400 °C. The heat exchanger for cooling had a counter-flow design. Two types of fluid channel arrangements were chosen for this device, which are shown in Fig. 8. Either both fluids flow in two levels as done similarly in many other applications or in one level, separated by walls as thin as 50 μm. The 32 channels for the product gas, 50 or 100 μm wide, were manufactured out of a silicon chip by deep plasma etching. Pyrex glass was then anodically bonded from both sides to the chip for sealing. Into one of the glass layers the 33 cooling fluid channels, 100 or 200 μm wide, were etched by HF. All channels were approximately 300 μm deep and 20 mm long. Interestingly, it was found that the product gas outlet temperature decreased with increasing gas flow rate due to the diminishing dominance of heat conductivity effects. 500 scm^3 per minute nitrogen as cooling fluid was cooled from 500 to 54 °C in less than 1 ms by the cooler at heat transfer coefficients from 30 to 40 W/(m^2 K).

Schouten et al. [31] applied a silicon-based micro-reactor for the study of the intrinsic kinetics of the catalytic partial oxidation of methane. The reactor, manufactured by photolithography, was put into a housing made of aluminium. The single micro-channel was 30 mm long and had a cross-section of 500 μm × 500 μm. The channel was covered by a 1.9 μm thick silicon sheet, which allowed for a good thermal contact between the Rh catalyst beneath it and the five Pt heating wires and the 12 Pt temperature sensors on top of it. Isothermal conditions of gas inlet temperature and wall side and bottom temperature generated highest *Nu* numbers and therefore heat transfer coefficients which was favourable for

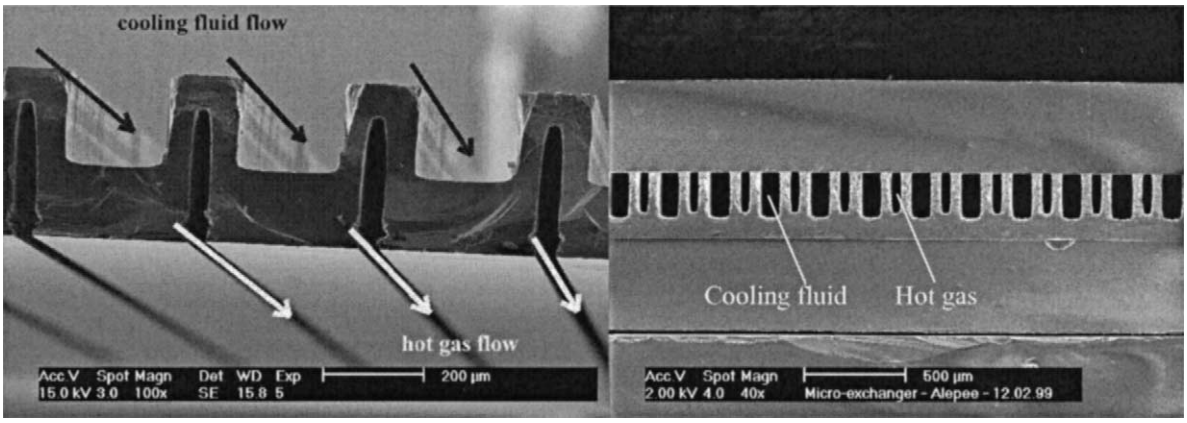

Fig. 8. Cross-sections of the double-sided (left) and one sided (right) silicon heat exchangers manufactured by Alepee et al. [30].

the minimisation of heat transfer limitations of the reaction under investigation.

McCreedy et al. [32] used a micro-reactor made of glass to perform the dehydration of ethanol. The micro-channels were introduced by photolithographic etching. A sulphated cobalt catalyst was dusted over the surface of the top cover block and immobilised this way. Additionally, a NiCr wire was immobilised in the reactor cover as a heating device. At a reaction temperature of 155 °C and a flow rate of 3 μl/min, which was adjusted using a syringe pump, only trace amounts of the ethanol feed remained unconverted and the main products were 68% ethylene, 16.% ethane and 15% methane. A further increase of the residence time by decreasing the flow rate via electro-osmotic pumping led to almost complete cracking of the ethanol to methane.

2.2. Chip-like micro-structured reactors carrying catalyst wires

Veser et al. [33] developed a single-channel reactor and applied it for the H_2/O_2 oxidation reaction. The reactor was designed as a modular and flexible tool for various high-temperature reactions. A stainless steel housing took up the silicon chips which were carrying the micro-channels. The wafers were coated with silicon oxide (400 nm thickness) and silicon nitride by low pressure chemical vapour deposition (LPCVD) alternatively. The chips were manufactured by photolithography and etching. The catalyst (for the application Pt) was introduced as a wire (150 μm thickness) which was heated resistively for igniting the reaction. The ignition of the reaction occurred at 100 °C and complete conversion was achieved at a stoichiometric ratio of the reacting species generating a thermal power of 72 W. Later, Veser [34] performed the reaction in a quartz glass micro-reactor with a diameter of 600 μm and 20 mm length. The ceramic housing of the reactor and the reactor itself were stable for temperatures exceeding 1100 °C. Again a Pt-wire of 150 μm diameter was used as a catalyst and electrically heated for start-up. Residence times down to 50 μs could be achieved. The fact that no homogeneous reactions, which are explosive, could be detected, demonstrates the possibility of separating homogeneous and heterogeneous reactions in micro-reactors due to the higher surface area to volume ratio of this reactor type. Increasing the flow rate led to increased temperatures of the gas exiting the reactor, which was attributed to reduced heat losses by conduction through the reactor walls. A thorough mechanistic investigation of the explosion limits revealed [34] that the first and the third explosion limit of the reaction are dependent on the reactor dimensions (see Fig. 9). The first explosion limit is reached, when the mean free path of the molecules gets smaller than the reactor dimensions, which was already the case at very low pressure (5 mbar). For the third explosion limit, which is responsible for explosions at ambient temperature, both the kinetic and the thermal explosion limit are increased. Veser states, that this is not achieved by thermal quenching but rather by “radical quenching” which means by kinetic effects. A core statement of the investigations is, that none of the three explosion limits can be crossed at ambient

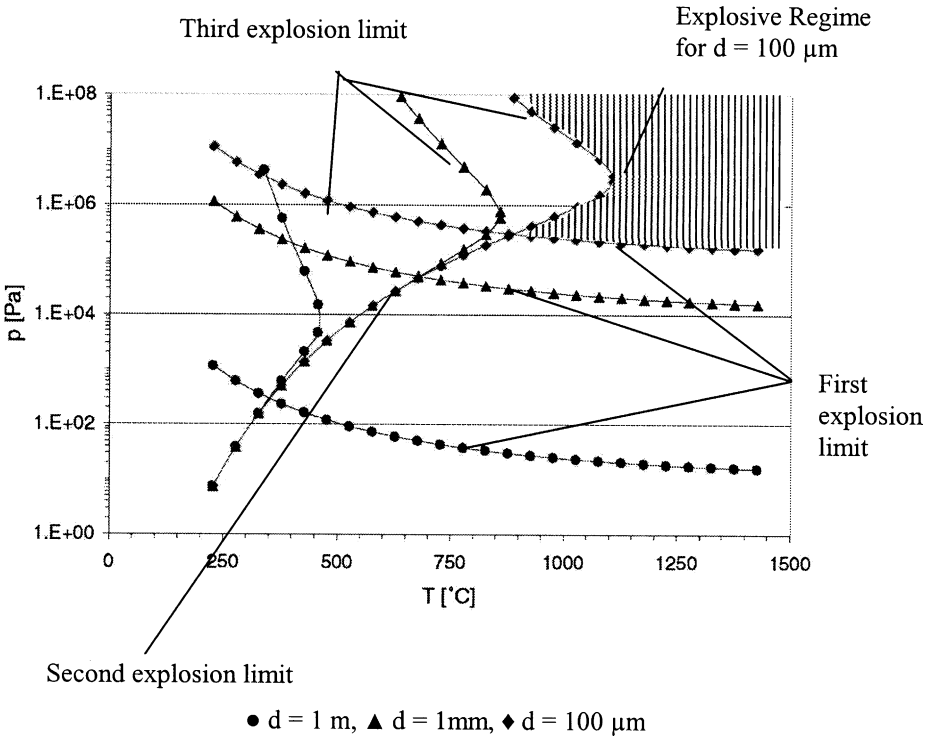

Fig. 9. Explosion limits for a stoichiometric H_2/O_2 mixture and different reactor diameters determined by Veser [34].

pressure in a 100 μm micro-channel, i.e. the reactor is "inherently" safe.

2.3. Micro-channel reactors with channel systems formed by the catalyst itself

Numerous investigations, which will be described below, were carried out on the ethylene oxide synthesis in various reactor types. The motivation for applying micro-technology in this reaction system is twofold. On one hand, the high overall heat of the reaction causes hot spots and heat removal problems in the industrial process, on the other hand only low concentrations of ethylene can be applied due to safety reasons. The application of micro-channels enhances the kinetic quenching of the reaction and thus enables operation in the explosive regime.

A micro-reactor was developed by Löwe et al. [35] for ethylene oxide synthesis. The reactor consisted of a two-piece housing which was sealed by graphite gaskets. The bottom piece contained two closely positioned square recesses made by die sinking, an electric discharge machining (EDM) process. In the recesses, stacks of platelets of micro-channels not connected and without seals, were inserted. The recesses were connected via a conduit that functioned as diffusion zone to guarantee mixing of the reactant gas before entering the reaction zone. The stacks of platelets were compressed when screwing the top and bottom housing pieces together. The first recess contained a stack of mixer platelets made by a combination of Laser-LIGA and electroforming. LIGA is the German acronym for LIthographie Galvanik Abformung, LIthographie corresponds to lithography, Galvanik to galvanization and Abformung stands for moulding. These platelets had curved micro-channels which made the fluid turn by 90°. In order to achieve equal individual flows in each curved channel different channel widths had to be used to compensate the differences in channel length. CFD simulation (FLUENT) was used to determine the mixer channel width and confirmed 99% mixing for all flow rates investigated. Two types of mirror-imaged platelet designs allowed in an alternating stack arrangement for creating gas multi-lamellae. The second recess contained originally a stack of silver reaction platelets made by LIGA and electroforming. In a later version, chemically etched silver and milled "Aluchrom" steel platelets were used [35]. Aluchrom is an aluminium containing stainless steel normally used as metallic support for car exhaust catalysts (Krupp VDM e-20Cr-5Al). Heating the aluchrom material to 1100 °C with oxygen creates an α-Al_2O_3 surface which is the only alumina species active for the ethylene reaction. The surface of the silver reaction channels was enhanced by means of oxidation. An increase in surface by a factor of 2–3 was reached based on chemisorption data. The silver catalyst was introduced by sputtering.

Kestenbaum et al. [36] used the micro-reactor manufactured at the Institut für Mikrotechnik Mainz GmbH (IMM) for the synthesis of ethylene oxide to demonstrate the safe operation of a highly explosive reaction mixture (explosion of ethylene oxide in air 2.6–100 vol.% at ambient pressure) in micro-channels. Contrary to the industrial process which applies alumina, supported pure silver was used as catalyst for the reaction in a stack of 14 platelets with 9 channels each 50 μm high and 500 μm wide (see Fig. 10). Maximum operating conditions of the reactor are 300 °C and 25 bar, heating was done externally. A reaction rate of 2.8×10^{-4} mol/(m^2 s) and an activation energy of 48 kJ/mol was found at a temperature of 280 °C, and a pressure of 5 bar. The rate values correspond well with literature values found for silver powder (1.7×10^{-4} mol/(m^2 s) from Tsybulya et al. [37] and

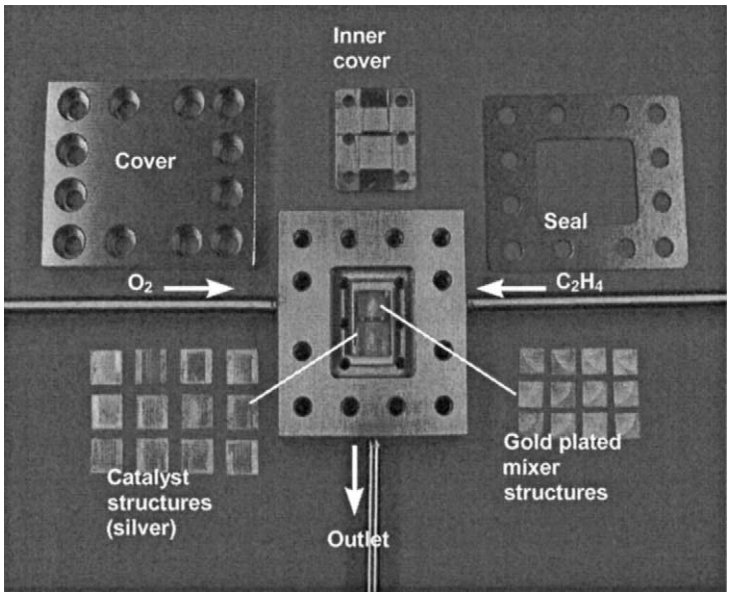

Fig. 10. Combined mixer/reactor for ethylene oxide synthesis developed by Löwe et al. [35]. *Source*: IMM.

45–62 kJ/mol from van Santen et al. [38]).The feed concentrations amounted to 6 mol% ethylene and 33 mol% oxygen. Conversions of up to 10% and ethylene oxide yields up to 5% were found at selectivities up to 50% the latter being inferior compared to the industrial process (90%) as no chloride species were added which are known to increase the selectivity. The space–time yields achieved were 0.18–0.67 t/(h m^3) which is superior compared to the industrial process. At a temperature of 290 °C and a pressure of 20 bar a rapid deactivation of the catalyst occurred. By XPS measurements carbon deposits were identified as the origin of the catalyst deactivation [39].

In a later publication, Kestenbaum et al. [39] used both 14 plates manufactured by Laser-LIGA, which were 300 μm thick carrying 50 μm deep channels and 21 etched silver-foils of 200 μm thickness and 80 μm channel depth in the reactor. Additionally, Aluchrom plates were used [35], which were 500 μm thick and carried sawed channels of some 90 μm depth. The silver layer of these plates was sputtered to a thickness of 1, 5 and 100 nm. First experiments were carried out with the etched plates. Increasing the ethylene concentration from 3.4 to 16.4 vol.% at a oxygen concentration of 50 vol.%, a pressure of 4 bar, a temperature of 290 °C and 235 ms residence time did hardly affect the selectivity. Additionally, the reaction rate followed a 0.53 reaction order for ethylene. On the other hand, increasing the oxygen concentration affected the selectivity and the reaction rate following a reaction order of 0.78. For the plates made by laser LIGA, the reaction rate increased from 4.5×10^{-5} mol/(m^2 s) at 239 °C to 1.5×10^4 mol/(m^2 s) at 308 °C which is related to a activation energy of 47 kJ/mol being very similar to the etched plates (49 kJ/mol) and corresponding to the literature [40,41]. At the same time, the selectivity towards ethylene oxide decreased in contrast to the etched plates from 64.1 to 45.1%. Increasing the pressure from 4 to 15 bar at a temperature of 290 °C and a constant residence time of 469 ms, increased the reaction rate by a factor of 3.5 and the selectivity towards ethylene oxide from 35 to 40%. The residence time had a strong effect on the reaction rates which deteriorated by an order of magnitude when the residence time was increased from 588 ms to 8 s. The selectivity was impaired as well. For the Aluchrom foils, a superior selectivity towards ethylene oxide was found for a silver layer thickness exceeding 1 nm, which even outperformed the etched plates. For the layer being merely 1 nm thick, the inferior values found were attributed to incomplete layer formation on the alumina surface. Further experiments were carried out at 290 °C, 5 bar and a residence time of 124 ms under addition of 35–100 ppm of dichloroethane. It acts as an inhibitor to the reaction, which has an Eley–Rideal mechanism oxygen being the adsorbed species. Therefore, the selectivity increased from 55 to 69%, however, the reaction rate deteriorated in parallel. Concentrations exceeding 300 ppm of dichloroethane lead to catalyst deactivation by silver-chloride formation. The selectivity of 69% is not much inferior to the industrial process, where promoters like Cs and Rh are added and values of 80% are achieved.

Hönicke et al. [58] also applied silver wafers for ethylene oxide synthesis. However, the reactor type was used for porous systems as well and is therefore discussed in Section 3.2.

Wörz et al. [42] proved the suitability of micro-reactors as measuring tools. The oxidative dehydrogenation of alcohols to the corresponding aldehydes was carried out industrially at 550 °C at Ag catalyst. The process was run isothermally under laboratory-scale conditions with a high selectivity of 90%. In an industrial reactor built later on for a similar process selectivities as low as 40% were found due to hot spot formation of up to 160 °C. Therefore a short shell and tube reactor was built for the process which achieved at a temperature of 450 °C at 50% conversion only hot spots of 60 °C at a selectivity of 85%. A micro-reactor was built made of Ag which showed at a reaction temperature of only 390 °C a higher conversion of 55% and a selectivity as high as 96% (see Fig. 11).

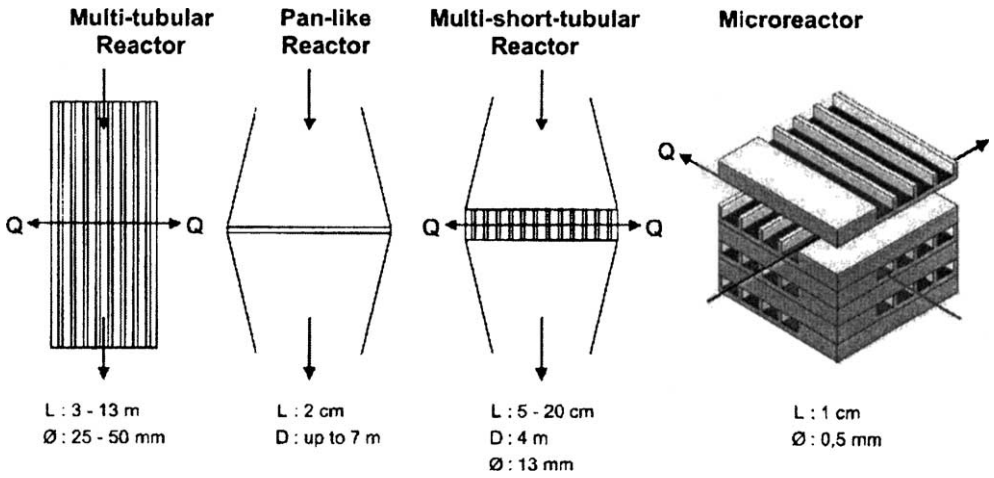

Fig. 11. Various reactor types applied for oxidative dehydrogenation from Wörz et al. [42].

Rebrov et al. [88] studied ammonia oxidation at a Pt monolith. However, other reactor types were applied as well and therefore the paper is discussed in Section 3.2.2.1.

3. Porous catalyst systems

3.1. Reactors containing catalyst particles

Ajmera et al. [43] introduced a micro-structured differential reactor, which takes up conventional catalyst particles. The intention for doing so was to use the reactor exclusively for testing of conventional catalyst particles rather than heading for a future micro-structured production device [44]. By a high parallelisation of the gas flow in an inlet region (channel dimensions 350 μm wide and 370 μm deep) 64 parallel channels were formed (see Fig. 12). These channels entered then one common catalyst bed which was 2.5 cm wide, 500 μm deep and 400 μm long. Due to the small length of the bed the pressure drop was minimised and a differential reactor was approached. After the bed 50 μm channels were placed as a frit for the catalyst particles. Finally, an area of very shallow channels 40 μm wide and 20–25 μm deep at a length of 2.2 mm fixed the pressure drop of the reactor which was only 7% higher for the reactor packed with catalyst compared to the empty reactor. Pressure drop amounted to 6 mbar at a flow rate of 100 scm^3/min. The reactor was made of a single crystal silicon by ion etching and covered with Pyrex glass by anodic bonding. Its maximum operation temperature was 550 °C. Sealing was done by an elastomer gasket which was pressed against the reactor by a metal cover which also took up the heating cartridges. The catalyst loading was done by vacuum. The reactor was applied for the oxidation of CO at Pt, Pd and Rh catalysts based on alumina particles of the size fraction 53–71 μm. 1 vol.% CO and 1 vol.% O_2 in He were fed at flow rates between 20 and 600 scm^3/min into the reactor revealing activation energies between 23 kcal/mol (Pt) and 30 kcal/mol (Pd) which agree well with literature [45–48]. Thus, the reactor may well be regarded as a novel and functional design of a differential reactor for catalyst testing and kinetics determination.

Ajmera et al. [49] investigated in a later paper the reactor performance for the same reaction system more in depth. The reactor was proven to work definitely under differential conditions. Pressure drop was ranging between 2 and 150 mbar which was regarded as negligible at a total pressure between 1 and 2.5 bar. By modelling an even velocity distribution was found for the catalyst bed at low *Re* numbers between 0.051 and 0.153. The residence time in the catalyst bed ranging around 0.6–8 ms was much longer than the time demand (0.02 ms) for gas particles to leave the recirculation zones having a diameter of 60 μm which corresponds to the size of the catalyst particles. However, for a residence time in the catalyst bed of 0.8 ms diffusion affected concentration profiles in the reactor and thus its performance. Due to the high heat conductivity of the silicon reactor housing isothermal conditions could be assumed. The reaction was performed at temperatures between 240 and 280 °C at a CO/O_2 ratio of 1 at alumina-based Pt, Pd and Rh catalysts. At CO/O_2 ratios higher than 0.08 the reaction was dominated by CO inhibition, CO desorption being the rate limiting step. A reaction order for p_{CO} of −0.79 and for p_{O_2} of 1–1.5 was found well

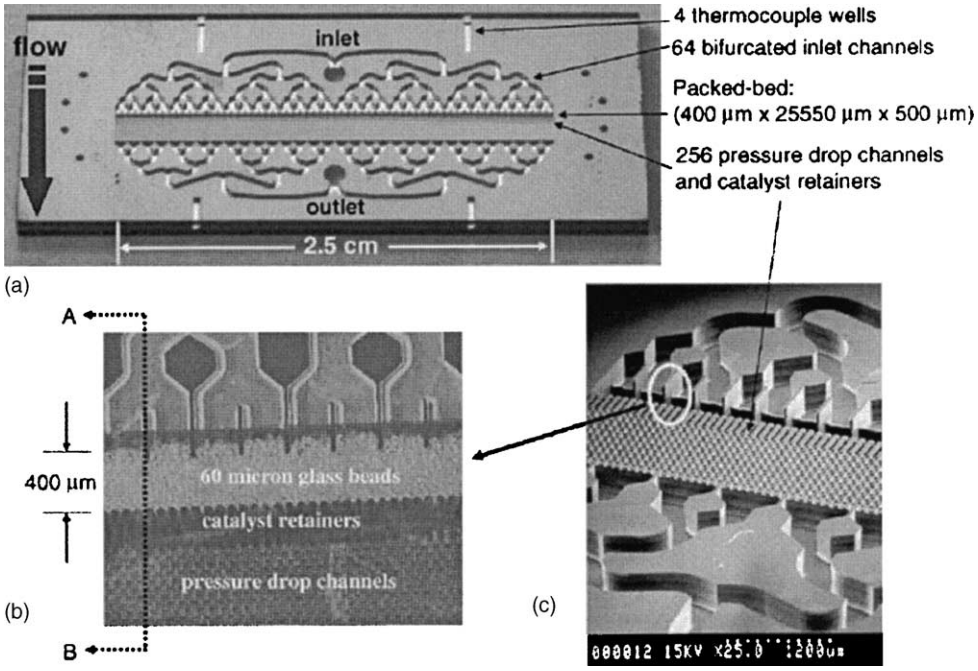

Fig. 12. (a) The silicon cross-flow reactor chip; (b) the micro-reactor packed with 60 μm glass beads; (c) scanning electron micrograph of the reactor designed and manufactured by Ajmera et al. [44].

in line with literature [50]. Calculation of the Weisz modulus revealed a value of 0.01 which is well below the lower boundary for internal diffusion limitation. Applying the Anderson criterion temperature gradient formation within the catalyst particles could be excluded (see Section 1). Thus, due to their small particle size internal gradients are not to be expected in the catalyst particles. Temperature gradients of less than 0.01 K were found for the reactor. Therefore, no internal or external mass and temperature gradients are to be expected for the reactor and the reaction system under investigation. Further simulation work was performed to quantify the effect of axial diffusion. It could be demonstrated for a total flow rate of 97 scm^3/min at a pressure of 2.5 bar and a feed concentration of CO and O_2 of 1 vol.% each, that the reactor performance got closer to a continuous stirred tank reactor (CSTR) behaviour, the lower the *Pe* number was. Impressingly, at a total conversion of 24.4% the gas composition of the feed already related to a conversion of as much as 18.4% at the reactor inlet due to diffusion effects. The mass transfer from the bulk to the catalyst surface was found not to be rate limiting as $Pe_{particle} \approx 1$.

Another single silicon crystal reactor of 10 mm × 40 mm × 1 mm size was developed by Ajmera et al. [51] for the synthesis of phosgene to demonstrate the feasibility of a safe and on-demand production of hazardous chemicals in microreactors. The manufacturing techniques applied were photolithography and silicon etching for the outer geometry and inductive coupled plasma etching for the channel systems. The reaction channel was 20 mm long, 625 μm wide and 300 μm deep with a total volume of 375 mm^3. The inlet and outlet of the reactor was formed by 25 μm wide channels and the channels were coated with a 0.5 μm thick SiO_2 layer as protection against chlorine. Cover and sealing of the reactor was similar to the former designs, four additional channels were incorporated in order to take up thermocouples. Again the catalyst loading (1.3 mg) was done by vacuum. Feed gas mixing was performed by a T-junction. The catalyst applied was activated carbon of a particle size of 53–73 μm and a specific surface area of 850 m^2/g. 4.5 scm^3/min feed composed of 33 vol.% CO and 66 vol.% Cl_2 were fed into the reactor at an inlet pressure of 1.35–1.40 bar and a temperature up to 220 °C. A pressure drop of 0.35 bar was observed. Complete conversion was found for reaction temperatures exceeding 175 °C which corresponds to a yearly production capacity of 3.5 kg for the reactor. The reactor has a potential for further improvement applying higher temperatures and flow rates. No catalyst deactivation was observed after 6–10 h TOS and no by-products were detected. As for the first reactor [49], isothermal conditions were achieved due to the big mass of the housing. Again, the useful criteria [49] for mass and heat transfer effects were applied revealing that plug flow has to be assumed (Pe = 180–360) and that less than 5% deviation of the data determined are to be expected due to temperature gradients. The Weisz-modulus amounts to 0.1–0.5 indicating minimal intra-particle mass-transfer limitations. External mass-transfer limitations could be regarded as negligible as well ($Pe_{particle} \approx 1$). An experimental activation energy of 7.6 kcal/mol was found for the reaction well in line with literature [52].

Allen et al. [53] presented reactors for hydrogen generation by ammonia cracking and for the oxidative coupling of methane. The micro-channels applied were manufactured by conventional milling (for channels up to 2.5 mm deep and 250 mm wide) and by laser ablation for channels being 1 mm deep and 300 μm wide. The reactor used for ammonia cracking had a diameter of 6.3 mm and a length of 50 mm. It took up a micro-structured plate with 20 channels 250 μm wide, 1.5 mm deep and 50 mm long. At flow rates of 70–250 scm^3/min full conversion was achieved at residence times as low as 6 ms. Oxidative coupling of methane to ethylene was performed revealing conversion levels of less than 1%.

Irving et al. [54] presented a micro-reactor filled with catalyst particles which is able to reform gasoline, diesel, methanol and natural gas by steam reforming at temperatures up to 800 °C. Not only this reactor, but also fuel mixing, heat exchanging, evaporation, and preheating were done in an integrated device made both of stainless steel and ceramics. Gasoline steam reforming at flow rates of 0.1 g/min gasoline feed was done at high S/C ratios between 5 and 8 revealing 70 vol.% hydrogen in the off-gas without methane formation and catalyst deactivation. Sulphur in the gasoline lead to H_2S formation. Applying lower S/C ratios for iso-octane steam reforming lead to methane concentrations as high as 5 vol.% in the reformate. As much as 3.75 g catalyst was used to achieve 100% conversion and methane concentrations well below 5 vol.% for a mixture of 60 vol.% iso-octane, 20 vol.% toluene and 20 vol.% dodecane at a feed rate of 0.3 g/min, and a S/C ratio of 4.

3.2. Reactors containing wash-coats or other coated catalyst

3.2.1. Stack-like reactors with external heating

Wießmeier [55] developed a stacked plate reactor and applied it for the partial hydrogenation of cyclododecatrien (CDT) to cyclododecene (CDE) at Pd catalyst. The ideas standing behind of it was the application of regular pore systems by anodic oxidation in order to achieve an improved residence time distribution in the reactor, which is beneficial for the consecutive reaction network [56]. Another aim was the elimination of axial temperature profiles by the improved heat conductivity of metal compared to ceramic monoliths and the elimination of radial concentration gradients due to the smaller channel size of micro-channels compared to the meso-channels of the ceramic monoliths [57]. A 103-fold surface area increase of the micro-structured aluminium plates used was achieved by anodic oxidation, which generates a regular pore structure of the alumina. The size of the pores generated this way ranged between 10 and 200 nm at a pore density of about 10^{14} pores/m^2. The impregnation of the alumina layers with Pd catalyst was done by a procedure

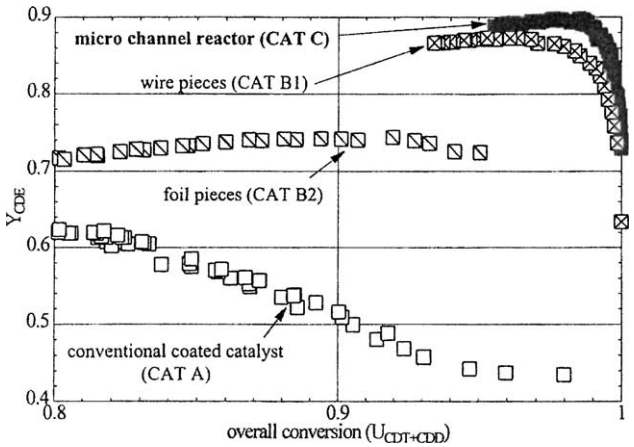

Fig. 13. CDE yield vs. overall conversion of CDT for different catalysts and fixed-bed structures determined by Wießmeier [55].

including an evacuation step and a liquid phase impregnation which generated Pd anchoring to the surface via oxygen bridges [57]. This was followed by a calcination and reduction procedure to gain the catalyst. The measurements were carried out close to ambient pressure at low partial pressures of CDT and H_2 (110 and 330 Pa). To check the time-on-stream behaviour of the catalyst, anodically oxidised and impregnated aluminium wires, which were cut into pieces, were used. At complete conversion of CDT selectivities towards CDE were ranging around 80%, the other products being cyclododecene (CDD) as intermediate and cyclododecane (CDA) as consecutive product of CDE. Complete reactivation of the catalyst was possible by oxidation in air. As a next step, two types of cut aluminium wires were tested having a different thickness of the oxidised alumina layer (15 and 80 μm) and thus a higher length of the pores. At conversion levels exceeding 90% an inferior performance of the longer pores was found which was attributed to the kinetically controlled formation of CDE, which has more time to react to the consecutive CDA in the longer pores at high conversion levels, where mass transport limitations of CDT and CDD occur. Finally, a comparison of a commercial Pd catalyst (average particle size 240 μm) and anodically oxidised and cut pieces of aluminium foils (pore depth 37 μm) and wires (pore depth 37 μm) with micro-structured aluminium wafers (same pore depth) was performed. It revealed that the commercial catalyst had a maximum CDE yield of 62% at a conversion of 80%, whereas the ordered pores of the foils yielded 74% CDE at 90% conversion. Decreasing the dead volume in the packing by introduction of wires lead to an even better yield of 86% at 95% conversion. The complete removal of dead volume in the micro-channels finally yielded 90% CDE at 98% conversion, which is an impressive prove of the beneficial effect of directed gas flow in micro-structured catalyst systems (see Fig. 13).

Kursawe et al. [58] developed a modular reactor made of all stainless steel parts which was designed for maximum operation conditions of 50 bar and 480 °C and was applied for benzene hydrogenation and ethylene oxide synthesis (see below). Easy handling and fast exchange of catalyst platelets were some of the design criteria (see Fig. 14). Sealing was done by an outer shell via copper gaskets. Two diffusers acted as gas-distribution devices and were placed in front of and behind the reactor core taking up the stack of three micro-structured platelets. All three parts were put into the shell subsequently. The micro-structured platelets were fabricated by means of thin-wire μEDM in aluminium or aluminium alloys such as Dural, $AlMg_3$ and AlMg 4.5 Mn at the Forschungszentrum Karlsruhe. Each platelet 50 mm long had 14 parallel micro-channels 300 μm wide and 700 μm deep. The surface of the micro-channels was rough which was regarded as beneficial for the coating techniques applied subsequently (see below). For the application of benzene dehydrogenation anodic oxidation was applied to achieve a porous alumina layer. Zn/Ru was introduced by impregnation afterwards. The catalyst prepared this way achieved conversions of 30% and selectivities towards cyclohexene up to 50% at a low benzene partial pressure of 110 Pa. For ethylene oxide synthesis both anodic oxidation and the sol–gel method were used to get a porous alumina carrier. The active compound, silver, was introduced by sputtering in both cases. A stepwise increase of the silver layer thickness from 100 to 400 nm revealed constant catalyst selectivity but an increase of conversion from 25 to 50% at 250 °C and 0.3 bar and a residence time of 95 ms. The catalyst stemming from the sol–gel route, which was based mostly on γ-alumina was much less active and showed merely 4–6% conversion at 3 bar and 230 °C at a residence time of 1.5 s.

A reactor of different dimensions, but similar geometry developed by the Forschungszentrum Karlsruhe (FZK) was applied by Kursawe et al. [59] for the ethylene oxide synthesis. Channel dimensions were 200 μm × 200 μm at a length of 50 mm. In fact, three different reactors were tested the main difference being the catalyst preparation procedure. The performance of silver wafers (reactor 1), $AlMg_3$ wafers coated with 200 nm silver (reactor 2) and anodically oxidised alumina covered with an 800 nm sputtered silver layer (reactor 3) was compared. Experiments were carried out at a relatively low pressure of 3 bar compared to the industrial process by feeding 20% ethylene in oxygen into the reactors. A maximum selectivity of up to 60% was found for all reactor types at conversions increasing from 5% (reactor 1) over 41% (reactor 2) to 45–70% (reactor 3). Optimum residence times were in the range of one to few seconds. An important comparison to conventional reactors was performed here: hackled silver foils, an aluminium wire coated by PVD with silver and anodically oxidised aluminium foils coated with silver by sputtering were tested in parallel at the same ratio of flow rate to surface area like it was set for the micro-reactors. These experiments revealed similar selectivities, but lower degrees of conversion and lower yields for the conventional reactors compared to their micro-structured counterparts. Fig. 15 (left) shows conversion, yields and selectivity for the three couples of reactors. Fig. 15 (right)

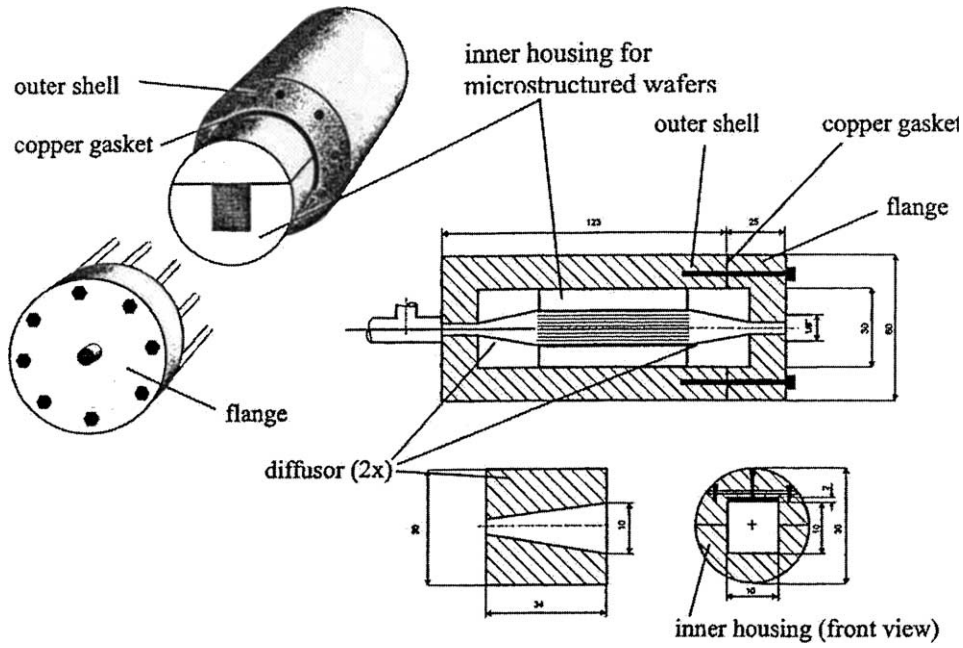

Fig. 14. Modular micro-channel reactor designed by Kursawe et al. [58].

shows a plot of the selectivity versus conversion of the micro-structured reactor 3 and the corresponding fixed-bed reactor. At considerably higher residence times, the fixed-bed reactor showed not only lower conversion, but also lower selectivity towards ethylene oxide.

Later on, the same authors [60] compared the performance of sputtered and industrial corundum supported catalysts for ethylene oxide synthesis in different micro-reactors. Industrial catalysts applied for ethylene oxide synthesis have a low surface area of 4 m^2/g because it is known, that higher surface areas of the alumina propagate the isomerisation of ethylene oxide and its combustion [61]. They are doped with various promoters like Cs, Ba, Re and K. Inhibitors like 1,2-$C_2H_4Cl_2$ and NO in ppm amounts and up to 10% of CO_2 are added to the feed in the industrial process. The rate determining step is the reaction of the adsorbed oxygen with ethylene. The industrial process is run at ethylene concentrations up to 40% and O_2 concentrations up to 8%. The catalysts applied here were both Ag directly introduced on the $AlMg_3$ carrier by sputtering a 1.2 μm thick layer and Ag impregnated onto a 1 μm thick α-alumina layer generated via the sol–gel route. Both the home-made reactor mentioned above [58] and the reactor developed by FZK [59] were applied for the tests again. It was made use of the higher number of channels (858) of the FZK reactor to achieve similar conversion levels of the less active sputtered catalyst compared to its alumina-based counterpart. Firstly, the home-made reactor was used to increase the thickness of the sputtered layer

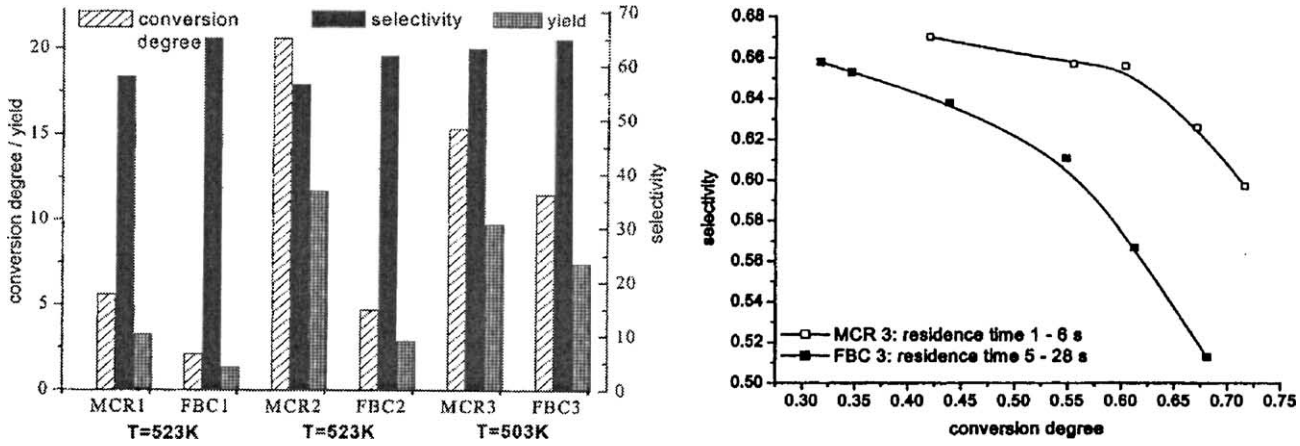

Fig. 15. Left: Comparison of fixed-bed (FB) and micro-reactors (MCR) for ethylene oxide synthesis carrying catalyst of types 1–3. An identical flow rate per surface area of 3.17 dm^3/m^2 was adjusted. Temperature 230 °C, pressure 3 bar, 20 vol.% ethylene in oxygen. Right: Selectivity vs. conversion of FCB 3 and MCR 3. Temperature 230 °C, pressure 3 bar, 20 vol.% ethylene in oxygen as determined by Kursawe et al. [59].

stepwise (50 nm) followed by a 24–48 h activation period necessary to achieve the full activity of the catalyst. Dense silver particles were found after this procedure leaving part of the aluminium surface open. At a 50 nm layer thickness a low conversion of about 5% was found at a relatively high selectivity of 55% which quickly degraded. Increasing the thickness of the sputtered layer up to 1.4 μm improved the conversion up to 42% at lower selectivities around 50%. The residence time of these experiments ranged from 0.23 to 2 s. Secondly, the effect of ethylene and O_2 concentration on conversion and selectivity was investigated for the corundum-based catalyst in the home-made reactor. Increasing the ethylene concentration from 3.5 to 60% led to a decrease of conversion from 21 to 1.5%, whereas selectivity was only slightly affected from 51.7 to 54.6%. Increasing the O_2 concentration from 11.6 to 80% led to an increase of conversion from 8.8 to 21.2%, whereas selectivity increased from 41 to 50.6%. A comparison of the alumina-based catalyst with the sputtered counterpart the latter determined in the reactor manufactured by FZK revealed an approximately 10% higher selectivity towards ethylene oxide independent of the conversion level for the sputtered catalyst at 3 bar and a temperature of 230 °C.

Födisch et al. [81] of the same group found a selectivity as high as 68% at 25% conversion at a temperature of 230 °C and a pressure of 3 bar for a Cs promoted Ag catalyst which was a superior performance compared to an industrial catalyst. The Ag was sputtered onto the 20 μm thick alumina layer generated by anodic oxidation and the promoter was introduced by wet impregnation prior to sputtering.

Kursawe et al. [62] applied a reactor of the same design for the hydrogenation of benzene to cyclohexene. Fifteen plates, 50 mm long were used. The catalytic active layer was prepared by anodic oxidation of the aluminium wafers and wet impregnation of Ru as catalyst. At a pressure of 1.1 bar and a temperature of 80 °C a residence time of 0.53 s was adjusted at a benzene partial pressure of 11 mbar and a methanol partial pressure of 44 mbar, the latter being added as reaction modifier. At a conversion of 13%, a selectivity of 20% towards cyclohexene was observed, which increased with time-on-stream. However, second-order deactivation of the catalyst was observed at the same time. Conversion decreased from 17 to 5% with increasing methanol partial pressure and selectivity towards cyclohexene up to 38% after 10 h TOS. Addition of Zn promoter had no substantial effect on conversion but increased the cyclohexene selectivity up to 32% after 15 h TOS. The same type of wafers was applied for ethylene oxide synthesis at 3 bar and a temperature of 250 °C. Silver was deposed on the aluminium by PVD. At an ethylene inlet concentration of 4%, the selectivity towards ethylene oxide of 45% was determined independent of the conversion ranging between 40 and 66%. Ethylene oxide yields between 19 and 29% were found and an adiabatic temperature rise of 630 K at 66% conversion. At a higher ethylene inlet concentration of 20%, an improved selectivity increased to 45% again independent of the conversion ranging between 15 and 39%. Ethylene oxide yields between 7.5 and 20% were found and the adiabatic temperature rise was as high as 1500 K at 39% conversion.

The reactor was then applied for cycloalkene formation by Dietzsch et al. [63]. Partial hydrogenation reactions were carried out at Pd and Ru/Zn catalysts to demonstrate the superior performance of micro-reactors in the highly selective production of intermediate products. Alumina layers of 18–24 μm thickness were formed on aluminium wafers by anodic oxidation and again channels of 200 μm × 200 μm size were used. After each catalytic run, a reactivation of the catalysts was performed by burning of the carbonaceous deposits at 420 °C and subsequent hydrogen treatment at 150 °C. Complete conversion was achieved at residence times around 100 ms at a temperature of 150 °C and a pressure of 1.1 bar for *c*,*t*,*t*-1,5,9-cyclododecatriene (CDT) and 1,5-cyclooctadiene (COD) at Pd catalysts. No deactivation of the catalyst was found for COD, but a 10% drop of conversion for CDT. The hydrogenation of COD was studied in more detail revealing an increase of conversion from 80 to 100% at decreasing selectivity towards cyclooctene from 99.5 to 88% by increasing the ratio of hydrogen to COD from 0.75 to 2. The yield of the product, cyclooctene, could be raised from 83 to 98% by adding 400 ppm CO to the feed. At lower residence times of 35 ms, conversion dropped to 75% compared to 99.5% at 115 ms. Rising the partial pressures of hydrogen and COD from 110 Pa by a factor of 10 impaired the cyclooctene yield, which decreased from 98 to 84% but increased the productivity by a factor of 10 as well. For benzene, hydrogenation at Ru/Zn catalysts a severe deactivation took place after 14 h TOS at a temperature of 180 °C and a residence time of 235 ms, which was higher compared to the reactions discussed above. Conversion dropped from 90 to 10% at increasing selectivity towards cyclohexene up to 36%, which reduced the formation of cyclohexane, which was exclusively formed at the beginning.

Kah et al. [64] used the reactor for the partial oxidation of 1-butene to maleic anhydride at $V_2O_5/P_2O_5/TiO_2$ catalysts, a highly exothermic reaction (−1300 kJ/mol) which is run in the industrial process at low hydrocarbon concentrations of 1.5% and selectivities around 60%. Going to higher concentrations leads to hot spot formation and thermal run-away of the reactors. Al and $AlMg_3$ wafers were treated by anodic oxidation to achieve Al_2O_3 layers of 40 μm thickness. Different reactors with 15, 25 and 37 wafers of various channel width (80, 200 and 400 μm) were tested and compared to a fixed-bed reactor containing Al-wires of identical geometric surface area which were anodically oxidised and impregnated in the same way like the wafers. Comparing the performance of the fixed-bed reactor with the micro-structured reactors at low hydrocarbon concentration (0.4%), the same degree of conversion was achieved at much lower residence times (750 ms compared to 25 ms) resulting in up to five times higher space–time yields in the micro-structured reactor. However, selectivities were lower in the micro-channel reactor and generally lower compared to the industrial pro-

cess. The reaction was run safely at 1-butene concentrations in the explosive regime (5%), atmospheric pressure and a temperature of 400 °C. Only small temperature rises at the outlet of up to 10 °C were measured due to conductive heat transfer from the micro-structured wafers. Conversions up to 95% were achieved at selectivities similar to the values found for low hydrocarbon concentrations.

Pfeifer et al. [65] used an externally heated reactor for methanol steam reforming. The focus of this work was to develop catalysts and a micro-structured reformer for a 200 W fuel cell for small-scale mobile applications. Four plates carrying 80 channels 64 mm long and 100 μm wide and deep could be introduced into the reactor. Various catalysts were tested for their performance:

- CuO/ZnO (1:1) catalyst based on nanoparticles sintered at 450 °C for 5 h; BET surface area of the plates coated with this catalyst amounted to 9.3 m^2/g and a maximum of the mesopore distribution was found at 100 nm; the layers had an average thickness of 20 μm ± 10 μm at the channel bottom.
- CuO/ZnO (1:1) catalyst based on nanoparticles sintered at 550 °C
- CuO/ZnO/TiO_2 (39:39:22) catalyst based on nanoparticles sintered at 450 °C for 5 h.
- Pd/ZnO (1:99) catalyst based on ZnO nanoparticles which were impregnated with Pd-acetate, calcined at 450 °C and reduced at 500 °C for 5 h in 1 vol.% H_2 for 5 h.
- CuO/ZnO/TiO_2 (25:2:3) catalyst based on TiO_2 nanoparticles which were impregnated with Cu/Zn $(NO_3)_2$ and calcined at 550 °C for 5 h.

The nanoparticles had an average particle size (APS) between 20 and 60 nm and BET-surface areas ranging between 17 and 58 m^2/g, which decreased with increasing calcination temperature reaching values below 1 m^2/g at 750 °C. To verify the absence of diffusion limitations, the modified residence time was varied, which was discussed at the introduction of this paper already. For the standard experiments, a 1:2 molar methanol/water mixture was fed together with 60 vol.% helium at a pressure of 3 bar into the reactor with a hydrodynamic residence time of 250 ms. The reaction started at 230 °C and showed maximum carbon dioxide yields between 235 and 250 °C. The best carbon dioxide yields were found for the catalyst based on TiO_2 impregnated with CuO/ZnO. The Pd catalyst showed a higher activity and less deactivation at 285 °C, but also higher CO yields which exceeded the thermodynamic equilibrium for the water-gas-shift reaction. It was assumed that the Pd could not form alloys with the Zn and therefore propagated CO formation in its elementary form. The activity of the Pd catalyst could be stabilised by small amounts of oxygen added to the feed, which was attributed to a removal of the coke. For the impregnated TiO_2 catalyst CO yields exceeding the water-gas-shift equilibrium were found as well. Merely the CuO/ZnO catalysts showed low carbon monoxide conversion at or (for the pre-reduced sample) even below the water-gas-shift equilibrium, however, at low degrees of conversion. Copper in its oxidised form is known to show low CO-formation. However, under the reducing atmosphere the copper is likely to be in a mixed oxidation state which propagates carbon monoxide formation.

Later on, Pfeifer et al. [66] focused on Pd/PdZn/ZnO systems for methanol steam reforming. The formation of a Pd/Zn alloy at higher reduction temperatures was identified as the crucial step. Additionally, it was found that pre-impregnation of the ZnO particles with palladium before the coating procedure decreased the carbon monoxide selectivity by a factor of 3. However, the CO concentration still exceeded the equilibrium of the water-gas-shift reaction, which was not the case for a pelletised catalyst of the same type and therefore attributed to an interaction between the metal of the micro-structured carrier and the catalyst. Chemisorption measurements with hydrogen and CO revealed a poor dispersion of less than 10% for PdZn. Temperature Programmed Oxidation (TPO) measurements revealed a slow destruction of the PdZn alloy, in air at temperatures exceeding 200 °C and therefore diffusion of oxygen into the reactor was seen as a possible reason for the increased CO selectivity. However, copper-based catalysts are known to be much more sensitive to oxidation. Two reformers having housings made of both stainless steel and copper were set up for a hydrogen output sufficient for a 200 W fuel cell. At 310 °C and a pressure of 1.25 bar, 80% methanol conversion was achieved. The S/C ratio of 1.9 led to a carbon monoxide concentration of 0.5 vol.% in the product. Instationary measurements were carried out at the reformer revealing equilibration times around 30 s in the heating zone of the reactor and 200 s at the maximum distance from the heating zone when a temperature step of 20 °C was made. The reaction followed the temperature immediately. Equilibration of the reactor took 140 s when switching from bypass to reactor on stream. Dimethyl ether was found as a by-product in amounts up to several hundred ppm exclusively at the stainless steel reformer.

Wunsch et al. [67] demonstrated the application of microreactors as a tool for hydrocarbon removal purposes in laboratories. As an example, methane was removed by combustion in an externally heated micro-reactor. The reactor contained 820 channels in total which were 200 mm long at a hydraulic diameter of 120 μm. Platinum was introduced as catalyst by wet impregnation on the micro-structured aluminium plates, which were anodically oxidised to an alumina layer thickness of 20 μm at 41 nm average pore diameter. A crystallite size of 2.6 nm was measured by chemisorption for the Pt particles. The catalyst was activated in a hydrogen/argon mixture at 500 °C for 5 h. Experiments were carried out at pressures between 1.1 and 5.5 bar and hydrodynamic residence times between 200 and 800 ms. The feed mixture was composed of 20 vol.% oxygen in nitrogen containing 120 ppm methane. The reaction started at 250 °C. At a temperature of 520 °C and a Pt loading of 0.4 wt.%, 85% methane conversion was determined at a pressure of

1 bar and almost complete conversion (99.8%) at a pressure of 5 bar. No selectivity towards carbon monoxide was detected. Increasing the methane concentration in the feed to 650 ppm lead to a conversion decrease from 99.8 to 95% at a temperature of 520 °C and a pressure of 4 bar. Addition of water, which is present in most practical applications, at a 20 vol.% level decreased the conversion by 9%. Increasing the Pt metal loading from 0.02 to 0.4 wt.% increased the conversion from 4 to 92% at a pressure of 2 bar and a temperature of 520 °C. Further addition of Pt up to 1.6 wt.% increased conversion well above 98%. Optimum reaction conditions were thus identified to be a temperature exceeding 500 °C, a pressure higher than 2 bar and a Pt metal loading above 1.4 wt.%.

Reuse et al. [68] applied a home-made reactor carrying micro-structured plates for the methanol steam reforming at a copper based low temperature water-gas-shift catalyst. The reactor took up 20 plates made of FeCrAl alloy of a size of 20 mm × 20 mm × 0.2 mm. The channel size was 200 μm × 100 μm. The catalyst was conditioned by oxygen and hydrogen treatment. Kinetic measurements were carried out. Kinetic expressions were determined for both a tubular fixed-bed reactor containing 30 mg catalyst particles and the micro-reactor coated with the catalyst particles. The experiments were carried out at a pressure of 1.5 bar and a flow rate of 80–270 cm^3/min. At a temperature of 200 °C no deactivation of the catalyst was observed. As the rate of reaction was found to show linear dependency of the residence time, differential conditions were assumed for the measurements. Because of the high activation energy of 56 kJ/mol determined mass transport limitations were excluded. Power law kinetics of the following form were determined for methanol steam reforming:

$$-R_{CH_3OH} = k_0 e^{-E_a/RT} p^m_{CH_3OH} p^n_{H_2O} p^o_{H_2} \quad (9)$$

Similar values were found for the reaction orders in both systems at lower rate of reaction for the micro-channels as shown in Table 2. The inhibition by hydrogen was obviously more pronounced in the micro-channels. Without hydrogen in the feed the reaction rate was on an average 34% higher for the coated catalysts.

Rebrov et al. [69] synthesised ZSM-5 zeolite in micro-channels and performed the selective catalytic reduction of NO with ammonia on the zeolite. The main focus of this work was to assess the performance benefits of zeolitic coatings in micro-channels compared to conventional zeolite-based pellets and powders. The reaction takes place at a temperature below 400 °C and a selectivity towards nitrogen close to 100%. Ce-ZSM-5 is commonly applied as catalyst for the reaction. The coatings were performed in a sandwich of two plates of 1 cm length and width at a thickness of 2 mm. The seven channels were accordingly 1 cm long and had a diameter of 500 μm. The catalytic tests were performed in a micro-reactor taking up 20 removable plates of 8 mm length and 4.3 mm width. The plates were positioned with a distance of 280 μm from each other in the housing of the reactor. A zeolitic film of one crystal thickness was formed under the optimum synthesis conditions which were determined to a water/silicon ratio of 130 and a template/aluminium ratio of 2 at a temperature of 130 °C after 35 h on a flat plate. The Si/Al ratio of the zeolite, which lowers the crystal size as well when decreased, was optimised to a value as low as 28. To get a uniform distribution of the zeolite in the micro-channels, a two-step procedure was developed, including a nucleation growth at high temperature at the horizontally oriented plates followed by a growth period at the vertically oriented plates, which was performed at lower temperature and water to silicon ratio. The crystals were oriented parallel to the surface of the carrier. Nitrogen adsorption revealed the typical micro-pore distribution of ZSM-5 for the coating. Thermal cycling of the coated plates revealed a good binding of the coating and no migration of Cr from the passive metal layer into the zeolite. By XRD analysis, high crystallinities of the coatings exceeding 90% were found. The crystallisation took place on the whole platelet and the crystal layer had to be removed mechanically from the flat surface. The zeolite coatings were then exchanged with cerium to get an active catalyst. The testing of the catalyst in NO reduction revealed 100% selectivity to nitrogen formation and a conversion maximum at 350 °C. At higher temperatures, the competing ammonia oxidation got more and more dominant. A feed composition of 683 ppm NO, 800 ppm NH_3 and 5 vol.% O_2 was adjusted. At a temperature of 350 °C and a flow rate of 66 cm^3/min, 30% NO conversion could be achieved.

Input from the earlier work [69] was used by Rebrov et al. [70] for further optimisation on 1 cm^2 sized 2 mm thick plates carrying channels of 200 μm diameter. The optimum template/aluminium ratio could be maintained, however, the water/silicon ratio had to be lowered to 108 at a silicon to aluminium ratio of 28 and a slightly lower temperature of 135 °C. Bigger crystals (6 μm × 4 μm × 3 μm) were formed this way compared to the former method. For the synthesis rather diffusion limitation occurred than crystal formation limitation. Stirring resulted in more uniform, but thinner coatings. Pre-treatment of the stainless steel support with dilute template solution improved the crystal growth in the upper part of the channels. Finally, 1.5 μm × 1 μm × 2 μm big crystals with a very narrow size distribution (within 0.2 μm) [31] were achieved by firstly putting the platelets in a concentrated synthesis mixture at a water/silicon ratio of 24 for 2 h at 160 °C. This resulted in 0.3 μm long crystals

Table 2
Reaction order of fixed-bed and micro-reactor determined by Reuse et al. [68] for methanol steam reforming

	Fixed bed	Micro-channels
m	0.70 ± 0.02	0.70 ± 0.1
n	0.1 ± 0.04	0.0 ± 0.1
o	−0.1 ± 0.1	−0.2 ± 0.1
k	$7.8 \times 10^{-5} \pm 0.9 \times 10^{-5}$	$4.8 \times 10^{-5} \pm 0.6 \times 10^{-5}$

which were further treated by applying the initial method for flat plates for 35 h at 130 °C. The zeolite was then exchanged with cerium to a 160% exchange level resulting in formation of additional extra-framework cerium oxide. By putting two plates on top of each other, a simple reactor was formed. A maximum rate of reaction was found at 300 °C at low conversion levels around 15%. As the rate of the reaction was not changing when increasing the flow rate, external mass transport limitations could be excluded. Similar, but always higher reaction rates were found for the zeolite coatings compared to pelletised zeolites, which is remarkable as the conventional measurements were carried out under extremely turbulent flow regime in a Berty-type recycle reactor. Therefore, diffusion limitations in the macropores of the pelletised zeolite created transport limitations obviously.

Cominos et al. [71] developed a micro-reactor for testing catalysts in methanol steam reforming for PEM fuel cells. The stainless steel device had outer dimensions of 75 mm × 45 mm × 110 mm and took up a stack of 5–15 plates carrying micro-channels of 500 μm width and 350 μm depth at a length of 50 mm. The feed distributed between the channels and plates from a common inlet region. By simulations applying the software CFD-ACE+ the flow distribution was proven to deviate by less than 2% for both the channels of one plate and for the individual plates. Home-made Cu/Zn catalysts were prepared by introducing γ-alumina wash-coats [72] of an average thickness of 10 μm as carrier material into the micro-channels. Their BET surface area was determined to 72 m^2/g and the average pore diameter amounted to 45 nm. The active components, Cu and Zn were introduced by wet impregnation in two different load levels (8 and 16 wt.%) and weight ratios (3:1 and 1:1). The experiments were carried out at a residence time between 200 and 100 ms and a total flow rate between 500 and 900 cm^3/min using five coated plates. A 23% decrease of the conversion was found when the flow rate was increased from 500 to 800 cm^3/min. However, the hydrogen content in the product decreased more pronounced by 36%, which was attributed to the slow kinetics of the reverse water-gas-shift reaction. Increasing the temperature from 200 to 275 °C increased the conversion from 37 to 65%. At temperatures exceeding 250 °C carbon monoxide formation started. When 15 plates were introduced into the reactor, 80% conversion was achieved at 290 °C temperature, a residence time of 600 ms and a steam-to-carbon (S/C) ratio of 2 resulting in a product containing more than 50% hydrogen and 0.25 vol.% CO, which pointed out the need of an additional gas purification device to remove the CO before the product could enter a fuel cell. From these results, a power output of the testing device of 43 W and a power density of 1.8 kW/dm^3 were calculated.

3.2.2. Stack-like reactors with integrated heat-exchanging capabilities

Combined heat exchangers/reactors offer the opportunity of exploiting the superior heat transfer capabilities of micro-structures combined with the enhanced catalyst effectiveness in micro-structured catalyst layers.

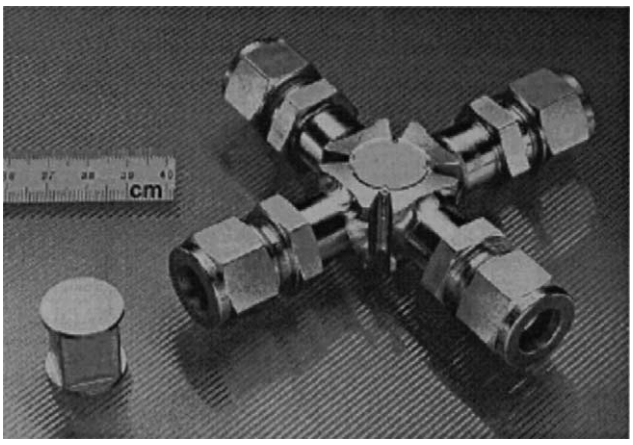

Fig. 16. Cross-flow heat exchanger/reactor. *Source*: FZK-Website.

3.2.2.1. Cross-flow heat exchangers/reactors. A well-known professional tool developed by FZK and available in small series, is a derivative of a micro-heat exchanger [73–76] which was developed prior. By insertion of catalytically active material, the 'micro-heat exchanger' functions as reactor (see Fig. 16). Quadratic platelets with straight micro-channels through are assembled to a stack so that two adjacent platelets have 90° turn. By this, a cross-flow configuration is created with two separated fluid passages for two heat transferring fluids or one reaction mixture and a heating/cooling fluid flow alternatively.

Micro-fabrication of the parallel channels was performed by mechanical surface cutting of metal tapes [73]. In the case of aluminium alloys, ground-in mono-crystalline diamonds were used [74]. In the case of iron alloys, ceramic micro-tools have to be used due to the incompatibility of diamonds with that material. Such a micro-structured platelet stack is provided with top and covers plates, diffusion bonded and connected to suitable fittings for the inlet and outlet ducts by electron beam welding.

Optimised micro-fabrication and advanced assembly led to the use of thin platelets, in an original version 100 μm thick at 80 μm micro-channel depth, so that very thin walls as low as 20 μm remain for separating the fluids, which limits the axial heat flow through the material walls and improves the efficiency especially of counter-flow heat exchangers. Due to the low wall thickness, also the total inner reaction volume with respect to the total construction volume or respectively the 'active internal surface' is very large. The latter surface amounts to 300 cm^2 (for both the heat transfer and reaction sides) at a cubic volume of 1 cm^3. Indeed, the micro-heat exchangers proved high heat transfer coefficients for gas [75] and liquid [76,77] flows.

Meanwhile, the reactor can be obtained in many materials such as aluminium alloys, copper, silver, titanium, and stainless steel. The number of stacked platelets, the dimen-

sions of the micro-channels on the platelets, and the fluidic connectors were demonstrated to be varied as well. Pressure tightness up to several hundred bar for gases and liquids was demonstrated.

As the reactors are diffusion bonded, all types of catalyst deposition techniques may be applied which allow for a deposition subsequent to the reactor bonding. Wießmeier et al. [78] applied anodic oxidation in a micro-structured reactor and used it for the hydrogenation of cyclododecatriene. Wunsch et al. [79] demonstrated anodic oxidation of aluminium or aluminium alloys ($AlMg_3$) in 5 wt.% oxalic acid. After 3–4 h a satisfactorily even film distribution in the range of 10–12 μm was achieved. The catalyst carriers were impregnated with Pt. However, due to the inaccessibility of the in situ generated catalyst, surface area data of the layers were only available as surface magnification factors. The coatings were successfully applied for the H_2/O_2 oxidation reaction. Gorges et al. [80] introduced anodic spark deposition (ASD), a modification of anodic oxidation for the formation of polycrystalline ceramic oxide layers on passivating metals. The method is therefore limited to Ti, Al and Zr surfaces. By local melting of the layer into the substrate strongly adhered coatings of up to 40 μm thickness could be generated and the incorporation of dopant elements got possible. By coating a ceramic green body with Ti, ASD could even be carried out on a nonconductive base material. Födisch et al. [81] applied electrophoretic precipitation of industrial catalyst powders.

Hönicke et al. [82] applied an FZK cross-flow heat exchanger manufactured of 100 μm thick copper foils of 14 mm × 14 mm size for the partial oxidation of propylene to acrolein at Cu_2O. Each of the 100 foils carried 80 microchannels of 80 μm hydraulic diameter. The active species was generated by oxidation of the copper foils achieving an oxide layer of several μm thickness. The reaction was investigated between 350 and 375 °C revealing a minimum selectivity towards acrolein at 363 °C. The maximum selectivity of 47% was found at a temperature of 350 °C and 5% conversion. Independent of the initial oxidation state (CuO or Cu_2O) of the catalyst, an intermediate state was achieved after sufficient TOS.

Hagendorf et al. [83] applied the reactor for the H_2/O_2 reaction in the explosive regime. Alumina was used as catalyst carrier introduced by in situ CVD and Pt as active component was in situ wet impregnated. Channel dimensions amounted to 100 μm × 200 μm for the reactor side and 70 μm × 100 μm for the cooling gas side (nitrogen). In this early work, in 1 cm^3 reactor volume complete conversion could be already achieved at temperatures below 220 °C generating 150 W of thermal energy which were removed by the cooling fluid.

Janicke et al. [84] applied the reactor for the same reaction in a by far more detailed study stressing the possibility of applying the system as a catalytic burner for automotive applications. Here channel dimensions of 140 μm × 200 μm were used for the reaction area and 70 μm × 100 μm for the cooling channels. Alumina layers were generated by CVD and Pt was introduced via up to threefold wet impregnation to improve the loading level. Catalyst characterisation was performed by SEM and EDX and even coatings of 10 μm thickness were found. Krypton adsorption was performed revealing a low surface area of 0.17 m^2/g as the coated carriers, and not the coating alone were analysed. A Pt particle size of 15 nm was determined by XRD which did not change during the reaction. At low Pt loadings, which correspond to a single impregnation procedure, the reactor was externally heated to 80 °C leading to complete conversion and a power generation of 72 W. Seventy percent of the heat generated was lost. At a flow rate of 1.6 dm^3/min a temperature increase of 300 K was observed.

Occasionally, owing to experimental errors, which occurred during the post-mounting catalyst deposition technique, in some cases hot spot formation and subsequent homogeneous reactions were observed in the reactor in- or outlet. At high Pt loadings, which correspond to a threefold impregnation procedure, ignition took place after an induction period with a gradual temperature increase from room temperature. The temperature could be easily controlled by the cooling gas flow rate. Interestingly, this induction period got shorter after several experiments which was attributed to the formation of a thin and highly active oxide layer at the surface of the platinum which was initially in the reduced state. At both levels of Pt loading, the coolant temperature at the exit was higher than the temperature of the products which was explained by hot spot formation. Further experiments were carried out by Janicke et al. [85] using cooling oil. Surprisingly, for a cross-flow heat exchanger, an exit temperature of 207 °C was determined for the heat carrier, whereas the product gas exited at 70 °C. This phenomenon was attributed to the fact, that most of the energy was transferred to the oil at the feed inlet. Subsequently, the product was then cooled by the cold oil not yet heated up.

Görke et al. [86] investigated the catalytic oxidation of hydrogen in an integrated cross-flow heat exchanger/reactor which was combined with a mixer for feed preparation. The reactor was build as a measurement tool for the determination of kinetics of fast and highly exothermic heterogeneous gas phase reactions. The reactor had a height of 1.6 mm at a width and length of 14 mm each. The channels were 200 μm wide and 70 μm thick and each of the 16 stainless steel foils of the stack carried 38 channels. Twelve foils were used for cooling the reactor with water and four foils were used as reaction zone which were impregnated with Pt directly on the stainless steel surface. Using 324 measuring points taken at temperatures between 35 and 75 °C, hydrogen concentrations between 1.6×10^{-3} and 11.0×10^{-3} mol/dm^3 and oxygen concentrations between 1.7×10^{-3} and 7.3×10^{-3} mol/dm^3 a kinetic expression for the reaction was determined on the basis of a Langmuir–Hinshelwood model. The Mears criterion was applied to verify that no mass-transfer limitation were to be expected for the system from the gas phase to the non-porous catalyst. No heat transfer

limitation in the boundary layer was found according to the Anderson criterion. The *Nu* number calculated amounted to 5.7. For a cooling flow of 7.5 dm^3/min the temperature increase of the water was 1.8 K at a power generation of 30 W of the reaction. The overall heat transfer coefficient was calculated to be as high as 15 kW/(m^2 K). No increase of the gas outlet temperature was observed proving that the heat was completely removed. From the kinetic experiments an activation energy of 17.3 kJ/mol and an adsorption enthalpy of 252 kJ/mol for oxygen was found for the highly endothermic reaction. The frequency factor was high as well (1.16×10^9 mol/(dm^3 s)) which points at the high reaction rate.

Rebrov et al. [87,88] developed an integrated cross-flow heat exchanger/reactor for the platinum-catalysed ammonia oxidation to N_2O. This highly exothermic reaction occurs at low temperatures, short residence times and high reaction rates. Nitrous oxide is used for the selective oxidation of methane to methanol and of benzene to phenol, respectively, in a single reaction step. Poor temperature management of the reaction impairs nitrous oxide selectivity, which has a maximum at a temperature of 325 °C [31]. Industrially, N_2O is either produced by ammonium nitrate decomposition or bio-chemically. Therefore, the application of micro-structured reactors has a potential to improve the performance of the process. Additionally, mass-transfer limitations are to be expected for the reaction at higher temperatures. The application of a micro-reactor for kinetic investigations is thought to extend the kinetically controlled temperature range to higher values [31]. The reactor applied had a Ni housing which could withstand temperatures up to 430 °C. The housing was divided into a heated zone where the feed was preheated and the reaction took place and a cooled zone for quenching of the products to a temperature of −20 °C. The zones were separated by a ceramic layer. Four types of reactors were tested in the scope of the investigations. The first one was a parallel plate reactor taking up a stack of 20 aluminium plates 4.34 mm wide and 0.3 mm thick. The channels were 7 mm long, 500 μm wide and 380 μm deep. The plates were treated by anodic oxidation and the resulting alumina layer of approximately 20 μm thickness was impregnated with Pt at three loading levels of 0.05 (referred to as reactor Al below), 0.2 wt.% (A2) and 1.3 wt.% (A3) on alumina. Pt is known to have an at least 2 orders of magnitude higher turn-over-frequency (TOF) for the reaction compared to all other metals, which may be more selective [31]. The catalyst was reduced in hydrogen at 400 °C for 1 h prior to testing. The second reactor (B) was a Pt monolith of the size 10 mm × 10 mm × 9 mm manufactured by conventional machining. The 49 channels had a diameter of 500 μm and a length of 9 mm. The third reactor (C) consisted of 14 plates 9 mm long, with 7 channels on each plate being 140 μm deep and 280 μm wide. To improve the heat transfer between the plates, they were mounted prior to the oxidation and impregnation steps. The fourth reactor (D), being the reason why this work is attributed to the heat exchanger based reactors, was designed as a cross-flow heat exchanger each plate carrying half-circles of one level of the tubular reaction cooling channels (see Fig. 17). The plates were made of aluminium and the thickness of the plates was 270 μm. The reaction channels had a diameter of 145 μm to avoid diffusion limitations, the cooling channels were 300 μm wide. Twenty reaction channels were machined into each of the plates. For the experiments, a residence time of 0.33 ms was assumed for the reaction channels resulting in a flow velocity of 20 m/s which is still laminar flow (Re = 220) and a pressure drop of 3.5%. The feed composition of the standard test performed amounted to 6 vol.% NH_3 in 88 vol.% O_2 and 6 vol.% He. Table 3 gives an overview of the results. Reactors Al and A2 have a low level of Pt loading, whereas reactors A3 and C are expected to have clusters of Pt on their surface, which explains their better performance. Clusters of at least five atoms are regarded as necessary for a good performance of the catalyst. For a cluster size of 2.3 nm a TOF of 40 s^{-1} was found. The best performance showed reactor C, which was attributed to the improved heat removal through the walls. In the A-type reactors the aluminium plates were melted together due to the poor heat transfer at ammonia concentrations exceeding 12 vol.%. Generally, a heat removal got necessary when ammonia concentration in the feed exceeded 10 vol.%. Reactor C was run autothermally at 14 vol.% ammonia concentration in the feed and a temperature of 325 °C. It was found that a large excess of 90 vol.% oxygen in the feed doubled the selectivity towards N_2O compared to a stochiometric feed composition. Quenching helped to avoid consecutive reactions of N_2O. Decreasing the residence time below 0.3 ms was beneficial for the selectivity towards N_2O. By calculation of the Damköhler number it was found that at temperatures exceeding 325 °C mass-transfer limitations need to be taken into consideration for the reaction system. Simulations were carried out in order to optimise the inlet and outlet dimensions and the dimensions of the individual channels concerning both flow distribution and axial/transverse temperature de-

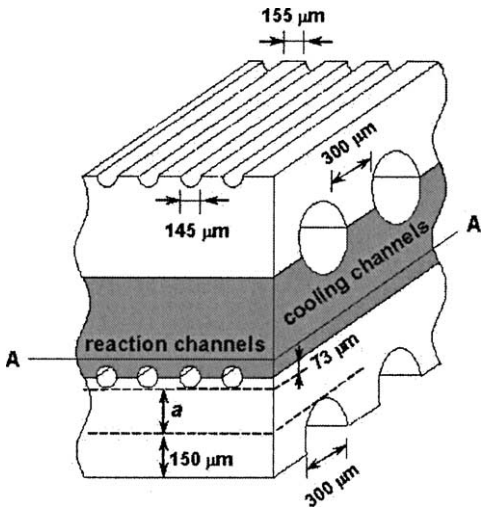

Fig. 17. Assembly of the micro-reactor D designed by Rebrov et al. [87].

Table 3
Conversion of ammonia and selectivity to nitrous oxide for various Pt loadings and micro-reactors, respectively (according to Rebrov et al. [88])

Reactor	Flow rate (1/min)	Pt loading (mg)	Conversion (%) at 320 °C	Selectivity (N_2O) (%) at 320 °C
A1	0.6	0.022	25	7
A2	1.175	0.086	50	24
A3	4.43	0.56	100	40
B	0.58	–	100	27
C	4.29	0.543	100	49

viations. This was done to equalise the residence time in the channels. The calculations revealed, that a temperature difference of 9 °C between two channels generates a conversion difference as large as 20%. From these simulations and the results generated experimentally at reactor C, a selectivity towards N_2O of 52% seemed to be achievable. The feed composition for future experiments in an optimised reactor was proposed to be 20 vol.% ammonia in oxygen at an inlet temperature of 175 °C and a cooling gas temperature of 20 °C.

Rebrov et al. [89] developed a kinetic model for the low temperature ammonia oxidation. Numerous literature data, which will therefore not be completely cited here, were used to set up a reaction scheme. The measurements were carried out in reactor C of a prior publication of Rebrov et al. [88]. The kinetic experiments were performed at a Pt-catalyst with 3.5 wt.% loading, which showed 40% dispersion and 2.3 nm particle size. Steady state data were generated after a 12 h pre-treatment in a 6 vol.% ammonia in oxygen feed. The ammonia concentration was then varied between 2 and 12 vol.% NH_3 in oxygen or oxygen/helium at residence times between 0.3 and 0.82 ms. For the kinetic modelling, a dual site mechanism was chosen, where adsorbed O_2, OH and H_2O ad-species occupy the hollow sites [90], and absorbed NH_3 and NH_2 ad-species occupy single-on-top adsorption sites [91,92] and adsorbed NH and N ad-species occupy single bridge sites [93]. The latter two types of sites were not distinguished here. Ammonia adsorption was assumed to proceed via an intrinsic precursor state, where a molecule is trapped and then diffuses to an empty site [94]. From literature, the adsorption was assumed to proceed non-activated [95], molecular [96] and the bonding to take place via the nitrogen atom [97]. The adsorbed oxygen was regarded as an immobile ad-species [98]. It was assumed that the oxygen concentration is restricted to one monolayer. Molecular chemisorbed oxygen was not included due to lack of kinetic data. A kinetic model of 19 reactions was then set up and reduced to a lumped model after sensitivity analysis. Ammonia decomposition was considered as one lumped irreversible reaction step with first order regarding the oxygen surface sites. The micro-channel reactor was simulated applying the kinetic model. Firstly, a single channel plug-flow model was applied. The kinetic parameters were determined by regression of the integral data from 103 experimental runs performed in the micro-reactor. Qualitatively, the simulation results agreed very well with the experimental data and revealed, that high oxygen partial pressure is necessary to achieve high N_2O selectivity. The maximum selectivity towards nitrous oxide was found at 330 °C for an ammonia partial pressure of 0.066 bar and an oxygen partial pressure of 0.88 bar. The TOF values predicted by the model for a temperature of 413 K agree well with data found in literature [99]. Between 873 and 923 °C a TOF of 60 s^{-1} was achieved at full ammonia conversion, however, mass-transfer limitations were observed under these conditions. An apparent activation energy of 129.6 kJ/mol was calculated based on the 13 step lumped model. The plug-flow model over-estimated the ammonia conversion and nitrous oxide selectivity, which were determined experimentally at temperatures exceeding 573 K. This could be attributed at least partially to the fact, that the feed was not preheated during the experiments. An improved prediction of the experiments could be achieved applying a complete Navier–Stokes model. Among other results, the detailed calculations revealed a thermal equilibration in the reactor after 6 mm length without preheating of the feed at a low residence time of less than 1 ms.

Moreover, Rebrov et al. [100] optimised the non-uniform flow-distribution of a micro-structured cross-flow heat exchanger/reactor made of aluminium to achieve an equal temperature distribution for kinetic measurements of ammonia oxidation. Target of the work was to run the highly exothermic reaction at 15–20 vol.% inlet concentration, which corresponds to an adiabatic temperature rise of 1800 °C and to improve the selectivity towards nitrous oxide. The diameter of the cylindrical channel system under investigation amounted to 145 μm, the length to 6.5 mm. Temperature was kept below 300 °C and the residence time below 0.33 ms. Each micro-structured plate carried 20 semi-cylindrical channels for the chemical reaction, which formed cylindrical channels with its counter-part. The thickness of the alumina layer carrying the catalyst was set at 8 μm and the catalyst loading to 7.5×10^{-3} mol Pt/m^2. The kinetic expressions applied were based upon a former publication of Rebrov et al. [88]. A reaction order of 0.02 was applied for the ammonia concentration, in a partial pressure range between 0.05 and 0.2 bar. For lower partial pressure values, a reaction order of 1 was used. The reaction order concerning oxygen was set to −0.06 for the entire partial pressure range used in the experiments. The following adopted power law was applied in the temperature range between 310 and 340 °C:

$$r_{NH_3} = \frac{k_1 k_2 p_{NH_3}}{(1 + k_1 p_{NH_3}) p_{O_2}^{0.06}} \quad (10)$$

Nine cooling channels were used for heat-removal by nitrogen. Four designs were checked the difference of them being the distance between reaction and cooling channels, which was varied from 125 to 670 μm. For this concept, preheating of the feed to 175 °C was assumed. Generally, a decrease of the plate thickness increased the axial heat transfer and decreased the temperature gradients, but also increased the reactor size, of course. Additionally, the benefits from the non-uniform flow distribution were deteriorated this way. Temperature gradients up to 20 °C were found and could be reduced to 3 °C by sending 35% more coolant through channels number six to nine. Additionally, any distance between 470 and 670 μm did not show substantial difference concerning the temperature distribution. Then inlet and outlet chamber geometry were optimised. An optimum asymmetric position of the inlet and outlet at a diameter of 1 mm each was determined. The angle between chamber wall and reactor channel front did not affect the flow pattern between values of 0 and 10° and was therefore set to 5°. Finally, the optimum distance between chamber wall and reactor channel front was found to be 300 μm. The latter parameter was not significant as well, as switching from 300 to 610 μm did only change the velocity distribution by 6%. Based upon these results, a reactor was manufactured of aluminium. It carried eight plates each with 20 reaction channels of 145 μm width at a distance of 155 μm and with nine cooling channels of 300 μm width at a distance of 300 μm at the reverse side. The plates were treated by anodic oxidation to gain an alumina layer of 8 μm thickness. Impregnation was performed by circulating Pt-solution through the channels. The catalyst was then oxidised in pure oxygen for 6 h at 450 °C and thereafter reduced in 10 vol.% hydrogen at 340 °C. For a total feed rate of 2 dm^3/min at a O_2/NH_3 ratio of 5.7, a selectivity towards nitrous oxide of 40% could be achieved. The coolant flow was 5.4 dm^3/min, the product outlet temperature amounted to 325 °C. The results generated at the optimised reactor were compared to a micro-reactor without heat exchanger made from aluminium [89]. For this reactor, temperature gradients of 14 °C existed in axial direction at full conversion of 6.6 vol.% ammonia in oxygen. Compared to this simple reactor, the selectivity to nitrous oxide could be significantly increased from 41 to 44% at a O_2/NH_3 ratio of 10.

Brandner et al. [101] developed a both heated and cooled reactor for temperature cycling experiments. Heating was done electrically and permanently by integrated cartridges of 6.3 kW electrical power while cooling was done periodically using a cooling fluid. Six micro-structured plates carrying 81 channels of 22.5 mm length, 350 μm width and 150 μm depth formed the cooling passage of the reactor while four reaction plates carried three meandring channels each 380 μm wide, 150 μm deep and 710 mm long (see Fig. 18). The total mass of the reactor was as low as 117 g. The reactor was sealed by diffusion bonding and electron beam welding. The coolant water was fed at pressure drops up to 10 bar and a flow rate between 15 and 45 dm^3/min through the reactor. To minimise the liquid hold up of the reactor during the heating period, the removal of the coolant was done by air at a pressure of 12 bar. At a heating power of 450 W and a water flow of 15 kg/h the reactor temperature could be increased from 70 to 250 °C within 30 s. However, the temperature of a 100 cm^3/min nitrogen flow did increase from 60 to 140 °C at the same time. At even higher heating power of 1700 W, a temperature jump of the reactor core from 120 to 225 °C could be achieved in 2.1 s with no measurable change of the nitrogen temperature which was attributed to an average temperature the outer regions of the reactor approached during temperature cycling. Later on, Brandner et al. [102] presented an updated version of the reactor which contained three separately controlled heating blocks and was expected to reach half-cycle times of 0.5 s at temperature differences of 100 °C.

3.2.2.2. Counter-flow heat exchangers/reactors. The application of counter-flow heat exchangers allows not only for a higher heat-exchanging efficiency compared to cross-flow heat exchangers but also for the adjustment of temperature gradients in the reaction zone. This has a potential for further improving yields and selectivities of various chemical reactions in a single integrated device in a more advanced way like it is done in industrial macro-scaled reactors. An alternative to the incorporation of heat-exchanging devices into the reactor, to cold gas (steam) injection or construction of multi-stage reactors is provided.

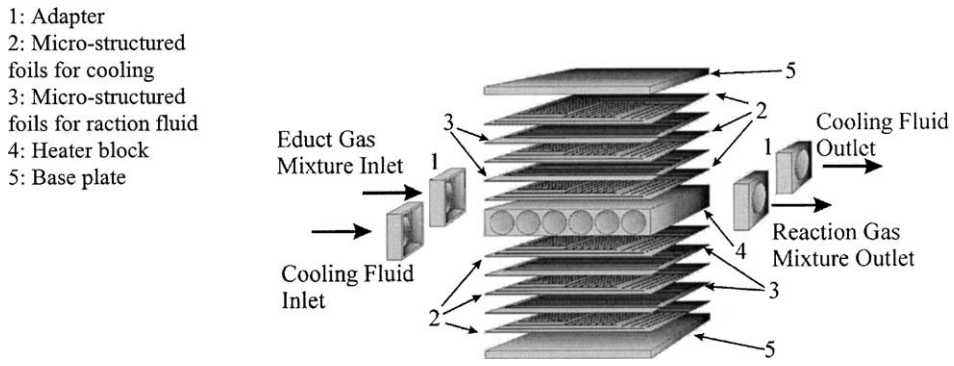

Fig. 18. Schematic explosion drawing of the micro-structured reaction device designed by Brandner et al. [101].

Fitzgerald et al. [103] presented a micro-structured iso-octane heat exchanger/steam-reformer heated by combustion gas with a total volume of 30 cm^3 which produced enough hydrogen for a 0.5 kW PEM fuel cell. At ambient pressure, a temperature of 650 °C, a residence time of 2.3 ms and a high S/C ratio of 6, up to 95% conversion were achieved at 90% hydrogen selectivity. Decreasing the S/C ratio decreased the iso-octane conversion, but not the hydrogen selectivitiy.

Walter et al. [104] applied an externally heated micro-reactor, which may be applied as a counter-flow heat exchanger as well (see below) from IMM for the partial oxidation of isoprene to citraconic anhydride in a heterogeneously catalysed reaction as an alternative to the industrial process which is by far more complex. The catalysts applied for the system contained vanadium and titanium oxide in various amounts. Conventional catalysts were made for comparison with surface areas in the range from 6 m^2/g for pure vanadium oxide up to 15 m^2/g for $V_{30}Ti_{70}O_x$. All conventional catalysts were prepared by impregnation on a TiO_2 support. The pure vanadium oxide catalysts performed best in conventional fixed-bed testing. Selectivitites found for the conventional catalysts were ranging between 27 and 30% being independent of the molar vanadium content in the range between 5 and 75%. The active compounds were introduced by both anodic oxidation and wash-coating into the micro-channels. After anodic oxidation of the micro-structured aluminium platelets they were impregnated with vanadyl and titanyl acetylacetonate resulting in a $V_{50}Ti_{50}O_x$ alumina-based catalyst. The impregnation procedure resulted in an accumulation of vanadium and titanium in the holes of the rough surface. Aluminium wires were prepared in parallel by anodic oxidation for surface area measurements. Surface areas in the range of 5 m^2/g were found. For the wash-coat preparation conventional catalyst was ground and introduced onto the micro-channels together with silicate solution. This resulted in 10–40 μm thick layers of high surface areas (35 m^2/g for pure vanadium oxide and even 110 m^2/g for $V_{50}Ti_{50}O_x$). An identical flow rate of 1.5 scm^3/min per channel was adjusted to get comparable results despite of the different amounts of plates introduced into the reactor. Each plate carried 34 channels of 20 mm length and a hydraulic diameter of 230–280 μm. Experiments were carried out at an isoprene concentration of 0.6 vol.% and a pressure of 1.2 bar. The selectivities found for the coatings were slightly lower compared to the fixed-bed catalyst for the wash-coats (22–25%) and significantly lower (12%) for the catalysts prepared by anodic oxidation. Maximum yields achievable were inferior for the wash-coats compared to the conventional catalysts. This was attributed to both the residual sodium found in the wash-coats stemming from the preparation procedure and deep oxidation of citraconic acid at the stainless steel and aluminium walls of the micro-reactor (the conventional reactor was made of ceramics). Additionally, the isothermal behaviour of the micro-reactor was claimed to be responsible for the inferior performance.

The same reactor was applied for forced temperature oscillations as an integrated heat exchanger/reactor for the dehydration of iso-propanol to propene and di-isopropyl-ether over γ-alumina catalysts by Rouge et al. [105] to increase the yields achievable in this reaction system. Simulations were carried out revealing that a 90% change of the first to the second temperature of a temperature cycle should be achievable within 3 s. The main limitation of the heat transfer was found between the heating oil and the stainless steel of the reactor. Most of the heat stored in the oil was expected to be lost at the reactor inlet and the heat to be transferred mainly through the solid by conductivity. Consequently, downstream the temperature changes took longer. Of course the housing took much longer to reach a new temperature. Nine couples of heat exchanger and reactor plates were applied for the experiments and channel dimensions were 300 μm width and 240 μm depth at a length of 20 mm. The plates carried again 34 channels each. They were isolated from the reactor housing by MACOR ceramic plates. A total of 110 mg catalyst was introduced into the reactor which had a total inner volume of 0.9 cm^3. The experiments were carried out at flow rates between 0.66 and 1.66 cm^3/s and an iso-propanol concentration of 0.92 mol/m^3. Temperature was cycled between 190 and 210 °C applying two oil circuits. After increasing the temperature desorption effects led to a peak of the iso-propanol concentration at the reactor outlet. Corresponding negative peaks were found when decreasing the temperature again. After that initial effect, the iso-propanol concentration approached a new steady state very slowly within 60 s. However, the propene concentration followed the temperature cycles immediately. These effects were attributed to the inhibition of the reaction by the reactant and water. Performing experiments at 10 s temperature cycling resulted in a 5 s shift for propylene and a 10 s shift for iso-propanol. The by-product ether was only formed to a minor extend. Further optimisation of the temperature cycling would be necessary to optimise the reactor performance.

Later on, Rouge et al. [106] worked on concentration cycling for the same reaction system in the same reactor. The intention was to make use of the so-called stop-effect, which shows an increased reaction rate, when the reactand is removed from the feed. Two species of active sites exist on the catalyst surface, which are both occupied by the feed molecule. As the second type of active site needs to be un-occupied for the dehydration reaction, the feed molecule inhibits its reaction. Simulations showed that periodic operation has a potential to improve the productivity of the process especially at short cycling times. The same type of plates like described in the earlier work was used but the number of plates was reduced to either 5 or 10 for the experiments. For five plates a Bodenstein number of 70 was found by residence time measurements which could be described by simulation in perfect agreement. Thus the micro-reactor behaved almost like a plug-flow reactor. It was found that the ratio of cycle period to residence time should be at least 2 in order to avoid a severe deterioration of the inlet signal in the

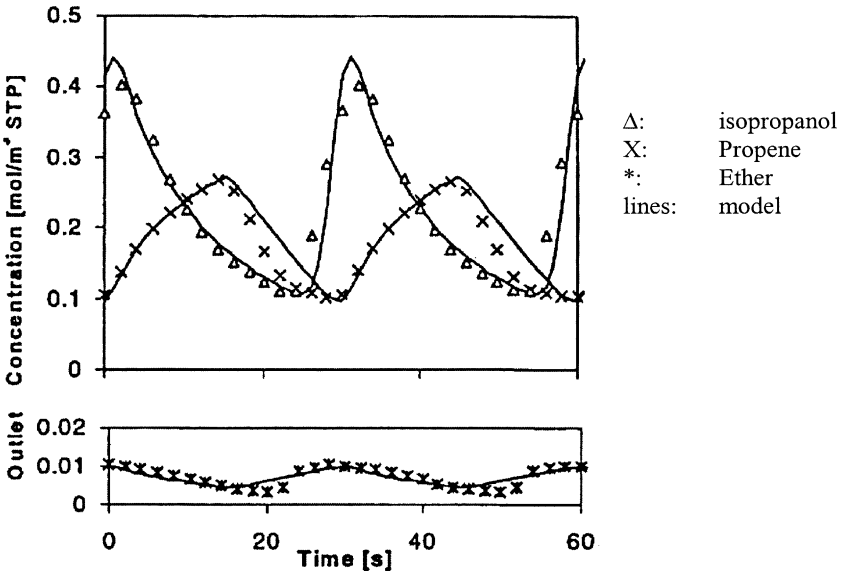

Fig. 19. Outlet concentrations during a periodic cycle at a iso-propanol switch from 0.86 mol/m^3 to 0 at $t = 0$ s (30 s cycle time, residence time 175 ms) determined by Rouge et al. [106] for the dehydration of iso-propanol.

reactor. The concentration cycling was done by switching between the feed flow and an inert gas flow. The experimental conditions were a pressure of 1.3 bar, a temperature of 200 °C and an iso-propanol concentration of 0.86 mol/m^3. A mixture of inert (nitrogen) and water at a concentration of 0.25 mol/m^3 was also introduced into the reactor during some of the experiments. When switching from alcohol feed to inert gas, a sharp peak of product (propene) was found due to the stop-effect (see Fig. 19). Accordingly, a similar peak was found for the water when the gas flow was switched from inert to feed. The product peak was not found when the gas flow was switched from propanol to water, as the latter only expelled the propanol from the sites, no free sites remaining for the reaction. Assuming therefore the following advanced model of the reaction, the dynamic behaviour of the reactor could be described:

$$\text{isopopanol} + \text{water} - \text{site type 1} \leftrightarrow \text{isopopanol} - \text{site type 1} + \text{water}$$

$$\text{isopopanol} + \text{site type 2} \leftrightarrow \text{isopopanol} - \text{site type 2}$$

$$\text{water} + \text{site type 2} \leftrightarrow \text{water} - \text{site type 2}$$

$$\text{isopopanol} - \text{site type 1} + \text{site type 2} \leftrightarrow \text{water} - \text{site type 1} + \text{propene} + \text{site} - \text{type 2}$$

Liauw et al. [107] demonstrated, that a stationary vortex may be formed at a conical inlet of a stack-like micro-reactor which deteriorates the residence time behaviour if feed concentrations are changed.

Steinfeld et al. [108] investigated the oxidative dehydrogenation of propane in a fixed-bed reactor and in the micro-reactor developed by IMM at VO_x/Al_2O_3 catalyst. At 460 °C inlet temperature, selectivity dropped from more than 70% to about 50% with increasing conversion (from 5 to 15%). In turn, carbon monoxide and dioxide selectivities increased. At 460 °C, the space–time yield was increasing linearly (maximum: 0.3 mol/(kg s)) when increasing the partial pressure for propene from 10 to 50 kPa. For the same temperature, the impact of oxygen partial pressure was less remarkable for both reactors. At higher temperatures (490 and 502 °C), more carbon dioxide formation was noted for the micro-reactor when increasing propene partial pressure which was explained by unspecific total oxidation due to the stainless steel walls having large specific area. For increasing the oxygen partial pressure at the same temperatures, carbon monoxide formation in the micro-reactor was high. Experiments at fixed flow rate allowed a comparison of the reactor performance as a function of the inlet temperature. The conversions rose steeply with increasing inlet temperature. It turned out that in all cases investigated higher propene and oxygen conversions resulted for the fixed-bed reactor. Propene conversions, for instance, differed as much as about 10%. Measurements of local temperatures confirmed that hot spots up to 100 °C were responsible for this difference.

3.2.2.3. Counter-flow heat exchangers/reactors for evaporation purposes. The heat generation of a chemical reaction may well be exploited to evaporate liquids in a micro-structured reactor.

Tonkovich et al. [109] applied micro-technology for methanol processing as a hydrogen source for fuel cells. They claim a 90% size reduction due to the introduction of micro-channel systems, which is crucial for mobile reform-

ing applications. The device makes use of the hydrogen off-gas of the fuel cell anode which is burnt in monoliths at palladium catalyst to deliver the energy for the fuel evaporation. A metallic nickel monolith 0.63 cm high was etched and impregnated with palladium to act as a reactor for the anode effluent. It was attached to a micro-structured device consisting of liquid feed supply channels and outlet channels for the vapour the latter flowing in counter-flow to the anode effluent. A bench-scale evaporator was firstly built consisting of one monolith and heat exchanger plates 5.7 cm wide and 7 cm long. The stainless steel channels manufactured by EDM were 254 μm deep and the vapour channel depth was varied from aspect ratios of 4–18 the latter being the optimum value as found by experiments. At Pd loadings of more than 5 wt.%, 80–90% hydrogen conversion was found for a synthetic anode effluent containing 6.7% hydrogen. The heat exchanging efficiency of the bench-scale evaporator increased linearly with the aspect ratio of the vapour channels and reached a value of 92% at an aspect ratio of 18. The full scale reactor/evaporator had a total size of 7.6 cm × 10.2 cm × 5.1 cm and was composed of four monoliths of 5 cm^2 cross-sectional area and four heat exchangers with 7.2 cm^2 cross-sectional area. This device was claimed to evaporate 208 cm^3/min methanol by converting 25 dm^3/min hydrogen at a level of 100%, an efficiency of 93.2% and a heat flux of 145 W/cm^2. The methanol vapour exited the device at 203.4 °C. Cleaning of the evaporation channels was said to be necessary on a regular basis by burning off the coke deposits formed during operation.

Drost et al. [110] developed an evaporator combined with a micro-scale combustion chamber for homogeneous combustion of hydrocarbons. The main focus of the work was to maintain a stable combustion of the fuel avoiding NO_x formation. Evaporation tests were carried out under isothermal conditions. Fifty-four parallel channels, 270 μm wide and 1000 μm deep at a length of 20.52 mm were cut into a copper substrate with a diamond saw. Basically, an unstable two-phase flow was found at the exit of the evaporator which was indicated by high *Nu* numbers in the range between 20 and 30. Then a combined combustor/evaporator was designed which consisted of a ceramic tube as combustion chamber placed in a stainless steel housing (dimensions 41 mm × 60 mm × 20 mm). Ignition wires were used to initiate the reaction. The combustion gases then entered cooling channels which were combined with evaporation channels for the water. Both channel systems manufactured by EDM were 35 mm long, 300 μm wide and 500 μm deep. An alternative design was developed for methane combustion, where a sintered metal plate served as flame arrestor. The device had a size of 50 mm × 50 mm × 10 mm. For a cooling water flow rate of 1.32 g/s, heat fluxes up to 28 W/cm^2 were achieved at a combustion efficiency of 82%. The best combustion efficiency of 91% was achieved at a heat flux of 6 W/cm^2. NO emissions of the system were determined between 5 and 15 ppm.

3.2.3. Reactors for screening of micro-structured catalyst carriers

Ouyang et al. [25] propagate the application of chip-like reactors for catalyst screening. There are two types of screening instruments. The first type is a high-throughput device for sample numbers higher than 100 which is used to find about 10 leads. The second type is designed in order to gain more information about these leads to identify the optimum catalyst. The advantages of micro-reactors for screening purposes are manifold. Their reduced size lowers the operation cost, their response times are shorter and they may be run safely even under explosive conditions. Ouyang et al. proposed to set up an array of micro-reactors, which was already described in Section 3.1, and to apply it for the second stage of catalyst screening.

Senkan et al. [111] developed a catalyst screening device which is based on pelletised samples of catalysts arranged in an array reactor for testing. The reactor, which ranges dimension-wise at the boarder-line between micro- and mesoscale, is composed of two silica ceramic slabs one of them carrying 20 channels having a size of 1 mm × 1 mm and a cylindrical well for the pellets. A second slab was covering and sealing the reactor. The gas flow rates in the individual channels were found to deviate by less than 5%. Four of these reactor arrays were put into an aluminium heating block which allowed for parallel testing of 80 catalyst samples. The temperature in a single array and between the arrays deviated by less than 1 °C. The pellets made of high surface area alumina had a diameter of 4 mm and a height of 1 mm. They were impregnated with various automatically premixed solutions of the active metals having different composition. The reactor was applied for the testing of Pt, Pd and In catalysts and combinations thereof. The catalytic dehydrogenation of cyclohexane was chosen as the reaction. Ten percent cyclohexane in argon was fed to the arrays with 4 ms contact time after a pre-reduction treatment. Sampling was done by inserting a sampling probe 2 mm deep into the sample exit channel for 5 s allowing for acquiring two to five data sets by mass spectrometry. This way the analysis of all 80 samples was possible within 10 min. Platinum and palladium were both found to be active for the reaction, but pure In showed no activity. However, a combination of 0.8% Pt, 0.1% Pd and 0.1% In was found to be the most active candidate (see Fig. 20). The array of catalysts was repeatedly analysed every 10 mm for 24 h showing that all samples deactivated by coking. The coke could be removed by calcination in air and most of the activity could be regained. It was found that the addition of 0.1% Indium had little impact on the initial activity but reduced the rate of the deactivation reaction considerably. The sample array was screened at four different temperatures and Arrhenius plots were made revealing an increasing importance of diffusion limitations with increasing temperature for the highly active samples.

Zech et al. [112] developed together with IMM an externally heated reactor which was able to take up 35 micro-structured plates within a volume of 10 cm^3. The plates had a

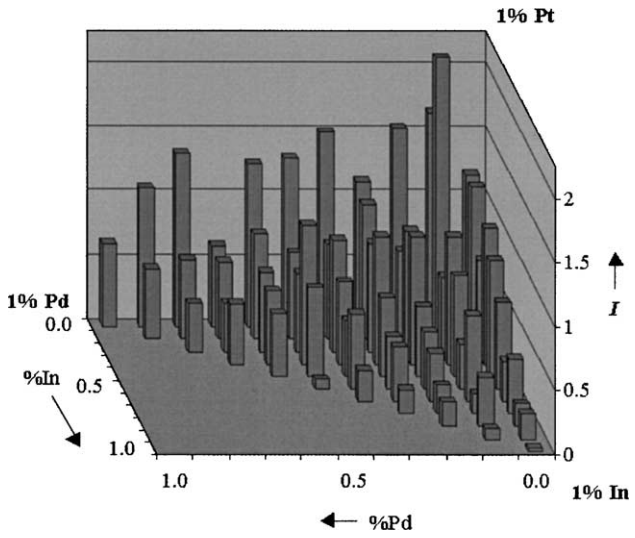

Fig. 20. Initial activity for benzene formation from cyclohexane of the Pt/Pd/In catalyst library determined by Senkan et al. [111].

channel width of 150 μm at various aspect ratios. The maximum temperature of the reactor amounted to 450 °C. Sampling was done by a capillary controlled by a CCD camera. The capillary moved up to 5 mm deep into the outlets of the 35 plates. Analysis was done by a mass spectrometer. The whole system was fully automated [113] and set not only the capillary position but also reaction conditions like residence time, feed concentration, temperature and pressure. Additionally, on-line data storage in an oracle database was approached. The response time of the whole system amounted to 15 s, which summed up to a sampling time demand of 1 min per sample. Even at gas flow rates of 1 cm^3/min for each wafer a sufficient signal-to-noise ratio was found for the device. The reproducibility of the results generated at the individual positions of the plates, which depended on the proper design of the diffuser at the reactor inlet, was optimised [113]. Reproducibility of the results generated at a given set of samples was proven as well. The cross-talking, between the individual plates, which is caused by the leakage rate from one plate to another, was determined by putting just one active plate into the reactor. Only a very low signal of 2% of the signal detected for the active plate was found for the neighbouring plates. Step changes of methane concentration in the feed revealed that all species detected at the reactor outlets followed within less than 30 s except for the water which took 200 s to achieve a new steady state. Methane oxidation at alumina-based Pt, V and Zr catalysts and combinations thereof was applied as a test reaction to proof the functionality of the reactor. The catalysts were prepared by wet impregnation of alumina wafers anodically oxidised both in sulphuric and oxalic acid. A methane-to-oxygen ratio of 1, 550 ms residence time, a pressure of 1.1 bar and a temperature of 450 °C was set for the experiments. The degree of conversion depended mostly on the Pt content of the samples. Zirconia enhanced the reactivity. Alumina layers generated by anodic oxidation were more active due to their higher surface area. Later on, Claus et al. [114] applied the reactor for the oxidative dehydrogenation of isobutene to isobutene on V, Zr and Mn catalysts.

Kolb et al. [115] developed a novel modular screening reactor for testing of up to 10 catalyst carrier plates. The reactor was made of Ti due to the reaction system it was designed for. It consisted of a core with drawers into which the micro-structured plates were put. By variation of the end-caps of the reactor two operation modes were possible. Firstly, parallel screening of up to 10 plates and secondly serial operation of up to 10 identically coated catalyst plates. The latter gave the opportunity of modifying the residence time via the catalyst mass under identical flow conditions. A steel housing was put around the titanium reactor which was designed for temperatures up to 500 °C due to the low stability of Ti at this temperature. This made the reactor rather bulky (160 mm × 70 mm × 120 mm). Heating of the reactor had to be done externally. The micro-structured plates had dimensions of 300 μm depth and 500 μm width at a length of 100 mm. Experiments performed with the reactor by Wörz at BASF at a proprietary reaction, revealed 60% yield for the desired product at residence times as low as 40 ms in the micro-reactor. This performance was superior to experiments performed in an aluminium capillary which corresponded well to the reactor design of the industrial process. A 2000% gain in space–time yield was found for the porous coated micro-structures compared to the aluminium capillaries. Later on a stainless steel version of the reactor was developed and applied for methanol steam reforming. This reactor was by far more compact (70 mm × 55 mm × 64 mm^3) compared to the former version. The cross-sectional area of the channels was maintained but the length of the channels was reduced to 50 mm. The reactor was heated by heating cartridges incorporated into the housing. The functionality of the reactor concerning cross-talking between the individual channels in the parallel operation mode was verified. Ziogas et al. [116] performed catalyst screening with the reactor at catalysts coatings, which were made of various base aluminas like corundum, boehmite and γ-alumina. Testing of Cu/Cr and Cu/Mn catalysts based on the different coatings for methanol steam reforming revealed differences in activity which were subscribed to both the different surface area and morphology of the carrier material. The functionality of the serial operation mode of the reactor was proven at the same reaction system indicating mass-transfer limitations for higher flow rates.

Müller et al. [117] applied the concept of using micro-structured titer-plates in a screening device for methane oxidation. The heart of the reactor consisted of a stainless steel reaction plate micro-structured by an etching process which contained up to 48 single reaction wells. The micro-channels of the well were 320 μm wide, 200 μm deep and 5.2 mm long. The parallel reactor for screening of the titer-plate consisted of several modules (see Fig. 21). The gas flow was preheated and evenly distributed in a distribution

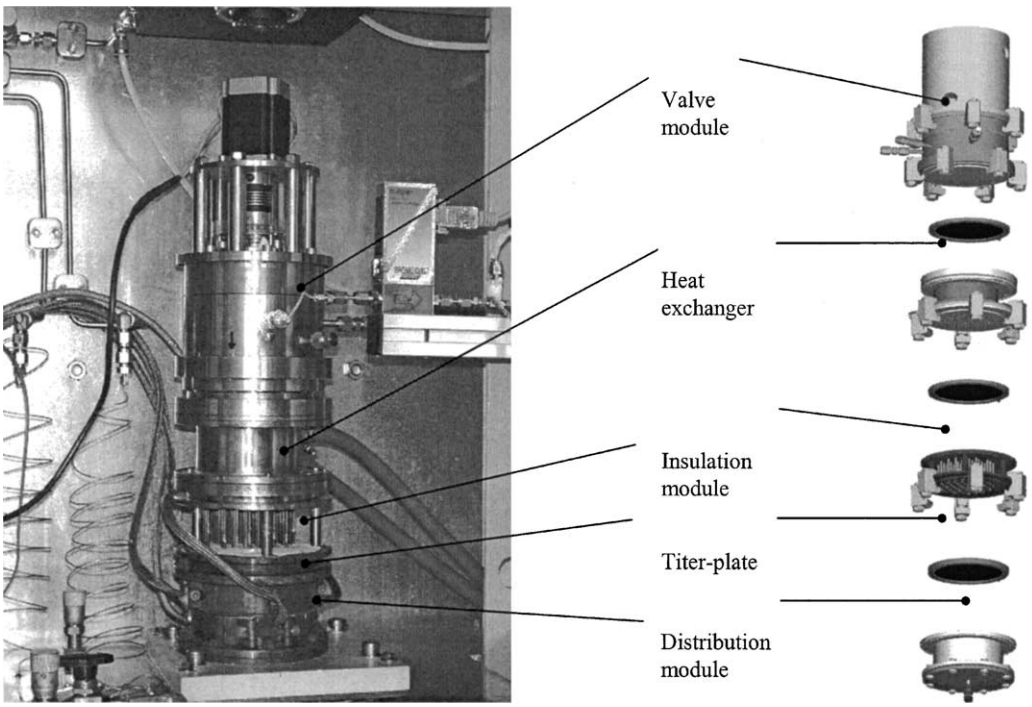

Fig. 21. Micro-structured screening reactor developed by Müller at al. [118].

module. After the reaction had taken place on the titer plate, the product passed an insulation module which separated the heated section of the parallel reactor from the unheated section and was further cooled by a heat exchanger module on top of it. The last module just above the heat exchanger module was a multiport valve which delivered the product gas to the gas-chromatograph. The heating capacity of the system allowed reaction temperatures up to 650 °C at pressure ranges between atmospheric pressure and 10 bar. Numerical calculations of the temperature field inside each titer plate verified very low mutual temperature effects between adjacent reaction chambers even for a "hot spot" situation (see Fig. 22), which was achieved by heat sinks positioned above and below the titer-plate. In order to fabricate appropriate titer plates coated with catalytically active layers, new coating techniques had to be developed [118]. Among others, simultaneous sputtering of metal and non-metal layers was used. During this process, the layer thickness of each component was either de- or increased, resulting in a homogeneous multi-component layer. Using this sputtering technique, the preparation time of a single titer plate with up to 48 reaction zones was reduced to less than 20 min. After the coating procedure, the titer-plates were inserted into the reactor to test the activity of the catalysts. The reaction conditions were held constant for all experiments. The reactor was heated up to 475 °C and held under a pressure of 1.2 bar. The heat exchanger was operated at 50 °C and the throughput for a single well was adjusted to 1 cm^3/min resulting in a residence time of 400 ms. A set of six binary mixtures of zirconium and platinum were produced by sputtering. Zirconium served as the inactive component which acted as a kind of dilutor for the known good activity of platinum. The samples showed good agreement between Pt content and catalytic activity. Catalysts prepared by the wash-coating method were used in order to check the reproducibility of the measurements. For another set of experiments, six metal salts (platinum, zirconium, molybdenum, nickel, silver, rhodium) were impregnated onto a titer-plate. The catalysts were pre-reduced inside the reactor with 5 vol.% hydrogen in 95 vol.% nitrogen at 250 °C. The results were recorded before and after the pre-reduction, indicating a good reproducibility in both cases. The conversion of methane with the rhodium catalyst was highest followed by platinum and could be improved by the pre-reduction. The activity could be maintained for 18 h TOS. To check for fluidic and thermal cross-talking the same six metal catalysts were coated in six rows on another titer-plate. Active catalysts were neighboured to less active catalysts. The two active rows (platinum and rhodium) did not have an effect on the neighboured less active rows (zirconium and silver). Thus cross-talking was not observed. In a next test, elementary, binary and ternary mixtures of the same metal catalysts were examined. Every mixture was deposited on four different wells to verify the reproducibility. Except for some of the ternary mixtures the results were well reproduced and consistent with the well-known high activity of rhodium and mixtures of rhodium and platinum. The latter showed the highest activity.

3.2.4. Ceramic micro-reactors for high-temperature applications

Knitter et al. [119] have designed and manufactured two types of ceramic micro-reactors by stereolithography,

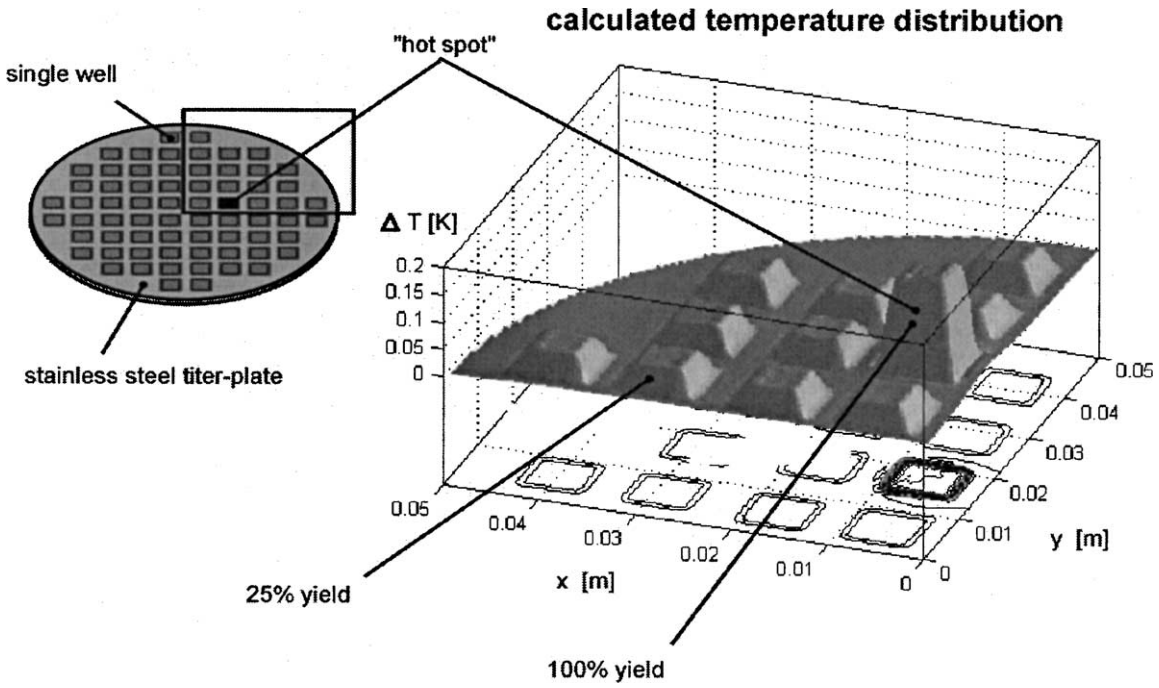

Fig. 22. Temperature distribution in the titer-plate determined by Müller et al. [118].

moulding in silicon, hot moulding and sintering which could withstand temperatures up to 1100 °C. The first reactor, a screening tool with exchangeable micro-structured platelets was sealed by highly polished surfaces (see Fig. 23). The second reactor had two separate and preheated inlets and took up two carrier plates. Glass ceramics were used for sealing of the second reactor. Due to the sealing techniques applied the reactors were not suitable for high pressure applications. Channel dimensions of both reactors ranged around 500 μm at a length of 20 mm. Lithium aluminate was used as a catalyst introduced into the catalyst carriers by a sol–gel method and subsequent calcination at 800 °C and sintering at 1000 °C.

Later on, Göhring et al. [120] applied the first type of ceramic micro-reactor for the partial oxidation of isoprene to citraconic anhydride at temperatures between 300 and 500 °C. $V_{75}Ti_{25}O_x$ was used as catalyst. The feed composition was 0.6 vol.% isoprene in air at a modified residence time of 6 g_{cat} min/mol_{tot}. Full conversion was achieved in the ceramic reactor at 400 °C already, whereas 430 °C were necessary for a metallic micro-reactor carrying channels of different material. Citraconic anhydride yields found for the ceramic reactor were higher at 420 °C than yields achieved with the metallic reactor. Oxidative coupling of methane was carried out in the second type ceramic reactor. $LiAlO_2$ as the active component was introduced in different ways on various carriers. Firstly, a sol–gel layer (1) was produced, secondly the metal salt solvents were in situ impregnated (2), thirdly micro-structures were machined into ceramic monoliths (3; 17% porosity) and fourthly polymer foam was coated with ceramic slurry revealing a monolithic structure (4) of 75% porosity. The experiments were carried out at ambient pressure and temperatures between 850 and 1000 °C at a feed flow rate of 100 cm^3/min and CH_4/O_2 ratios between 1 and 10. Similar yields were found for both monolithic catalysts being superior compared to the coated catalysts. Maximum conversion was achieved for all catalysts at a CH_4/O_2 ratio of 1 at 1000 °C which was as high as 60% for the ceramic monolith (3). The maximum C_2 selectivity of 30% was found for the ceramic monolith (3) at a conversion of 15%, a temperature of 900 °C and a CH_4/O_2 ratio of 4.

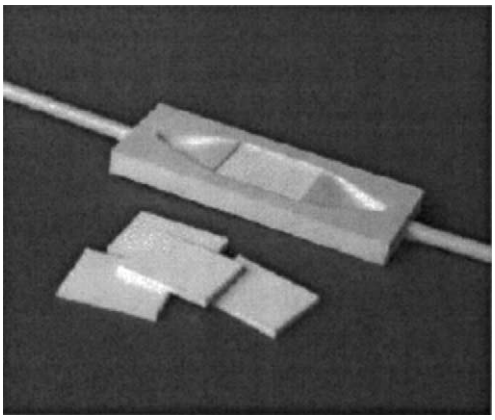

Fig. 23. Ceramic micro-reactor with catalyst carrier plates designed and manufactured by Göhring et al. [120].

A silicon nitride ceramic-based 2D-micro-combustor was presented by Tanaka et al. [121]. Micro-electro-mechanical system machining was applied to manufacture 2 and 4 cm^3 hydrogen combustors, which worked without a catalyst. The ceramic material was chosen, as silicon, glass and metals were believed to be not suitable for the high temperature

combustion reaction. The combustor was manufactured from silicon powder by spark plasma sintering at 200 bar and 1215 °C to get the silicon green compact. After mechanical micro-milling, the compact green was reaction sintered in nitrogen atmosphere. All layers of the combustor were stacked without bonding. The combustor was composed of two chambers. In the first chamber, mixing of hydrogen and air by shear flow was performed and the flame was maintained ideally in the centre of the chamber to minimise heat losses. The second chamber was designed to achieve complete combustion. Five types of combustors with different chamber depth and opening angle of the fillets for combustion air were tested. Experiments were carried out at a flow speed in the fuel nozzle of 11.5 m/s which corresponds to a *Re* number of 1300. The residence time in the first chamber amounted to 1 ms, and the heating power to 310 W. The location of the homogeneous reaction was visualised with an infrared imager. It was found that the chamber depth had to be significantly higher than the quenching distance of 640 μm assumed for the reaction to achieve complete combustion. Residual hydrogen between 0.1 and 0.2% was found for hydrogen equivalent ratios between 0.28 and 1. Lower values decreased the combustion temperature which led to incomplete combustion, higher values made the flow speed of the gases too high and thus shifted the combustion to the second chamber.

4. Combinations of micro-structured process engineering components for specific applications

Hessel et al. [122] demonstrated the Andrussov synthesis in one of the first combined laboratory-scale synthesis units consisting of a gas/gas micro-mixer, a reaction zone and a subsequent heat exchanger (see Fig. 24). The highly exothermic reaction, which is the formation of HCN out of methane and ammonia in a nitrogen/oxygen atmosphere (air), takes place at a temperature exceeding 1000 °C and a residence time of less than 1 ms. Educts were preheated to 600 °C in a mixing zone. The reaction zone was composed of the catalyst material itself (Pt) and consisted of 20 channels 250 μm long and 70 μm wide. After leaving the reaction zone the gases were cooled down in a cross-shaped counter flow heat exchanger. At almost complete methane conversion HCN yields up to 31% were found, which was approximately half the value achieved in the industrial process (60%) due to undesired total oxidation of methane to CO and CO_2. A comparison of the yields of this micro-reactor to metallic and ceramic monoliths (pore sizes ranging from 600 to 1200 μm) reveals superior performance of the smaller micro-channels compared to monoliths working in the laminar flow regime as small dimensions are beneficial at the low residence times applied.

Haas-Santo et al. [123] made use of the FZK cross-flow heat exchanger/reactor described in Section 3.2.2.1 for the oxidation of excess hydrogen stemming from electrolytic cells of future space vehicles. The equipment consisted not only of a micro-structured reactor (1 cm^3 volume) with integrated cooling channels but also of a micro-mixer for feed mixing and a micro-structured heat exchanger (1 cm^3 volume) put downstream for product cooling. All channel systems had dimensions of 200 μm × 70 μm. The reaction channels were coated by the sol–gel technique revealing a 2–3 μm thick alumina layer with pore diameters ranging between 1 and 5 nm having a maximum at 4 nm. Due to the preparation technique no surface area data could be obtained but a surface enhancement factor of 430 m^2/m^3 was determined. Pd was introduced as active component by wet impregnation. Subsequently, the catalyst was activated at 80 °C and reduced in H_2. Experiments performed with the miniaturised process engineering device at FZK revealed complete conversion after 120–150 s TOS at a flow rate of 1 μl/min H_2 and a stoichiometric amount of O_2. The cooling air flow was 20 μl/min. Direct ignition of the reaction occurred at 25 °C and outlet temperatures of the cooling air up to 220 °C were observed. The catalyst was stable for 200 h TOS. At Astrium laboratories, the project partner of FZK, three to five electrolysis cells were used to generate a H_2 flow of up to 1.16 μl/min revealing a liquid product (water) temperature of 40 °C at a cooling gas flow of 30 μl/mm. Steady state

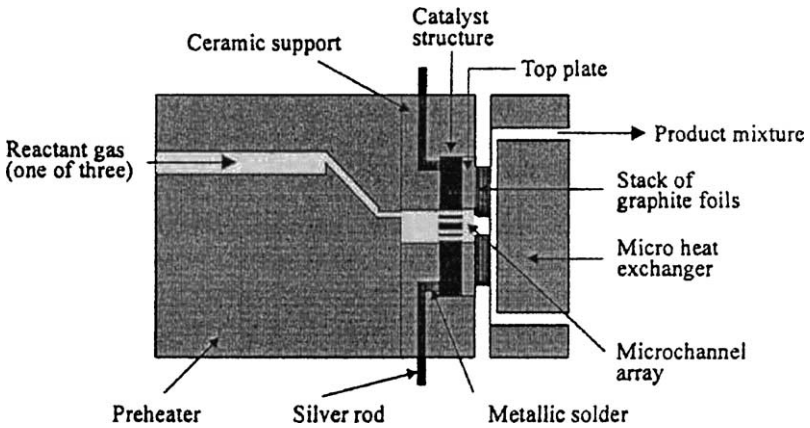

Fig. 24. Schematic of the micro-reactor assembly from Hessel et al. [122] for the Andrussov reaction.

of the system was achieved after 20 min when changing the number of cells feeding the system.

Mayer et al. [124] used an electrically heated micro-heat exchanger, a micro-mixer and a honeycomb reactor all developed by FZK for the partial oxidation of methane to syngas. There are various reasons for the application of micro-reactors in this reaction. Firstly, a safe operation of the explosive mixture is possible [125]. Due to the channel diameters being smaller than for conventional ceramic monoliths, the surface to channel volume is higher. Compared to packed beds or porous solid foams, a smaller pressure drop is achievable. The reaction takes place at temperatures around 1000 °C, a pressure of 25 bar and residence times in the order of few to several hundred milliseconds. Conventionally, the process is performed at metal loaded ceramic supports. From calculations hot spot formation up to 2320 °C might occur which was expected to be minimised by the metallic catalyst. The process was run autothermally by a combination of exothermic methane oxidation and endothermic reforming. The metallic honeycomb served as a medium for axial heat transfer between both reaction zones. Rhodium was chosen as reactor material which was the catalytically active species as well and has a high thermal conductivity of 120 W/(m K). 200 μm wide and 5 mm long channels were manufactured for the honeycomb reactor by mechanical micro-machining of pure rhodium foils of 220 μm thickness. By wire-EDM 60 μm wide channels 130 μm deep were produced. Twenty-three foils carrying 28 channels each were electron beam and laser welded to get a sealed honeycomb which was pressure resistant up to 30 bar. During diffusion bonding, which was followed as an alternative route for sealing, large angled grin boundaries were formed. The honeycomb structure was then put into a ceramic holder carrying the heating wire of 150 W heating power. The maximum temperature of the reactor amounts to 1200 °C. The feed was mixed in the micro-mixer, preheated in the heat exchanger to 300 °C, fed to the reactor and quenched in conventional equipment afterwards. 1 dm^3/min to 10 dm^3/min feed composed of 60 vol.% methane, 30 vol.% oxygen and 10 vol.% argon for the standard experiments were sent through the reactor at a pressure between ambient and 25 bar. The activity increased with TOS up to 20 h. At 650 °C, mostly water and carbon dioxide were produced at a 10% conversion level. After ignition of the reaction at catalyst temperatures between 550 and 700 °C, a temperature exceeding 1000 °C was reached within 1 min and mainly carbon monoxide and hydrogen were formed. Conversion levels of 62% for methane and 98% for oxygen were achieved at 1190 °C for the fully activated catalyst. Due to the low residence time high selectivities towards hydrogen (78%) and carbon monoxide (92%) were found under standard testing conditions at a low carbon dioxide selectivity of 10% which decreased with increasing temperature. Full oxygen conversion was achieved when the methane/oxygen ratio was decreased from 2 to 1.5. Under these conditions, methane conversion was 96% and hydrogen and carbon monoxide selectivities of 80% and 85% were found. These effects were assumed to stem from the increased heat generation by enhanced methane combustion. Changing the GHSV from $2 \times 10^5\ h^{-1}$ to $1.2 \times 10^6\ h^{-1}$ lead to a 10% drop of methane conversion and deteriorated hydrogen and carbon monoxide yields which was at least partially attributed to mass transport limitations. To check for mass transport limitations, the channel dimensions were varied from 60 to 120 μm width at constant depth of about 130 μm. No effect of the channel diameter on conversion and selectivities was found at 900 °C. At 1090 °C, the reaction was in an autothermal mode. No deactivation of the catalyst could be observed during 200 h TOS. However, some 0.1 wt.% material was lost from the monolith which was attributed to sublimation effects [66]. To check for the effect of using air instead of pure oxygen, the inert gas content was increased at constant GSHV, which lead only to a slight deterioration of the hydrogen and carbon monoxide selectivities due to the decreasing generation of heat. The thermodynamic equilibrium could not be reached likely because of the low residence time of less than 1 ms. Homogeneous reactions might well have taken place as the residence time before the quenching section was 30 times higher than the residence time in the reaction zone. At flow rates exceeding 3 dm^3/min, autothermal conditions were reached. Increasing the pressure from 1 to 12 bar at constant flow rate, lead to lower conversion and selectivities towards hydrogen and carbon monoxide. At 12 bar, a selectivity of 3% towards ethylene was found. At a pressure of 20 bar, using air instead of oxygen and a 20 mm long honeycomb, lower methane conversion and selectivities towards CO and hydrogen were found as well. Higher pressures lead to soot formation in the section after the honeycomb and before the quench. It was proposed to control the heat formation by adding methane downstream in the reaction zone by nozzles to avoid product back diffusion. Compared to results from literature [126] the degree of conversion and the hydrogen selectivities of the rhodium monolith outperformed both metal coated foam monoliths, Pt–Rh gauzes and extruded monoliths. This was partially attributed to the expected higher activity of the rhodium monolith, but also to the lower cross-sectional channel area of the metallic monolith, which reduced mass-transfer limitations and the improved heat conductivity, which enhanced the transport from the exothermic to the endothermic area of the monolith.

An early work from Tonkovich et al. [127] dealt with a heat exchanger/reactor containing catalyst powder for the partial oxidation of methane for distributed hydrogen production. The intention was to run the reaction safely in a micro-structured reactor due to the short residence times applied and the improved heat removal avoiding hot spot formation. A 5 wt.% rhodium catalyst was applied on mesoporous silica. The reactor with a total size of 7 cm × 3.8 cm × 0.4 cm consisted of nine plates each carrying 37 channels of 254 μm width and a large depth of 1.5 mm at a length of 35 mm. Before the reactor, a heat exchanger was installed as preheater supplied with energy from a heating

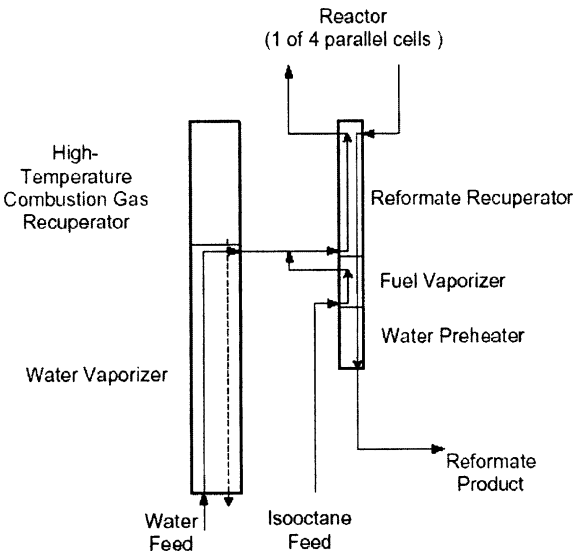

Fig. 25. Flow scheme of the supply system of the steam reformer developed by Whyatt et al. [128].

fluid. After the reactor, the products were quenched in another heat exchanger by cooling fluid. All three devices were integrated into a stack and sealed with nickel gaskets. A feed of 100 cm^3/min methane and 50 cm^3/min oxygen was introduced into the reactor at a pressure loss of less than 2.5 mbar. The residence time of the reaction was as high as 50 ms. Sixty percent conversion was found together with a high carbon monoxide selectivity of 70% at a temperature of 700 °C.

Later on, Whyatt et al. [128] presented results generated at a combined system of independent evaporators, heat exchangers and reformers for iso-octane steam reforming. Four integrated reformers/heat exchangers switched in series were fed by four independent water vaporizers which got their energy by combustion of anode-off gas performed in an independent burner (see Fig. 25). The fuel was evaporated in a second unit which also preheated the steam/iso-octane vapour in a second stage. This unit was heated by the hot reformate. The reactors were designed as cross-flow heat exchangers. Their energy supply was stemming from the burner off-gas which was sent to the water evaporators afterwards. The machining of micro-structured components was done by photochemical etching and diffusion bonding. The reformers achieved up to 98.6% conversion at a reaction temperature of 750 °C, a S/C ratio of 3 and a product composition of 70.6% H_2, 14.6% CO, 13.7% CO_2 and 0.9% CH_4. Doubling the reformate output was claimed to be feasible in 20 s. The reformate was sufficient to feed a 13.7 kW PEM fuel cell. An overall efficiency of 44% of the whole system was calculated assuming 90% conversion and 100% selectivity for the water-gas-shift reaction and 54% overall efficiency for the fuel cell.

Then Whyatt et al. [129] designed two reformer reactors of 107 and 68 cm^3 total volume for reforming of methane, propane, butane, ethanol, methanol, iso-octane and a mixture of hydrocarbons simulating sulphur-free gasoline. The two reactors were tested in a test-bench in combination with micro-structured heat exchangers for feed preheating using product (hot reformate) and evaporators for water and liquid feed preheating. The experiments were carried out at ambient pressure. All hydrocarbons were tested at a S/C ratio of 3, all alcohols at a corresponding oxygen to carbon ratio. Decreasing conversion was found for the various fuels with increasing feed-rates except for methanol due to the very high reaction temperature of 725 °C. Table 4 summarises some of the results presented for the various fuels. The proprietary catalyst did show only minor deactivation after 70 h TOS. It was deactivated reversibly by sulphur.

Jones et al. [130] presented an integrated and miniaturised device for methanol steam reforming consisting of two evaporators/preheaters, a reformer and a combustor with a total volume of less than 0.2 cm^3 for a power range between 50 and 500 mW, which corresponds to flow rates of 0.03–1 cm^3/h liquid methanol/water mixture. The energy for the steam reforming reaction was transferred from the combustor device having 3 W power capacity which was fed by a H_2/O_2 mixture for start-up and later on by up to 0.2 cm^3/h methanol and up to 14 cm^3/min air. The combustor was said to have a volume of less than 1 mm^3, the reformer volume being higher (5 mm^3). From Table 5 given by Holladay et al. [131], it can be seen that even at an efficiency as bad as 5% a fuel reformer outperforms a Li-ion battery. In this later paper, more detailed data on the device were given. The flow rate of methanol for the reforming reaction is said to be 0.02–0.1 cm^3/h and more than 99% conversion were achieved. The flow rate going to the burner ranged between

Table 4
Conversion, power density, reaction temperature and reformate composition for various fuels according to Whyatt et al. [129]

Fuel	Methane	Propane	Butane	Methanol	Ethanol	Iso-octane	Sulphur-free gasoline
C_1 feed-rate (10^{-4} mol/s)	8.13	8.34	11.62	8.07	10.4	7.51	10.8
Conversion (%) to C_1	95	99.8	99	100	98.9	100	99.6
Power density (kW/dm^3)	2.26	4.06	5.98	1.69	2.25	1.70	2.27
Reaction temperature (°C)	725	775	751	725	724	725	725
Dry reformate composition							
H_2 (%)	75.7	72.3	71.6	70.4	70.0	70.9	70.1
CO (%)	12.7	14.8	14.6	14.1	13.7	14.7	14.9
CO_2 (%)	10.4	12.0	12.9	14.9	15.2	13.3	14.1
CH_4 (%)	2.0	0.7	0.8	0.6	0.9	1.1	0.9

Table 5
Energy density of various cells and fuels from Holladay et al. [131]

Technology	Energy density (kW_e h/l)	Energy density (kW_e h/kg)	Comments
Primary cells	–	–	Not rechargeable
Alkaline	0.330	0.125	–
Zn-air	1.050	0.340	–
$Li/SOCl_2$	0.700	0.320	–
Secondary cells	–	–	Rechargeable
Lead acid	0.070	0.035	–
Ni-cad	0.055	0.035	–
Ni-metal hydride	0.175	0.050	–
Li-ion	0.200	0.120	–
Li-polymer	0.350	0.200	Anticipated
Hydrocarbons			
Methanol	4.384	5.6	Thermal energy
Butane	7.290	12.60	Thermal energy
iso-Octane	8.680	12.34	Thermal energy

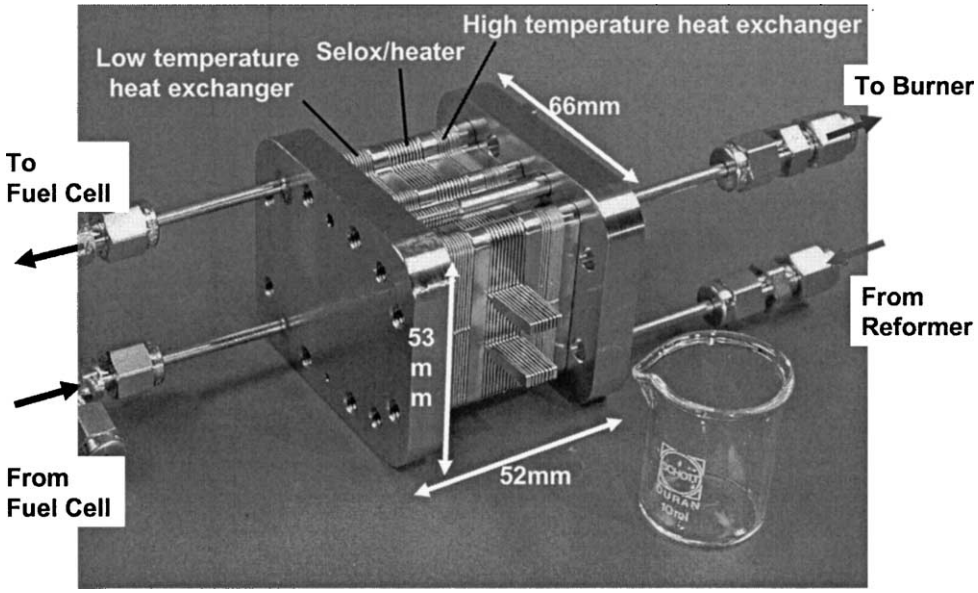

Fig. 26. Integrated reactor/heat-exchanger for the selective oxidation of carbon monoxide. *Source*: IMM.

0.1 and 0.4 cm^3/h. Combustion air flow was 8–20 cm^3/min. The burner temperature exceeded 400 °C. The thermal power of the device was 200 mW at an efficiency of 9%. Assuming a efficiency of the fuel cell of 60% and a hydrogen conversion of 80%, the net efficiency of the system amounted to 4.5% and the power output was 100 mW.

Delsmann et al. [132] presented the concept of an integrated reformer system developed in the framework of the European project MiRTH-e. There, an integrated system is built based upon methanol steam reforming to supply hydrogen to a fuel cell, which is designed to generate 100 W electrical power. The vaporisation of the feed is done in an integrated vaporiser/heat exchanger making use of the hot off-gas of the anode afterburner. The energy supply for the endothermic steam reforming comes from the residual hydrogen of anode off-gas, which is oxidised at a $Pt/A1_2O_3$ catalyst. A Cu/ZnO catalyst is applied for steam reforming [31]. Finally, the anode off-gas of the fuel cell is used to take up the heat generated by the selective oxidation reactor. Fig. 26 shows a prototype of the integrated selective oxidation reactor/heat exchanger manufactured by IMM. An overall efficiency of 35% was calculated for the design.

5. Novel approaches for micro-structured reactors

This last chapter has the intention to show up some alternative methods of achieving micro-structured reactors and proposals for new materials, which were presented recently in the literature. It does not at all claim for completeness. Besides metallic and ceramic monoliths, which will not be covered by this paper, few alternative approaches for manufacturing micro-structures will be discussed.

Schouten et al. [31] proposed the application of refractory metals and aluminium intermetallics which have high melting points, and a good corrosion resistance, which may be

further improved by niob and hafnium films. The materials have low thermal expansion and some of them have high heat conductivity in the range between 25 and 50% of the value known for aluminium.

Wolfrath [133] applied aluminoborosilicate glass fibres for the dehydrogenation of propane, a highly exothermic reaction ($\Delta H_r = 129$ kJ/mol). The high reaction temperatures required by the thermodynamics lead to thermal cracking, which lowers the selectivity due to coke deposition on the catalyst surface. Thus, the coke has to be removed by combustion periodically [134]. The fibres, having a diameter of 7 μm and a surface area of 2 m^2/g were leached with HCl to remove the non-silicon compounds revealing a surface area of 290 m^2/g. Covered with γ-alumina by precipitation the fibres had still a surface area of 100–230 m^2/g and were thermally stable up to 800 °C. Pt and Sn were introduced as catalysts by impregnation. The reactor was filled with threads of filaments which were for some experiments enclosed in a tubular Pd/Ag (23 wt.%) membrane of 70 μm thickness. The porosity of the filamenteous packing amounted to 0.8. The residence time distribution of the packing was found to be narrower compared to packed beds of 130 and 1100 μm average particle size. The pressure drop was five times smaller for the packing compared to a packed bed of 130 μm average particle size. Catalyst testing was performed at 550 °C, 1.4 bar and a residence time of 3 s at constant catalyst mass of 0.375 g. Similar conversion but a higher selectivity (95%) compared to the packed bed (88%) were found. Introducing the membrane into the reactor lead to a conversion of 30%, which exceeded the equilibrium value of 22%.

This was attributed to a permanent and efficient removal of the hydrogen out of the product stream by radial diffusion. Selectivity was increased to 97%, which was attributed to the lower hydrogen concentration surpressing hydroisomerisation and hydrogenolysis reactions [134,135]. However, an enhanced deactivation of the catalyst was observed. The principle of the reactor may be used in future to carry out reaction and regeneration of the catalyst in parallel (see Fig. 27). Long-term runs were performed at 550 °C, 1 bar and a residence time of 170 ms [134]. Pure propane was fed in the first zone, whereas hydrogen was oxidised by air in the second. The feeds were switched between the zones every 85 min [134]. After the first cycle, conversion dropped from 16 to 7% and the catalyst could not be fully regenerated. After four cycles, the conversion profiles were better reproducible between 7 and 5%. However, the selectivities were determined between 95 and 97%, which exceeds by far the values found for the industrial process (80–90%).

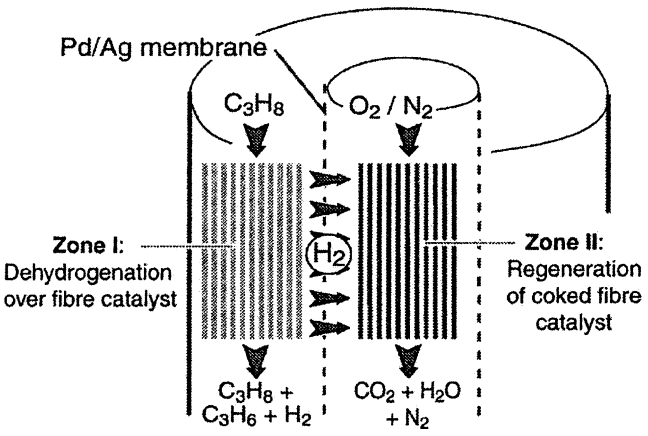

Fig. 27. Scheme of the membrane reactor with both zones packed with filamentous catalyst from Wolfrath et al. [133].

Another approach to gain the advantages of microstructures in order to avoid high pressure drops, heat and mass-transfer limitations and unequal flow distributions was presented by Louis et al. [136]. ZSM-5 zeolites were coated on stainless steel grids as an alternative to granulates or pellets usually applied in zeolitic catalysis. The H-ZSM-5 coatings were tested for the one-step oxidation of benzene by nitrous oxide to phenol. The grids had a total area of 9 cm^2, a wire diameter of 250 μm and a mesh size of 800 μm. Fifteen grids formed a stack separated by steel rings. By acid pre-treatment of the grids defects were generated which are known to become crystallisation centres during the synthesis of the zeolite. The synthesis gel was prepared and after 2–3 h ageing it was poured into the support packing. After three synthesis runs of 40 h duration at 171 °C the coating was calcined and exchanged with ammonium chloride to get the protonised form. A Si/Al ratio of 65 and a BET surface area of 302 m^2/g were found for the zeolite. Loadings of about 10, 55 and 95 g/m^2 zeolite, the latter corresponding to a layer thickness of 38 μm were found after the individual synthesis steps. Three loadings were regarded as an upper limit, as the grids tended too loose their void fraction at higher loadings. The coatings were tested for benzene oxidation at ambient pressure and a temperature of 350 °C at a feed flow rate of 60 cm^3/min and a composition of 3.8–14.6 mol% benzene and 0.4–16.7 mol% nitrous oxide in nitrogen. Increasing the nitrous oxide/benzene ratio was beneficial for the conversion, which was found to be in line with literature [137,138], but phenol selectivity deteriorated. Phenol selectivities as high as 99% were found at four times molar excess of benzene. For nitrous oxide/benzene ratios greater than 1.25, a rate law with zero order concerning nitrous oxide was found. The following expression was set up for the reaction assuming a plug flow reactor:

$$X = 1 - (1 + (n-1)k\tau' C_{B0}^{n-1})^{1/1-n} \quad (11)$$

C_{B0} being the benzene inlet concentration. For a modified residence time $\tau' = 696$ kg s/m^3 and a reaction order $n = 0.6$, the rate constants shown in Table 6 were determined for the coating, home-made H-ZSM-5 powder and a commercial catalyst from Süd-Chemie.

Thus, the coating had a 70% higher activity compared to the randomly packed beds. It was not excluded, that this superior performance was at least partially caused by iron incorporation from the steel grid into the zeolite.

Table 6
Comparison of rate constants determined Louis et al. for the partial oxidation of benzene by N_2O [136]

Catalyst type	k (10^{-4} mol$^{0.4}$ m$^{1.8}$/(kg s))
Structured coating	1.7
Home-made H-ZSM-5 powder	1.0
Comm. H-MFI-90	1.2

6. Summary

With recognising chemical micro-processing using micro-reactors as a novel means for chemistry and chemical engineering, more and more work is dedicated to the field of heterogeneous catalysis and the list of publications made here is indeed impressive meanwhile. A selection of this work is referred and reported in this review.

Diverse gas-phase reactions have been investigated in micro-reactors, among them (partial) oxidations, hydrogenations, dehydrogenations, dehydrations, and reforming processes. Particular attention has been drawn to achieve excellent temperature control and to prevent hot-spots. So, for many reactions increases in selectivity were found. Especially, many examples of partial oxidations were described, including processes of utmost industrial importance such as ethylene oxide synthesis. Within consecutive processes as, e.g. given for multiple hydrogenations, high selectivity was achieved for species that are thermodynamically not the most stable molecule such as monoenes. Also, increases in conversion were achieved, e.g. by processing at high pressure and high temperature, often in the explosive regime. As a consequence, high space–time yields were reported as well. Frequently, reactor performance better compared to fixed-bed technology was achieved. However, in many cases it turned out the state-of-the-art catalysts are not active enough and need to be improved ("engineered catalysts") to come up to the demands of this novel tool of chemistry. Process safety was found to be high when using micro-reaction devices; intrinsic safety in former explosive regimes was ascribed. With respect to process optimisation, fast serial screening of process parameter variation was conducted, at low sample consumption.

Besides scouting studies, followed by thorough micro-reactor technology evaluation and benchmarking to conventional technology, the investigations tend more and more to undergo detailed catalytic studies, aiming at reaction mechanism, kinetics and catalyst properties. It is not only the more accurate setting of process parameters, but the performance of studies under former 'hidden conditions' that makes micro-reactors attractive. Thereby, they considerably expand the possibilities of the tool portfolio for heterogeneous catalysis.

It is particularly noteworthy that first criteria are proposed to judge if mass and heat transfer limitations are present. Knowing such borders will boost micro-reaction technology to its maximum performance, but will avoid operation beyond.

7. Outlook

While this article focused on fundamental science investigations, a few examples of commercial applications were given as well, e.g. for industrial process optimisation with bench-scale tools, for sub-kW energy generation in small units by fuel processing, and for highly-parallel catalyst screening. Much more such work is on-going or undisclosed. Taking this into account, there are more than vistas for much larger micro-channel based processing units; the build-up of pilot-plant scale devices, having gas flows in the m^3/min range or energy generation/consumption in the 1–50 kW range, is currently undertaken by several groups and reports on their functioning will be given in near future.

As a result of all these scientific and technical investigations undertaken so far, we now have a clear view what can be done with micro-reactors. It is not only that we qualitatively know what, e.g., improved heat transfer may induce in micro-channel processing; there exists well-documented quantitative information on the achievements to be expected, as e.g. particularly given for the ethylene oxide synthesis and the oxidation of ammonia. This in turn poses demands on optimising micro-fabrication, rendering devices to be more effective, costly, or productive. From literature and probably more by self-made experience, we also know about the limits and obstacles when using micro-reactors. In a short sentence, the field is beyond infancy and has become mature.

When we define the achievement of proper micro-fabrication techniques as Phase I, relating to a time period of 1990–2000 or so, one could say that we are now busy with Phase II, a comprehensive characterisation of micro-reaction devices, mainly involving experts from chemistry and chemical engineering, e.g. from heterogeneous catalysis. This covers a period maybe starting 1998 up to now. Since about two years, Phase III has been marked the beginning of; dedicated to the commercial supply of micro-reactors and the truly and sober search for commercial applications.

Formerly, wide-spread use of micro-devices for scientific and industrial investigations on gas-phase processing was strongly hindered by restricted supply as a consequence of the enormous efforts and thus high costs to make such micro-structures. In turn, the supply of micro-reactors is today much better than in recent years. Several companies, most of them located in Germany, define micro-reactors as their core business or at least as major business branch. Such distribution chains are supplemented by similar supply and further development offers by institutes. As a consequence, micro-reactors and gas-phase micro-devices meanwhile can be purchased off-the-shelf. A first catalogue with many such products is on the market. Even complete plants are available. In the micro-technology domain, the commercial success thereof sometimes being questioned, micro-reactors have be-

come an accepted field with first evidence for commercial prospect, hopefully increasing in future. Industry stands undoubtedly behind this technology and is more and more using it [139].

References

[1] M. Fichtner, T. Ludwig, R. Wunsch, K. Schubert, Scientific Reports Forschungszentrum Karlsruhe, FZKA 6080, Karlsruhe, 1998, p. 121.
[2] W.E. TeGrotenhuis, D.L. King, K.P. Brooks, B.J. Golladay, R.S. Wegeng, in: Proceedings of the 6th International Conference on Microreaction Technology, 2002, New York, AIChE (2002) p. 18.
[3] J.B. Anderson, Chem. Eng. Sci. 18 (1963) 147.
[4] J.M. Commenge, L. Falk, J.P. Corriou, M. Matlosz, in: Proceedings of the 5th International Conference on Microreaction Technology, 2001, Springer, Berlin, 2002, p. 131.
[5] O. Levenspiel, Chemical Reaction Engineering, Wiley, New York, 1999, p. 388.
[6] S. Walter, M. Liauw, in: Proceedings of the 4th International Conference on Microreaction Technology, 2000, New York, AIChE (2000) 209.
[7] R. Aris, Proc. R. Soc., Lond., Ser. A 235 (1956) 67.
[8] J.M. Commenge, L. Falk, J.P. Corriou, M. Matlosz, AIChE J. 48 (2002) 345.
[9] K.F. Jensen, S.K. Ajmera, S.L. Firebaugh, T.M. Floyd, A.J. Franz, M.W. Losey, D. Quiram, M.A. Schmidt, Microfabricated chemical systems for product screening and synthesis, in: W. Hoyle (Ed.), Automated Synthetic Methods for Speciality Chemicals, Royal Society of Chemistry, London, 2000, p. 14.
[10] K.F. Jensen, S.L. Firebaugh, A.J. Franz, D. Quiram, R. Srinivasan, M.A. Schmidt, Integrated gas phase micro-reactors, in: J. Harrison, A. van den Berg (Eds.), Micro Total Analysis Systems, Kluwer Academic Publishers, Dordrecht, 1998, p. 463.
[11] K.F. Jensen, Chem. Eng. Sci. 56 (2001) 293.
[12] R. Srinivasan, I.-M. Hsing, P.E. Berger, K.F. Jensen, S.L. Firebaugh, M.A. Schmidt, M.P. Harold, J.J. Lerou, J.F. Ryley, AIChE J. 43 (1997) 3059.
[13] T. Pignet, L.D. Schmidt, Chem. Eng. Sci. 29 (1974) 1123.
[14] I.M. Hsing, R. Srinivasan, M.P. Harold, K.F. Jensen, M.A. Schmidt, Chem. Eng. Sci. 55 (2000) 3.
[15] A.J. Franz, D.J. Quiram, R. Srinivasan, I.-M. Hsing, S.L. Firebaugh, K.F. Jensen, M.A. Schmidt, in: Proceedings of the 2nd International Conference on Microreaction Technology, 1998, New York, AIChE (1998) 33.
[16] A.J. Franz, S.K. Ajmera, S.L. Firebaugh, K.F. Jensen, M.A. Schmidt, in: Proceedings of the 3rd International Conference on Microreaction Technology, 1999, Springer, Berlin, 2000, p. 197.
[17] A.J. Franz, K.J. Jensen, M.A. Schmidt, in: Proceedings of the 3rd International Conference on Microreaction Technology, 1999, Springer, Berlin, 2000, p. 267.
[18] A. Zheng, F. Jones, J. Fang, T. Cui, in: Proceedings of the 4th International Conference on Microreaction Technology, 2000, New York, AIChE (2000) p. 284.
[19] T. Cui, J. Fang, J. Maxwell, J. Gardner, R. Besser, B. Elmore, in: Proceedings of the 4th International Conference on Microreaction Technology, 2000, New York, AIChE (2000) p. 488.
[20] R. Besser, M. Prevot, in: Proceedings of the 4th International Conference on Microreaction Technology, 2000, New York, AIChE (2000) p. 278.
[21] R.S. Besser, X. Quyang, H. Surangalikar, Chem. Eng. Sci. 58 (2003) 19.
[22] R. Besser, X. Quyang, H. Surangalikar, in: Proceedings of the 6th International Conference on Microreaction Technology, 2002, New York, AIChE (2002) p. 254.
[23] H. Surangalikar, X. Quyang, R.S. Besser, Chem. Eng. J. 4140 (2002) 1.
[24] S. Zhao, R. S. Besser, in: Proceedings of the 6th International Conference on Microreaction Technology, 2002, New York, AIChE (2002) p. 289.
[25] X. Ouyang, R. Besser, in: Proceedings of the AIChE Spring Meeting Topical Conference, 2002, New York, AIChE, p. 254.
[26] K. Kusakabe, D. Miyagawa, Y. Gu, H. Maeda, S. Morooka, in: Proceedings 5th International Conference on Microreaction Technology, 2001, Springer, Berlin, 2002, p. 70.
[27] E. Cao, K.K. Yeong, A. Gavriliidis, in: Proceedings of the 6th International Conference on Microreaction Technology, 2002, New York, AIChE (2002) p. 76.
[28] D.A. Robb, P. Harriott, J. Catal. 35 (1974) 176.
[29] A.V. Pattekar, M.V. Kothare, S.V. Karnik, M.K. Hatilis, in: Proceedings of the 5th International Conference on Microreaction Technology, 2001, Springer, Berlin, 2002, p. 332.
[30] Ch. Alépée, R. Maurer, L. Parette, L. Vulpecu, Ph. Renaud, A. Renken, in: Proceedings of the 3rd International Conference on Microreaction Technology, 1999, Springer, Berlin, 2000, p. 514.
[31] J.C. Schouten, E.V. Rebrov, M.H.J.M. de Croon, Chimia 56 (2002) 627.
[32] N.G. Wilson, T. McCreedy, J. Chem. Soc., Chem. Commun. (2000) 733.
[33] G. Veser, G. Friedrich, M. Freygang, R. Zengerle, in: Proceedings of the 3rd International Conference on Microreaction Technology, 1999, Springer, Berlin, 2000, p. 674.
[34] G. Veser, Chem. Eng. Sci. 56 (2001) 1265.
[35] H. Löwe, W. Ehrfeld, K. Gebauer, K. Golbig, O. Hausner, V. Haverkamp, V. Hessel, T. Richter, in: Proceedings of the 2nd International Conference on Microreaction Technology, 1998, New York, AIChE (1998) p. 63.
[36] H. Kestenbaum, A. Lange de Olivera, W. Schmidt, F. Schüth, W. Ehrfeld, K. Gebauer, H. Löwe, T. Richter, Stud. Surf. Sci. Catal. 130 (2000) 2741.
[37] S.V. Tsybulya, G.N. Kryukova, S.N. Goncharova, A.N. Shmakow, B.S. Balzhinimaev, J. Catal. 154 (1995) 194.
[38] R.A. van Santen, P.C.E. Kuipers, Adv. Catal. 35 (1987) 265.
[39] H. Kestenbaum, A. Lange de Olivera, W. Schmidt, F. Schüth, W. Ehrfeld, K. Gebauer, H. Löwe, T. Richter, D. Lebiedz, I. Untiedt, H. Züchner, Ind. Eng. Chem. Res. 41 (2002) 710.
[40] R. Haul, G. Neubauer, J. Catal. 105 (1987) 39.
[41] R. Grant, R.M.A. Lambert, J. Catal. 92 (1985) 364.
[42] O. Wörz, K.-P. Jäckel, T. Richter, A. Wolf, Chem. Eng. Technol. 24 (2001) 138.
[43] S.K. Ajmera, C. Delattre, M.A. Schmidt, K.F. Jensen, in: Proceedings of the 5th International Conference on Microreaction Technology, 2001, Springer, Berlin, 2002, p. 414.
[44] S.K. Ajmera, C. Delattre, M.A. Schmidt, K.F. Jensen, Sens. Actuators B 82 (2002) 297.
[45] D.R. Rainer, M. Koranne, S.M. Vesecky, D.W. Goodman, J. Phys. Chem. B 101 (1997) 10769.
[46] S.H. Oh, G.B. Fisher, J.E. Carpenter, D.W. Goodman, J. Catal. 100 (1986) 360.
[47] S.H. Oh, C.C. Eickel, J. Catal. 128 (1991) 526.
[48] R.H. Venderbosch, W. Prins, W.P.M. van Swaaij, Chem. Eng. Sci. 53 (1998) 3355.
[49] S.K. Ajmera, C. Delattre, M.A. Schmidt, K.F. Jensen, J. Catal. 209 (2002) 401.
[50] G.S. Zafiris, R.J. Gorte, J. Catal. 140 (1993) 418.
[51] S.K. Ajmera, M.W. Losey, K.F. Jensen, M.A. Schmidt, AIChE J. 47 (2001) 1639.
[52] E.N. Shapatina, V.L. Kuchaev, B.E. Penkovoi, M.I. Temkin, Kinet. Catal. 17 (1976) 559.
[53] W.L. Allen, P.M. Irving, W.J. Thomson, in: Proceedings of the 4th International Conference on Microreaction Technology, 2000, New York, AIChE (2000) p. 351.

[54] P.M. Irving, W.L. Allen, T. Healey, Q. Ming, in: Proceedings of the 5th International Conference on Microreaction Technology, 2001, Springer, Berlin, 2002, p. 286.
[55] G. Wießmeier, D. Hönicke, in: Proceedings of the 2nd International Conference on Microreaction Technology, 1998, New York, AIChE (1998) p. 24.
[56] G. Wießmeier, D. Hönicke, Ind. Eng. Chem. Res. 35 (1996) 4412.
[57] G. Wießmeier, K. Schubert, D. Hönicke, in: Proceedings of the 1st International Conference on Microreaction Technology, 1997, Springer, Berlin, 1997, p. 20.
[58] A. Kursawe, R. Pilz, H. Dürr, D. Hönicke, in: Proceedings of the 4th International Conference on Microreaction Technology, 2000, New York, AIChE (2000) p. 227.
[59] A. Kursawe, D. Hönicke, in: Proceedings of the 4th International Conference on Microreaction Technology, 2000, New York, AIChE (2000) p. 153.
[60] A. Kursawe, D. Hönicke, in: Proceedings of the 5th International Conference on Microreaction Technology, 2001, Springer, Berlin, 2002, p. 240.
[61] C. Mao, M. Vannice, Appl. Catal. A 122 (1995) 61.
[62] A. Kursawe, E. Dietzsch, S. Kah, D. Hönicke, M. Fichtner, K. Schubert, G. Wießmeier, in: Proceedings of the 3rd International Conference on Microreaction Technology, 1999, Springer, Berlin, 2000, p. 213.
[63] E. Dietzsch, D. Hönicke, M. Fichtner, K. Schubert, G. Wießmeier, in: Proceedings of the 4th International Conference on Microreaction Technology, 2000, New York, AIChE (2000) 89.
[64] S. Kah, D. Hönicke, in: Proceedings of the 5th International Conference on Microreaction Technology, 2001, Springer, Berlin, 2002, p. 397.
[65] P. Pfeifer, M. Fichtner, K. Schubert, M.A. Liauw, G. Emig, in: Proceedings of the 3rd International Conference on Microreaction Technology, 1999, Springer, Berlin, 2000, p. 372.
[66] P. Pfeifer, M. Fichtner, K. Schubert, M.A. Liauw, G. Emig, in: Proceedings of the 6th International Conference on Microreaction Technology, 2002, New York, AIChE (2002) p. 125.
[67] R. Wunsch, M. Fichtner, K. Schubert, in: Proceedings of the 3rd International Conference on Microreaction Technology, 1999, Springer, Berlin, 2000, p. 625.
[68] P. Reuse, P. Tribolet, L. Kiwi-Minsker, A. Renken, in: Proceedings of the 5th International Conference on Microreaction Technology, 2001, Springer, Berlin, 2002, p. 322.
[69] E.V. Rebrov, G.B.F. Seijger, H.P.A. Calis, M.H.J.M. de Croon, C.M. van den Bleek, J.C. Schouten, Appl. Catal. A 206 (2001) 125.
[70] E.V. Rebrov, G.B.F. Seijger, H.P.A. Calis, M.H.J.M. de Croon, C.M. van den Bleek, J.C. Schouten, in: Proceedings of the 4th International Conference on Microreaction Technology, 2000, New York, AIChE (2000) p. 250.
[71] V. Cominos, S. Hardt, V. Hessel, G. Kolb, H. Löwe, M. Wichert, R. Zapf, A methanol steam micro-reformer for low power fuel cell applications, Chem. Eng. Commun., in press (2004).
[72] R. Zapf, C. Becker-Willinger, K. Berresheim, H. Bolz, H. Gnaser, V. Hessel, G. Kolb, P. Löb, A.K. Pannwitt, A. Ziogas, Trans. IChemE 81 (Part A) (2003) 721.
[73] W. Bier, W. Keller, G. Linder, D. Seidel, K. Schubert, ASME, DSC-Micro-structures, Sens. Actuators 19 (1990) 189.
[74] K. Schubert, W. Bier, G. Linder, D. Seidel, Ind. Diamond Rev. 50 (1990) 5.
[75] W. Bier, W. Keller, G. Linder, D. Seidel, K. Schubert, H. Martin, Chem. Eng. Proc. 32 (1993) 33.
[76] K. Schubert, J. Brandner, M. Fichtner, G. Linder, U. Schygulla, A. Wenka, Microscale Thermophys. Eng. 5 (2001) 17.
[77] K. Schubert, W. Bier, J. Brandner, M. Fichtner, C. Franz, G. Linder, in: Proceedings of the 2nd International Conference on Microreaction Technology, 1998, New York, AIChE (1998) p. 88.
[78] G. Wießmeier, D. Hönicke, in: Proceedings of the 2nd International Conference on Microreaction Technology, 1998, New York, AIChE (1998) p. 152.
[79] R. Wunsch, M. Fichtner, K. Schubert, in: Proceedings of the 4th International Conference on Microreaction Technology, 2000, New York, AIChE (2000) p. 481.
[80] A. Gorges, J. Käßbohrer, G. Kreisel, S. Meyer, in: Proceedings of the 6th International Conference on Microreaction Technology, 2002, New York, AIChE (2002) p. 186.
[81] R. Födisch, A. Kursawe, D. Hönicke, in: Proceedings of the 6th International Conference on Microreaction Technology, 2002, New York, AIChE (2002) p. 140.
[82] D. Hönicke, G. Wießmeier, Workshop on Microsystem Technology 1995, DECHEMA Monographien, Vol. 132, VCH, Weinheim 1996, p. 93.
[83] U. Hagendorf, M. Janicke, F. Schüth, K. Schubert, M. Fichtner, in: Proceedings of the 2nd International Conference on Microreaction Technology, 1998, New York, AIChE (1998) p. 81.
[84] M.T. Janicke, H. Kestenbaum, U. Hagendorf, F. Schüth, M. Fichtner, K. Schubert, J. Catal. 191 (2000) 282.
[85] M.T. Janicke, A. Holzwarth, M. Fichtner, K. Schubert, F. Schüth, Stud. Surf. Sci. Catal. 130 (2000) 437.
[86] O. Görke, P. Pfeifer, K. Schubert, in: Proceedings of the 6th International Conference on Microreaction Technology, 2002, New York, AIChE (2002) p. 262.
[87] E.V. Rebrov, M.H.J.M. de Croon, J.C. Schouten, in: Proceedings of the 5th International Conference on Microreaction Technology, 2001, Springer, Berlin, 2002, p. 49.
[88] E.V. Rebrov, M.H.J.M. de Croon, J.C. Schouten, Catal. Today 69 (2001) 183.
[89] E.V. Rebrov, M.H.J.M. de Croon, J.C. Schouten, Chem. Eng. J. 90 (2002) 61.
[90] J.M. Bradley, A. Hopkinson, D.A. King, J. Phys. Chem. 99 (1995) 17032.
[91] D.A. King, in: G.F. Froment, K.C. Waugh (Eds.), Dynamics of Surfaces and Reaction Kinetics in Heterogeneous Catalysis, Elsevier, Amsterdam, 1997, p. 79.
[92] N. Materer, U. Starke, A. Barbieri, R. Döll, K. Heinz, M.A. van Hove, G.A. Somorjai, Surf. Sci. 325 (1995) 207.
[93] R.J. Gorte, J.L. Gland, Surf. Sci. 102 (1981) 348.
[94] P. Kisliuk, J. Phys. Chem. Soilds 3 (1957) 95.
[95] D. Brennan, D.O. Hayward, B.M.W. Trapnell, Proc. R. Soc. Lond., Ser. A 256 (1960) 81.
[96] J.L. Gland, J. Kollin, Surf. Sci. 104 (1981) 478.
[97] B.A. Sexton, G.E. Mitchell, Surf. Sci. 99 (1980) 523.
[98] J.L. Gland, E.B. Kollin, Chem. Phys. 107 (1997) 6443.
[99] J.J. Ostermaier, J.R. Katzer, W.H. Manogue, J. Catal. 33 (1974) 457.
[100] E.V. Rebrov, S.A. Duinkerke, M.H.J.M. de Croon, J.C. Schouten, Chem. Eng. J. 93 (2003) 201.
[101] J. Brandner, M. Fichtner, K. Schubert, M.A. Liauw, G. Emig, in: Proceedings of the 5th International Conference on Microreaction Technology, 2001, Springer, Berlin, 2002, p. 164.
[102] J. Brandner, G. Emig, M.A. Liauw, K. Schubert, in: Proceedings of the 6th International Conference on Microreaction Technology, 2002, New York, AIChE (2002) p. 275.
[103] S.P. Fitzgerald, R.S. Wegeng, A.Y. Tonkovich, Y. Wang, H.D. Freeman, J.L. Marco, G.L. Roberts, D.P. VanderWiel, in: Proceedings of the 4th International Conference on Microreaction Technology, 2000, New York, AIChE (2000) p. 358.
[104] S. Walter, E. Joannet, M. Schiel, I. Boullet, R. Philips, M.A. Liauw, in: Proceedings of the 5th International Conference on Microreaction Technology, 2001, Springer, Berlin, 2002, p. 387.
[105] A. Rouge, A. Renken, in: Proceedings of the 5th International Conference on Microreaction Technology, 2001, Springer, Berlin, 2002, p. 230.
[106] A. Rouge, B. Spoetzl, K. Gebauer, R. Schenk, A. Renken, Chem. Eng. Sci. 56 (2001) 1419.
[107] M.A. Liauw, M. Baerns, R. Broucek, O.V. Buyevskaya, J.-M. Commenge, J.-P. Corriou, L. Falk, K. Gebauer, H.J. Hefter, O.-U. Langer, H. Löwe, M. Matlosz, A. Renken, A. Rouge, R. Schenk,

N. Steinfeld, St. Walter, in: Proceedings of the 3rd International Conference on Microreaction Technology, 1999, Springer, Berlin, 2000, p. 224.
[108] N. Steinfeld, O.V. Buyevskaya, D. Wolf, M. Baerns, in: M.J.J. Spivey, E. Iglesia, T.H. Fleisch (Eds.), Studies in Surface Science and Catalysis, Elsevier, 2001, p. 185.
[109] A.I.Y. Tonkovich, D.M. Jimenez, J.L. Zilka, M.J. LaMont, Y. Wang, R.S. Wegeng, in: Proceedings of the 2nd International Conference on Microreaction Technology, 1998, New York, AIChE (1998) p. 186.
[110] M.K. Drost, C. Call, J. Cuta, R. Wegeng, J. Microscale Thermophys. Eng. 1 (1997) 321.
[111] S. Senkan, K. Krantz, S. Ozturk, V. Zengin, I. Onal, Angew. Chem. Int. Ed. 38 (1999) 2794.
[112] T. Zech, D. Hönicke, A. Lohf, K. Golbig, T. Richter, in: Proceedings of the 3rd International Conference on Microreaction Technology, 1999, Springer, Berlin, 2000, p. 260.
[113] T. Zech, D. Hönicke, in: Proceedings of the 4th International Conference on Microreaction Technology, 2000, New York, AIChE (2000) p. 379.
[114] P. Claus, D. Hönicke, T. Zech, Catal. Today 67 (2001) 319.
[115] G. Kolb, V. Cominos, K. Drese, V. Hessel, C. Hofmann, H. Löwe, O. Wörz, R. Zapf, in: Proceedings of the 6th International Conference on Microreaction Technology, 2002, New York, AIChE (2002) p. 61.
[116] A. Ziogas, V. Hessel, G. Kolb, H. Löwe, R. Zapf, in: Proceedings of the 5th European Congress of Chemical Engineering (ECCE), 2003, Granada, Published on CD.
[117] A. Müller, W. Ehrfeld, V. Hessel, H. Löwe, A. Lohf, Th. Richter, in: Proceedings of the 3rd European Congress of Chemical Engineering (ECCE), 2001, Nürnberg, Published on CD.
[118] A. Müller, K. Drese, H. Gnaser, M. Hampe, V. Hessel, H. Löwe, S. Schmitt, R. Zapf, Catal. Today 81 (2003) 377.
[119] R. Knitter, D. Göhring, M. Bram, P. Mechnich, R. Broucek, in: Proceedings of the 4th International Conference on Microreaction Technology, 2000, New York, AIChE (2000) 455.
[120] D. Göhring, R. Knitter, P. Risthaus, St. Walter, M.A. Liauw, P. Lebens, in: Proceedings of the 6th International Conference on Microreaction Technology, 2002, New York, AIChE (2002) 55.
[121] S. Tanaka, T. Yamada, S. Sugimoto, J.-F. Li, M. Esashi, J. Micromech. Microeng. 13 (2003) 502.
[122] V. Hessel, W. Ehrfeld, K. Golbig, C. Hofmann, S. Jungwirth, H. Löwe, T. Richter, M. Storz, A. Wolf, O. Wörz, J. Breysse, in: Proceedings of the 3rd International Conference on Microreaction Technology, 1999, Springer, Berlin, 2000, p. 151.
[123] K. Haas-Santo, O. Görke, K. Schubert, J. Fiedler, H. Funke, in: Proceedings of the 5th International Conference on Microreaction Technology, 2001, Springer, Berlin, 2002, p. 313.
[124] J. Mayer, M. Fichtner, D. Wolf, K. Schubert, in: Proceedings of the 3rd International Conference on Microreaction Technology, 1999, Springer, Berlin, 2000, p. 187.
[125] M. Fichtner, J. Mayer, D. Wolf, K. Schubert, Ind. Eng. Chem. Res. 40 (2001) 3475.
[126] D.A. Hickmann, L.D. Schrnid, J. Catal. 136 (1992) 300.
[127] A.Y. Tonkovich, J.L. Zilka, M.R. Powell, C.J. Call, in: Proceedings of the 2nd International Conference on Microreaction Technology, 1998, New York, AIChE (1998) 45.
[128] G.A. Whyatt, W.E. TeGrotenhuis, J.G.H. Geeting, J.M. Davis, R.S. Wegeng, L.R. Pederson, in: Proceedings of the 5th International Conference on Microreaction Technology, 2001, Springer, Berlin, 2002, p. 303.
[129] G.A. Whyatt, C.M. Fischer, J.M. Davis, in: Proceedings of the 6th International Conference on Microreaction Technology, 2002, New York, AIChE (2002) p. 85.
[130] E. Jones, J. Holladay, S. Perry, R. Orth, B. Rozmiarek, J. Hu, M. Phelps, C. Guzman, in: Proceedings of the 5th International Conference on Microreaction Technology, 2001, Springer, Berlin, 2002, p. 277.
[131] J.D. Holladay, E.O. Jones, M. Phelps, J. Hu, J. Power Sources 108 (2002) 21.
[132] E.R. Delsmann, J. Rebrov, M.H.J.M. de Croon, J.C. Schouten, G.J. Kramer, V. Cominos, T. Richter, T. Veenstra, A. van den Berg, P. Codben, F. de Bruijn, C. Ferret, U. d'Ortona, L. Falk, in: Proceedings of the 5th International Conference on Microreaction Technology, 2001, Springer, Berlin, 2002, p. 368.
[133] O. Wolfrath, L. Kiwi-Minsker, A. Renken, in: Proceedings of the 5th International Conference on Microreaction Technology, 2001, Springer, Berlin, 2002, p. 192.
[134] L. Kiwi-Minsker, O. Wolfrath, A. Renken, Chem. Eng. Sci. 57 (2002) 4947.
[135] T. Matsuda, I. Koike, N. Kubo, E. Kikuchi, Appl. Catal. A: Gen. 96 (1993) 3.
[136] B. Louis, P. Reuse, L. Kiwi-Minsker, A. Renken, Appl. Catal. A 210 (2001) 103.
[137] E. Suzuki, K. Nakashiro, Y. Ono, Chem. Lett. 6 (1988) 953.
[138] V. Sobolev, G.I. Panov, A.S. Kharitonov, V.N. Romannikov, A.M. Volodin, K.G. Ione, J. Catal. 139 (1993) 435.
[139] U.-H. Felcht, Chem. Eng. Technol. 25 (4) (2002) 345.